

# Global Biogeochemical Cycles<sup>®</sup>

## RESEARCH ARTICLE

10.1029/2025GB008540

### Key Points:

- Despite poor climate and limited management, terrestrial ecosystems of Russia remained a stable carbon sink  $\sim 600 \text{ Tg C yr}^{-1}$  in 2000–2019
- All methods used in the carbon account give comparable results within their uncertainties, though some show different temporal trends
- Climate change, rising disturbances, and poor land management may greatly reduce the biospheric services of Russia's terrestrial ecosystems, particularly forests

### Supporting Information:

Supporting Information may be found in the online version of this article.

### Correspondence to:

A. Shvidenko,  
shvidenko@iiasa.ac.at

### Citation:

Shvidenko, A., Ciais, P., Patra, P. K., Bastos, A., Maksyutov, S., Lauerwald, R., et al. (2025). A system reanalysis of the current greenhouse gases budget of terrestrial ecosystems in Russia. *Global Biogeochemical Cycles*, 39, e2025GB008540. <https://doi.org/10.1029/2025GB008540>

Received 12 FEB 2025

Accepted 9 OCT 2025

### Author Contributions:

**Conceptualization:** Anatoly Shvidenko, Philippe Ciais






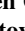


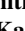
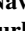





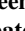


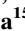


**Data curation:** Shamil Maksyutov, Dmitry Schepaschenko

**Formal analysis:** Anatoly Shvidenko, Philippe Ciais, Prabir K. Patra, Ana Bastos, Shamil Maksyutov, Ronny Lauerwald, Dmitry Belikov, Naveen Chandra, Mikhail Glagolev, Irina Terentieva, Dmitry Karelin, Juliya Kurbatova, Irina Kurganova, Anna Romanovskaya, Vladimir Korotkov, Liudmila Mukhortova, Anatoly Prokushkin, Vadim Mamkin, Andrey Krasovskiy, Dmitry Schepaschenko

**Funding acquisition:** Florian Kraxner

**Investigation:** Anatoly Shvidenko, Philippe Ciais, Prabir K. Patra, Ana Bastos, Shamil Maksyutov,

## A System Reanalysis of the Current Greenhouse Gases Budget of Terrestrial Ecosystems in Russia

Anatoly Shvidenko<sup>1</sup> , Philippe Ciais<sup>2</sup> , Prabir K. Patra<sup>3</sup> , Ana Bastos<sup>4</sup> , Shamil Maksyutov<sup>5</sup> , Ronny Lauerwald<sup>6</sup> , Benjamin Poulter<sup>7</sup> , Dmitry Belikov<sup>8</sup> , Naveen Chandra<sup>3</sup> , Mikhail Glagolev<sup>9,10</sup> , Irina Terentieva<sup>11</sup> , Dmitry Karelin<sup>12</sup> , Juliya Kurbatova<sup>13</sup> , Irina Kurganova<sup>14</sup> , Anna Romanovskaya<sup>15</sup> , Vladimir Korotkov<sup>15</sup> , Liudmila Mukhortova<sup>16</sup> , Anatoly Prokushkin<sup>16</sup> , Eric Gustafson<sup>17</sup> , Florian Kraxner<sup>1</sup> , Vadim Mamkin<sup>13,18</sup> , Natalia Lukina<sup>19</sup> , Andrey Krasovskiy<sup>1</sup> , Eugene Vaganov<sup>20</sup> , and Dmitry Schepaschenko<sup>1</sup> 

<sup>1</sup>International Institute for Applied Systems Analysis (IIASA), Laxenburg, Austria, <sup>2</sup>Centre d'Etudes Orme des Merisiers, Laboratoire des Sciences du Climat et de l'Environnement IPSL-LSCE, CEA CNRS UVSQ, Gif sur Yvette, France, <sup>3</sup>Research Institute for Global Change, JAMSTEC, Yokohama, Japan, <sup>4</sup>Institute for Earth System Science and Remote Sensing, Leipzig University, Leipzig, Germany, <sup>5</sup>National Institute of Environmental Studies, Tsukuba, Japan, <sup>6</sup>University Paris-Saclay, INRAE, AgroParisTech, UMR ECOSYS, Palaiseau, France, <sup>7</sup>NASA Goddard Space Flight Center, Greenbelt, MD, USA, <sup>8</sup>Center for Environmental Remote Sensing, Chiba University, Chiba, Japan, <sup>9</sup>Faculty of Soil Science, Lomonosov Moscow State University, Moscow, Russia, <sup>10</sup>Institute of Forest Science, Russian Academy of Sciences, Moscow, Russia, <sup>11</sup>Department of Geography, University of Calgary, Calgary, AB, Canada, <sup>12</sup>Institute of Geography RAS, Moscow, Russia, <sup>13</sup>A.N. Severtsov Institute of Ecology and Evolution of Russian Academy of Sciences, Moscow, Russia, <sup>14</sup>Institute of Physicochemical and Biological Problems in Soil Science, RAS, Pushchino, Russia, <sup>15</sup>Yu. A. Izrael Institute of Global Climate and Ecology, Moscow, Russia, <sup>16</sup>V.N. Sukachev Institute of Forest, Siberian Branch of the Russian Academy of Sciences, Krasnoyarsk, Russia, <sup>17</sup>Institute for Applied Ecosystem Studies, Northern Research Station, US Forest Service, Rhinelander, WI, USA, <sup>18</sup>National Research University Higher School of Economics, Moscow, Russia, <sup>19</sup>Center for Forest Ecology and Productivity of the Russian Academy of Sciences, Moscow, Russia, <sup>20</sup>Siberian Federal University, Krasnoyarsk, Russia

**Abstract** This study synthesizes the budgets of three greenhouse gases (GHG, namely CO<sub>2</sub>, CH<sub>4</sub>, N<sub>2</sub>O) for Russia over two decades (2000–2009 and 2010–2019) using bottom-up and top-down approaches, as part of the Regional Carbon Cycle Assessment and Processes, Phase 2 (RECCAP2). Published estimates of natural sources and sinks of these GHGs in Russia vary widely. Here, bottom-up estimates are based on eddy covariance measurements, the Integrated Land Information System of Russia (ILIS-LEA), field data, Dynamic Global Vegetation Models (DGVMs), and regional models. The bottom-up approach estimated Net Ecosystem Exchange (NEE) at  $-0.64 \pm 0.17$  and  $-0.57 \pm 0.14 \text{ Pg C yr}^{-1}$ , for decades 2000–2009 and 2010–2019, respectively. Top-down atmospheric inversions provide similar NEE carbon flux estimates with comparable uncertainties at  $-0.56 \pm 0.26$  and  $-0.73 \pm 0.27 \text{ Pg C yr}^{-1}$  for the two decades. Differences between these approaches arise from distinct flux components and structural assumptions. ILIS-LEA indicates a slightly declining carbon sink in 2010–2019, driven by increased disturbances. In contrast, DGVMs suggest a stable carbon sink over both decades but they do not fully simulate the effects of disturbances and recovery. Top-down inversions reveal an increasing CO<sub>2</sub> sink, suggesting with additional observed constraints on biomass carbon increment that soil and non-forest biomes absorb more carbon than predicted by DGVMs and ILIS-LEA models. A Bayesian averaging approach estimates natural ecosystems acting as a GHG sink with a land-to-atmosphere flux of  $-1.55 \pm 0.91$  and  $-1.47 \pm 0.82 \text{ Pg CO}_2\text{-eq. yr}^{-1}$ . Accounting for both natural and anthropogenic emissions across the Russian territory shifts the net GHG balance to a source around  $1.2 \text{ Pg CO}_2\text{-eq. yr}^{-1}$ .

**Plain Language Summary** Greenhouse gas (GHG) budgets for terrestrial ecosystems are complex and uncertain, requiring multiple methods for accurate assessment. In this study, we used a systems analysis approach to estimate the GHG budgets of Russia's terrestrial ecosystems, combining top-down (scaling down global estimates) and bottom-up (scaling up local and regional data) methods. These included empirical observations and process-based simulations to quantify the sources, sinks, and fluxes of key GHGs. Our analysis shows relatively small differences between the results of the different approaches but helps to clarify their respective strengths and limitations. A Bayesian synthesis of flux estimates confirms that Russia's ecosystems acted as a net CO<sub>2</sub> sink during the first two decades of the 21st century. However, some ecosystems may shift toward becoming net GHG sources in the future. When national anthropogenic emissions are included, Russia's

Ronny Lauerwald, Dmitry Belikov,  
Naveen Chandra, Mikhail Glagolev,  
Irina Terentieva, Dmitry Karelin,  
Juliya Kurbatova, Irina Kurganova,  
Anna Romanovskaya, Vladimir Korotkov,  
Liudmila Mukhortova,  
Anatoly Prokushkin, Vadim Mamkin,  
Andrey Krasovskiy,  
Dmitry Schepaschenko

**Methodology:** Anatoly Shvidenko,

Philippe Ciais, Prabir K. Patra,

Dmitry Schepaschenko

**Software:** Naveen Chandra,

Andrey Krasovskiy,

Dmitry Schepaschenko

**Writing – original draft:**

Anatoly Shvidenko, Prabir K. Patra

**Writing – review & editing:**

Anatoly Shvidenko, Philippe Ciais, Prabir

K. Patra, Ana Bastos, Shamil Maksyutov,

Ronny Lauerwald, Benjamin Poulter,

Mikhail Glagolev, Dmitry Karelin,

Juliya Kurbatova, Irina Kurganova,

Anna Romanovskaya, Eric Gustafson,

Florian Kraxner, Natalia Lukina,

Eugene Vaganov, Dmitry Schepaschenko

overall GHG balance indicates a net source. In recent decades, significant progress has been made in understanding the role of terrestrial ecosystems in the global cycles of CO<sub>2</sub>, CH<sub>4</sub>, and N<sub>2</sub>O, including within Russia. This study builds on those advances, providing new insights into the contribution of Russia's vast landscapes to global GHG dynamics and emphasizing their critical importance in shaping future biogeochemical trends.

## 1. Introduction

### 1.1. Importance of Russia in the Global Carbon Budget

Russia is the largest country on Earth, containing one-fifth of the world's forests and spanning all natural zones of the Northern Hemisphere (Figure S1 in Supporting Information S1), with a large heterogeneity of climate, soil, vegetation, and degrees of transformation of natural landscapes. Permafrost zones cover two-thirds of the country, including vast, sparsely populated, and largely ungovernable territories that have undergone significant social and economic changes over several centuries. There are many official statistics on land ecosystems and carbon and other GHGs, but most are incomplete or outdated. Most previous peer-reviewed publications were largely based on global model results and reported an average carbon sink (excluding a few outliers) in the range of 400–800 Tg C yr<sup>−1</sup> in 2000–2019. This Russian carbon sink accounts for 40%–80% of the global land net carbon sink derived from atmospheric inversions or the atmospheric oxygen budget (Friedlingstein et al., 2025). Despite its critical importance in the global budget, there is no up-to-date study of Russia's recent carbon balance or its emissions of CH<sub>4</sub> and N<sub>2</sub>O. This study aims to fill this knowledge gap by estimating Greenhouse gas (GHG) budgets for Russia's ecosystems, separating natural and anthropogenic fluxes of CO<sub>2</sub>, CH<sub>4</sub>, and N<sub>2</sub>O for the first two decades of this century, as part of the RECCAP-2 project. Unlike the earlier RECCAP-1 analysis, which covered only the 2000s and relied mainly on global model results, this study integrates empirical regional data to provide an observation-based budget of CO<sub>2</sub> fluxes over the last two decades using an upgraded version of the Land-Ecosystem approach (LEA) carbon accounting system (Shvidenko & Nilsson, 2003).

### 1.2. Recent Climate Trends in Russia and How They May Impact Terrestrial GHG Fluxes

Between 1976 and 2021, Russia experienced an average warming rate 2.5 times larger than the global average (+0.49°C decade<sup>−1</sup>). The maximum warming rates were recorded in spring (+0.78 to +0.85°C decade<sup>−1</sup>). Over the Arctic coast, the average warming rate was +1.5°C decade<sup>−1</sup>. Precipitation increased at a rate of +0.84 mm yr<sup>−1</sup> (+1.8% yr<sup>−1</sup>), with changes occurring mostly in spring and winter (Roshydromet, 2022). With longer growing seasons and wetter conditions, we could expect net primary productivity to increase, driving larger carbon uptake over time. Wetter and warmer conditions over Arctic peatlands and other wetlands are also expected to increase CH<sub>4</sub> emissions, as observed across high northern latitudes. For N<sub>2</sub>O emissions, very few measurements are available, and ecosystems can act as sources or sinks depending on the water table and ecosystem type. Under wetter conditions, we expect N<sub>2</sub>O emissions from the permafrost region to increase, while N<sub>2</sub>O uptake will increase in upland soils (Voigt et al., 2020).

However, the amount of snow, which mediates winter cooling of soil and provides water for plants during the growing season, has increased in most of the Siberian taiga since 1980, but has decreased in the Lena river basin (Pulliainen et al., 2020). Early snowmelt can increase water stress during the growing season, especially in Siberia where the growing season water balance is negative (Meroni et al., 2002). The severity and frequency of drought and extreme weather events has increased markedly, particularly by the end of 2010s in the Asian part of Russia (Kharuk et al., 2021), resulting in a substantial increase of fire and outbreaks of destructive insects in forests. Severe heat waves have been observed regularly in several Russian regions during recent decades. A significant greening trend was observed since 1982 in both European Russia and the major part of Siberia (Piao et al., 2020), with smaller trends in northcentral Siberia, indicating increased productivity and leaf area in these regions.

From recent changes in climate extremes and observed increases in fires and insect outbreaks, we expect the overall impact of climate change on Russia's ecosystems to be mostly negative, despite long-term climate trends increasing net primary productivity. Terrestrial ecosystems significantly increase ecosystem productivity during years with sufficient and regular summer rainfall. Conversely, in dry years, they can lose up to half of their Net Primary Production (NPP), particularly after heatwaves, catastrophic wildfires, and outbreaks of dangerous insects.

### 1.3. Main Sources of Uncertainty for Estimating the GHG Balance of Russia and Novelty of This Study

The current shortcomings in assessing GHG emissions and absorption by terrestrial ecosystems in Russia using empirical bottom-up approaches can be grouped as follows: (a) insufficient or absent systems approach; (b) unsatisfactory amount, accuracy, or adequacy of initial information; (c) oversimplification of accounting schemes; (d) inadequate assessment of uncertainties. In this study, we attempted to address these issues.

The methodological novelty of this study lies in following the major principles of applied system analysis while taking into consideration the specifics of the systems studied. The Integrated Land Information System (ILIS), a multi-level Geographical Information System with a spatial resolution of 150 m, was developed as the information basis of the study, particularly for applying in bottom-up LEA. The spatial component of ILIS represents ecosystems by a Hybrid Land Cover (HLC) derived from the integration of multi-sensor remote sensing data (above 10 different products) and ground information on vegetation, soil, landscapes, etc. ILIS contains information for Russian terrestrial ecosystems for 2009 and 2019 including updated forest inventory data.

A set of multidimensional, spatially distributed regional modeling systems for assessing key biometric indicators of ecosystems (mostly forest) has been developed based on comprehensive databases of field measurements and is used for: (a) assessing the structure and dynamics of live biomass by tree species and components (Schepaschenko et al., 2017); (b) assessing NPP and other indicators of forest biological productivity (Shvidenko et al., 2007; Shvidenko, Schepaschenko, Nilsson et al., 2008, Shvidenko, Schepaschenko, Vaganov et al., 2008); (c) estimating heterotrophic soil respiration (Mukhortova et al., 2021; Schepaschenko et al., 2025); and (d) assessing the amount and dynamics of dead wood in ecosystems (Shvidenko et al., 2023).

The final results were obtained using independent approaches, the empirical LEA, Dynamic Global Vegetation Models (DGVM) from TRENDY v11, Eddy Covariance (EC) and Atmospheric Inverse Modeling (IM), each with their corresponding uncertainties. A Bayesian approach was applied to estimate the integrated uncertainty.

## 2. Materials and Methods

### 2.1. Overall Methodological Approach

The biospheric functions and services of terrestrial ecosystems form natural real-existing, open, dynamic, and highly complex systems. In research, such natural systems can be represented by a model that is an artificial system mirroring the structure and properties of the natural systems. In this study, we attempted to follow the basic principles of applied systems analysis, taking into account the specific characteristics of the studied natural terrestrial systems of boreal Eurasia. These systems belong to the class of underspecified or fuzzy systems (Shvidenko et al., 1996) and constitute problems of full complexity (Schellnhuber, 2003). A key feature of such systems is their stochastic nature, which prevents the assessment of structural uncertainty using individually any method of GHG accounting. This requires the use of multiple independent methods, followed by harmonization (mutual constraints) of the final results (McGlynn et al., 2022; Nilsson et al., 2000, 2007; Quegan et al., 2011; Shvidenko et al., 1996, 2010a, 2010b, 2015).

Our approach to estimating the GHG budgets of Russian terrestrial ecosystems satisfies two fundamental requirements of applied system analysis: comprehensiveness and verifiability. Comprehensive accounting should consider all ecosystems, processes, and fluxes, explicitly in time and space, with landscapes as a primary unit for territorial up-scaling methods (Ciais et al., 2022). Partial accounting (e.g., limited to “managed” ecosystems) is not applicable because it may not present information about the entire system. Verifiability means that there is a possibility of assessing reproducibility and traceability based on reliably estimated uncertainty allowing certified accounting in future studies.

In this study, uncertainty is defined as the cumulative insufficiency in the estimates of the studied system, regardless of whether these insufficiency are a consequence of lack of knowledge, poor information, potential double counting, or other causes. Given that the membership functions of the studied systems are stochastic, the calculated uncertainty is not complete because it lacks a solid background for assessing the structural uncertainty. Thus, we provide here a “full” uncertainty assessment by comparing the results and uncertainties across multiple independent methods that, to some extent, provides multiple constraints of uncertainties of individual methods.

Other principles of system analysis relate to the strict logical structuring of the assessment process and minimization of uncertainty. The sources of uncertainty are numerous, particularly in bottom-up assessments:

inconsistencies in definitions and classifications across disciplines; shortcomings of experimental data; lack of planned experiments at various stages of the accounting; unknown or insufficient precision in measurements; inadequate basis for upscaling; short time series; lack of numerical description of some important processes; oversimplified modeling assumptions; gaps in the observation systems; and many others (Nilsson et al., 2000; Shvidenko et al., 1996). In some instances, the results rely on numerical expert judgments and estimates.

In this study, we address uncertainties through the independent application of different methods of GHG accounting: inventories created for different purposes; diverse sets of measurements in situ (including EC); and numerous empirical and “semi-empirical” regional models (LEA); DGVM; and top-down atmospheric models approaches, with subsequent harmonization of the results obtained. The empirical information support, despite its high and often poorly constrained uncertainty, plays a key role in understanding the major biogeochemical cycles of vegetation that impact the climate system of the planet.

## 2.2. Uncertainty in Forest Area: Russian versus FAO Definitions

A primary and difficult-to-manage source of uncertainty, particularly in empirical bottom-up approaches such as LEA, is the inconsistency of input data (definitions, classification schemes, etc.). A key source of uncertainty in previous estimates of the carbon budget for Russia's forests has been terminological ambiguity. Russian forest land-cover terminology distinguishes between two notions: (a) forest or land covered by forest, which denotes areas actually covered by trees at the time of inventory, including shrubs within lands managed by forest authority where “high forests” cannot develop because of harsh environmental conditions; and (b) unforested land, which refers to areas designated for forest growth but temporarily not covered by trees. Together, these two categories form forest land in the Russian land-cover classification. The FAO definition considers “forest” to include both established forests and currently treeless areas that are expected to become forest in the future, but it does not include shrubs. The FAO definition, with its focus on land use rather than land cover, makes mapping with remote sensing challenging (Hansen et al., 2013, Text S1 in Supporting Information S1). Furthermore, the lower boundary of relative stocking (often used as a synonym for canopy closure) is 24% in the Russian definition (34% for young forests), while the FAO definition includes “forest” starting from 10% relative stocking. Notably, the FAO definition requires mandatory restoration of temporarily treeless forest lands during a defined period that is not considered by the Russian definition.

The differences in estimated forest areas according to these definitions are significant. Around the 2020s, the Russian definition (Forest State Register, excluding shrubs) estimated 715 M ha of forest, while the FRA FAO 2020 reported 815 M ha. Some forest categories defined by FAO cannot be reliably identified via remote sensing (e.g., old not regenerated harvested areas or burns). In this study, we defined as “forest” all areas actually covered by trees of major forest-forming species (MFFS) and encompassed more than 90% of the forest area according to the Russian national definition.

Russia conducted the first cycle of the State (National) Forest Inventory (SFI) between 2007 and 2021, with some aggregated country-level results published by Filipchuk et al. (2023). The updated national estimates of forest area and growing stock have increased substantially and are now more consistent with ILIS-LEA. However, since spatially distributed SFI data are not available, this study relies on information from ILIS-LEA. We separately report data for “forest” and for major categories of other “forest land” and shrub land-cover classes from ILIS-LEA to ensure consistent comparisons across forest land categories.

## 2.3. Uncertainty Estimation

We used standard tools for assessing uncertainties within the bottom-up approach—error propagation theory and Monte Carlo analysis. In its general form, the GHG budgeting by individual substances (for instance, carbon) is presented as a consecutive chain of recurrent functionals, for example,

$$U = f(V_i), V_i = \varphi(V_{ij}, Q_{ij}), \dots, Y_{ij}, \dots, k = \phi(X_{ij}, \dots, 1, X_{ij}, \dots, 2, \dots, X_{ij}, \dots, n),$$

where  $U$  is a final result (e.g., carbon flux or pool),  $V_{ij}$ ,  $Q_{ij}$  are the intermediate results of the aggregated levels (e.g., for process  $i$  and (or) aggregated unit  $j$ ), etc., and at the lowest level of the set  $X \dots \in [X_{\dots,1}, X_{\dots,2}, \dots, X_{\dots,n}]$  relates to primary measurements.

Then, because all calculations are based on a traceable numerical model, all variables of which have derivatives, standard errors of a function  $Y = f(X_i)$ , where  $X_i$  is a random quantity with standard error  $m_i$ ,  $i = 1, 2, \dots, k$ , could be calculated approximately at each hierarchical stage of the carbon accounting (Kendall & Stuart, 1966), for example, for the initial step of calculation by using functional

$$m_y^2 = \sum_{i=1}^k \left( \frac{dY}{dX_i} m_i \right)^2 + 2 \sum_{i>j} \left( \frac{dY}{dX_i} \right) \left( \frac{dY}{dX_j} \right) r_{ij} m_{X_i} m_{X_j}, \quad (1)$$

where  $dY/dX_i$ —partial derivative of  $Y$  by  $X_i$ , and  $r_{ij}$ —is the correlation coefficient between  $X_i$  and  $X_j$ . Usually, inclusion of the second item of (1) is important because many  $X_i$  in Equation 1 are statistically interdependent.

Usually,  $m_y$  is interpreted based on the assumption of Gaussian error distribution, a simplification that does not change the interpretability and magnitude of the results compared to more complicated approaches, for example, Tschebishev's theorem. Note that errors of initial variables are often presented as summarized errors (including a systematic component), which might have a bias. The bias must not be too large (not exceed 10%–15% of random errors). In our assessments, we used a confidence probability of 0.9.

Uncertainty derived through error propagation is strictly connected to the specificity of the methods of calculation. On one hand, a number of fundamental indicators of ecosystems are calculated based on a large number (up to many thousands) of primary measurements; therefore, their means have very high accuracy. For example, live biomass and NPP of Russian forests were determined with errors of 4%–6% (Nilsson et al., 2000), and similar accuracy was also achieved in the current study. On the other hand, subtraction of values that are close in magnitude is often used, leading to significant relative errors in the result, sometimes exceeding hundreds of percent. Positively defined values (i.e., most indicators of ecosystems) have no practical meaning if their errors are greater than 100%. Therefore, multiple-constraint comparison of results—particularly within and between top-down and bottom-up analyses, are essential components of uncertainty analysis. In a few cases where data were insufficient for a reliable uncertainty assessment, we partially relied on expert estimates of uncertainties, mostly accepting those around 35%.

Uncertainties of DGVM and atmospheric inversion models (IM) are of a different nature than in the bottom-up approach, since they are calculated by averaging results for ensembles of models, and we do not know precisely how independent individual models really are. Therefore, a direct comparison between bottom-up and top-down methods is, to some extent, devoid of scientific basis. Nevertheless, we compared results from different methods because it reflects the influence of the accuracy of individual method results on the systems assessment of the validity of the methods used.

The Bayesian approach is used for different purposes in studying land-atmosphere processes (Li et al., 2016; Shvidenko et al., 2015; Zhou et al., 2012). Here, we used a Bayesian approach to apply mutual constraints to the result obtained by different methods, attempting to take into account different levels of certainty of the ensembles' constituents. For example, for Net Ecosystem Exchange, NEE (Quegan et al., 2011) we used

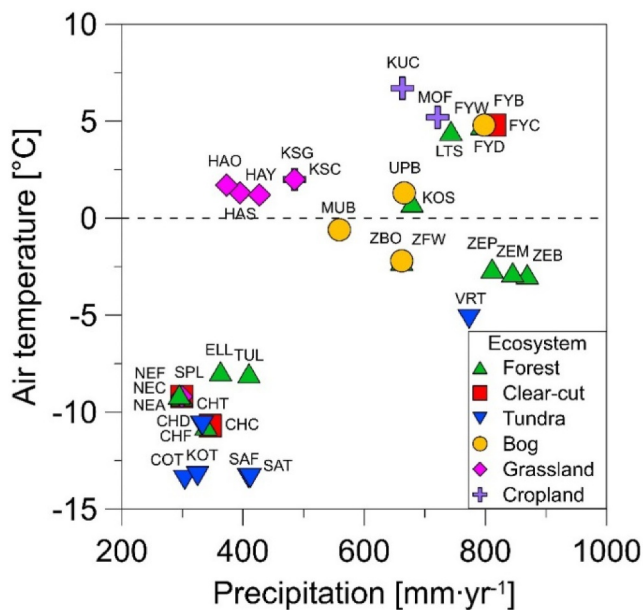
$$NEE(\text{BAYES}) = \sum_i^n \frac{NEE_i}{V_i} / \sum_i^n \frac{1}{V_i},$$

where  $n$ —number of methods,  $n = \geq 2$ ,  $NEE_i$ —Net Ecosystem Exchange (NEE) of method  $i$ , all values are assumed to have unbiased and Gaussian distributions with variance  $V_i$ ,  $i \geq 2$ .

#### 2.4. Upscaling of CO<sub>2</sub> fluxes From Eddy Covariance (EC) Flux Tower Measurements

Eddy Covariance (EC) flux towers measure local net ecosystem CO<sub>2</sub> exchange (NEE) that can be separated into total ecosystem respiration (TER) and gross primary production (GPP). Flux towers might not capture immediate CO<sub>2</sub> losses during disturbances such as fires. Published measurements from 35 sites across Russia were used. The location of each station is shown in Figure S2 in Supporting Information S1, and meta-information is provided in Table S1 in Supporting Information S1. The EC sites are classified into established forests, forests with recent disturbances (e.g., clear-cuts or burnt), bogs, tundra, grasslands and croplands. Annual and growing season cumulative fluxes were analyzed using site-specific growing season length (mostly a number of days with average





**Figure 1.** Distribution of eddy covariance flux stations on the mean annual air temperature—annual precipitation space. The names and locations of the stations are given in Table S1 in Supporting Information S1.

daily temperature  $\geq 5^{\circ}\text{C}$ ). Average fluxes from EC stations, covering periods of 1–15 years (3 years on average), were computed from all available data for each station. The sites were associated with Köppen climate classes based on long-term air temperature and precipitation data for 1981–2010 (Karger et al., 2017). The distribution of the 35 sites in the temperature—precipitation space (Figure 1) covers a longitudinal gradient of the mean annual temperature and annual precipitation, particularly for forest and the bog sites. Siberian sites, except for grasslands and croplands in southern Siberia, are situated in areas with negative annual air temperature and precipitation below  $400\text{ mm yr}^{-1}$ . In contrast, European Russia sites are situated in areas with positive annual air temperatures and higher precipitation levels.

## 2.5. Land Ecosystems C Fluxes From the Landscape-Ecosystem Approach (LEA)

The bottom-up empirical estimates of  $\text{CO}_2$  fluxes in this section were mostly obtained using the landscape-ecosystem approach (LEA) based on the ILIS of Russia, ILIS (Dolman et al., 2012; Schepaschenko et al., 2011; Shvidenko & Schepaschenko, 2014). The ILIS-LEA model uses a HLC data set (HLC) in the form of multi-scale GIS and numerous attributive databases (Figure S3 in Supporting Information S1). The major strength of ILIS-LEA is the integration of empirical data and regional empirical models to merge and harmonize land and forest inventories, ecological monitoring data, remote sensing data and in situ information about ecosystems and landscapes. The ILIS-LEA system also uses quality controlled, critically analyzed and updated

official sources on land use/land cover changes in Russia, such as the State Land Account, State Forest Register, and official statistics (Shvidenko et al., 2010a, 2010b). This allows for a better integration of the diversity of information sources as well as understanding the potential inconsistencies and discrepancies among them. It is based on the HLC map (Figure S3 in Supporting Information S1) that integrates and harmonizes multi-sensor remote sensing products (Schepaschenko et al., 2011; See et al., 2015).

The ILIS-LEA model incorporates databases and calculations to assess the major terms of carbon pools and fluxes (Shvidenko et al., 2010a, 2010b) using a combination of flux-based and stock-change methods. The initial version of ILIS-LEA was developed for the period 2000–2009 with a spatial resolution of  $1\text{ km}^2$ . In 2010, the system was updated for this period and further extended to cover 2000–2019 with a spatial resolution of  $150\text{ m}^2$ . The ILIS-LEA model version used in this study includes updated forest inventory data as a substitute for attributes that cannot be reliably measured by remote sensing (Shvidenko et al., 2010a, 2010b). About 50% of Russian forests have not been inventoried for more than 30 years (Vashchuk, 2016) and the State Forest Register contains obsolete and likely biased information (Schepaschenko et al., 2021). The land cover map used in ILIS-LEA and shown in Figure S3 in Supporting Information S1 was produced by integrating multi-source remote sensing information and updated ground forest inventory data from  $\sim 1700$  forest enterprises and protected forest territories (Shvidenko & Schepaschenko, 2021). Taking into account the availability of spatially distributed detailed land cover data, a number of regional “semi-empirical” models of carbon pools and fluxes were developed and applied, particularly for forest (e.g., for assessment of live biomass, Coarse Woody Debris (CWD), NPP, and heterotrophic respiration for assessment of disturbances). More information on methods and empirical material used is found in Text S1 in Supporting Information S1.

## 2.6. Global Bottom-Up and Top-Down Models

$\text{C-CO}_2$ . We used results from 13 DGVMs from the TRENDY v11 Intercomparison project (Sitch et al., 2024). TRENDY v11 provides updated results of land-use change fluxes and vegetation dynamics covering the full decade of the 2010s. Sitch et al. (2024) also reported  $\text{CO}_2$  fluxes for Russia using 15 DGVMs included in Friedlingstein et al. (2023) with factorial simulations—unforced fluxes under constant climate - land cover and  $\text{CO}_2$ , constant climate and rising  $\text{CO}_2$ , variable climate and  $\text{CO}_2$ , and variable climate,  $\text{CO}_2$  and historical land cover change. Model outputs were analyzed for 2000–2009 and 2012–2021.

We used results of the eight CO<sub>2</sub> atmospheric inversions from the Global Carbon Budget (GCB) 2023 that provides global maps of CO<sub>2</sub> fluxes re-gridded at 1 × 1° resolution and at monthly time intervals (Friedlingstein et al., 2023). The inversions cover the period 2000–2019 and are based on in situ measurements of CO<sub>2</sub> mixing ratio. The inversion design is summarized in Table 4 and A4 of (Friedlingstein et al., 2023). The inversions follow a common submission format and prior gridded fossil fuel data set with a monthly resolution (Jones et al., 2021). We use CO<sub>2</sub> fluxes based on these inversions corrected for CO<sub>2</sub> fluxes due to lateral displacement processes, harvested wood and food products, and riverine export of carbon, as described by Deng et al. (2022). This correction of inversions removes CO<sub>2</sub> fluxes that are not causing carbon stock changes and transforms CO<sub>2</sub> fluxes maps into land carbon storage change maps, facilitating an accurate comparison to the land carbon storage changes estimated by bottom-up methods.

Finally, we used information three book-keeping models from Global Carbon Project (GCP) (2023) for comparative analysis, namely BLUE (Hansis et al., 2015), H&C2023 (Houghton & Castanho, 2023) and OSCAR (Gasser et al., 2020). Source: Supplemental data of GCB 2023 (Version 1.1), GCP, National Land Use Change Carbon Emissions 2023 (<https://doi.org/10.18160/gcp-2023>).

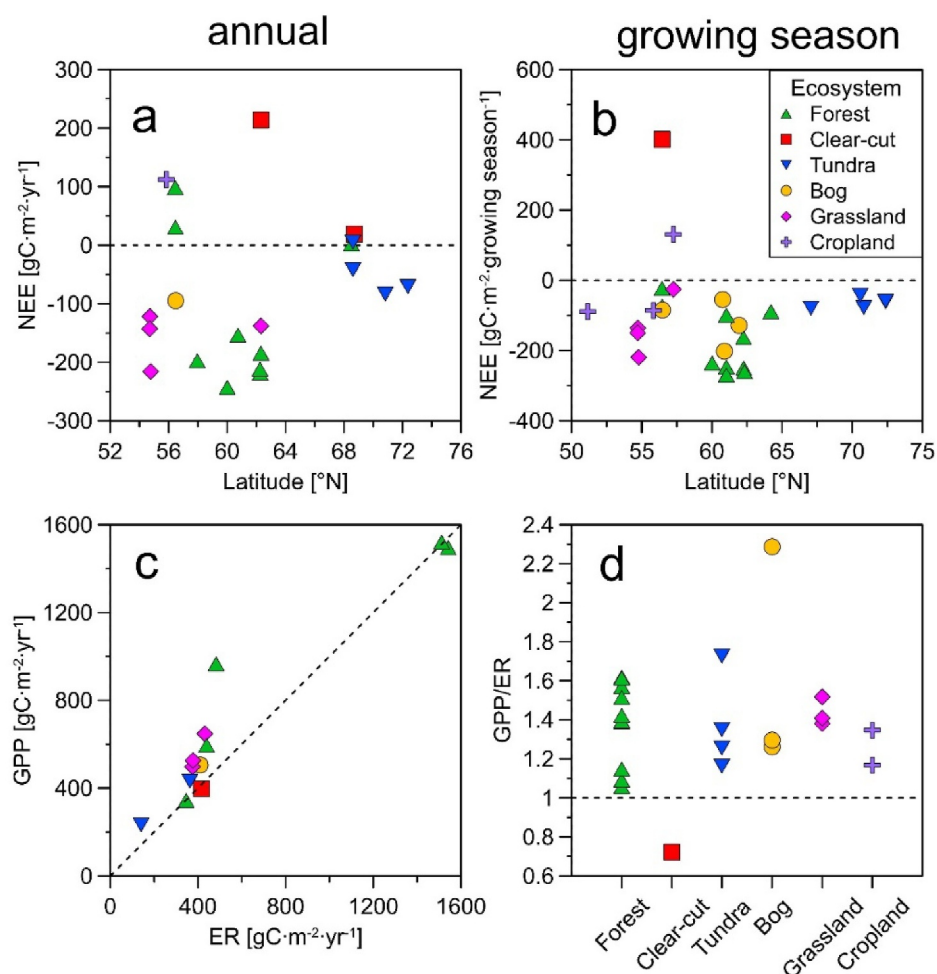
**CH<sub>4</sub>.** The CH<sub>4</sub> atmospheric inversions used to estimate methane fluxes are those from eight inverse modeling (IM) systems reporting for the global methane budget (Saunois et al., 2020). An ensemble of 21 inversions includes 10 surface-based inversions covering 2000–2017 and 11 satellite-based inversions covering 2010–2017 (Saunois et al., 2020). The MIROC4-ACTM inversion by Chandra et al. (2021) was also added to cover the full decade of 2010–2019. The protocol suggested a set of common prior source and sink estimates along with a set of in situ atmospheric observations. However, their use was not compulsory, and the inversions differ in terms of prior fluxes and handling of observation data. Satellite-based inversions use GOSAT CH<sub>4</sub> total columns, and the concentration products assimilated differ by the modeling group (see (Saunois et al., 2020), Supplement). As a result, the ensemble of CH<sub>4</sub> inversions derived a wider range of results than would follow from a stricter intercomparison protocol. The majority of the inversions were driven with a single prescribed climatological OH from TransCom (Patra et al., 2011), which leads to attributing most of the inter-annual variations in atmospheric methane concentration to variations in emissions.

**N<sub>2</sub>O.** The N<sub>2</sub>O atmospheric inversions used here are from four inversion systems used in the GCP Nitrous Oxide Budget (Tian et al., 2020): GEOS-Chem (Wells et al., 2015), PyVAR-CAMS (Thompson et al., 2014), with two ocean priors, MIROC4-ACTM (Patra et al., 2022) and INVICAT (Wilson et al., 2014). The prior fluxes and flux uncertainties are documented by Tian et al. (2020). All inversions used ground-based observations from the NOAA discrete sampling network and included observations from additional networks (for details see (Tian et al., 2020)). The inversions accounted for photolysis and oxidation of N<sub>2</sub>O in the stratosphere, resulting in atmospheric lifetimes in the range of 118–129 years (Deng et al., 2022). The flux estimates by a set of DGVMs are also included for comparison. The set of DGVMs from the RECCAP2 database are DLEM (Tian et al., 2015), LPJ-GUESS (Olin et al., 2015), ORCHIDEE-CNP (Goll et al., 2017) and VISIT (Ito et al., 2018).

### 3. Results

#### 3.1. Bottom-Up Fluxes From Eddy-Covariance Measurements

The mean annual NEE across the EC sites (Figure 2) varied between a sink of −243 g C m<sup>−2</sup> yr<sup>−1</sup> (ELL forest near Chersky) and a source of 213 g C m<sup>−2</sup> yr<sup>−1</sup> (the NEC clearcut forest near Yakutsk). Most sites were annual carbon sinks (Figure 2a). Forest and grassland sites typically provided the most substantial sinks. The tundra sites were mostly small CO<sub>2</sub> sinks (NEE = from 5 to −85 g C m<sup>−2</sup> yr<sup>−1</sup>). The only bog site with full annual measurements (FYB, Fyodorovskoe, European Russia) had a larger sink (NEE = −95 g C m<sup>−2</sup> yr<sup>−1</sup>) than tundra. CO<sub>2</sub> sources were detected at the NEC clearcut forest, and also in the drained tundra site (CHD near Chersky), a larch forest stand (CHF near Chersky) and a mechanically disturbed clearcut forest (CHC, near Chersky). During the growing season, nearly all ecosystems acted as CO<sub>2</sub> sinks (Figure 2b). Growing season NEE at the forest sites varied from −23 g C m<sup>−2</sup> yr<sup>−1</sup> (FYD) to −270 g C m<sup>−2</sup> yr<sup>−1</sup> (ZEP). A growing season CO<sub>2</sub> source was detected at a grassland site near Tyumen in West Siberia (KSC), and the largest growing season source was at a clear-cut site (FYC, Fyodorovskoe, European Russia) at 401 g C m<sup>−2</sup> yr<sup>−1</sup>. Tundra sites showed growing season NEE values similar to annual NEE (between −42 g C m<sup>−2</sup> yr<sup>−1</sup> at KOT to −79 g C m<sup>−2</sup> yr<sup>−1</sup> at VRT), indicating minimal non-growing season flux contribution. For bog sites, the growing season NEE was a larger sink than in tundra, ranged between −55 (ZBO) and −202 g C m<sup>−2</sup> yr<sup>−1</sup> (MUB), greater than the annual NEE, suggesting significant non-growing



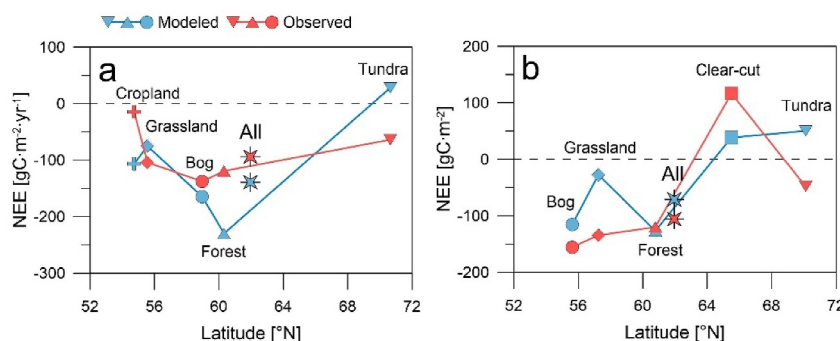
**Figure 2.** CO<sub>2</sub> ecosystem-atmosphere flux estimates obtained using eddy covariance measurements: annual (a) and growing season (b) Net ecosystem exchange versus latitude of the stations; (c) annual gross primary production (GPP) versus ecosystem respiration (total ecosystem respiration (TER)); (d) growing season GPP/TER ratio across the different ecosystem types.

season emissions. Grassland and cropland growing season NEE ranged between 131 g C m<sup>-2</sup> yr<sup>-1</sup> (KSC) and -219 g C m<sup>-2</sup> yr<sup>-1</sup> (HAO) (Figure 2b).

We compared NEE data from the selected sites (Figure 2) with gridded upscaled NEE maps obtained with machine learning models trained by data from EC towers worldwide from the FLUXCOM project (Jung et al., 2020). The FLUXCOM results we used are generated from remote sensing data on a global 0.08° grid but did not incorporate in their training set most of the site data shown in Figure 2. The mean FLUXCOM NEE for Russia was a sink of  $-0.44 \pm 0.16$  Pg C yr<sup>-1</sup> for the 2001–2015 period, which corresponds to a mean rate of  $-27.1$  g C m<sup>-2</sup> yr<sup>-1</sup> over a land area of 1623.8 M ha. Figure 3 shows mean NEE by ecosystem type from FLUXCOM data and the observations in our data set (Section 2.2). Overall, the latitude gradients of NEE for both growing season (Figure 3a) and annual NEE (Figure 3b) are broadly similar, with differences to FLUXCOM of less than 100 g C m<sup>-2</sup> yr<sup>-1</sup>.

GPP and TER data show a wide range of variations across sites. GPP ranged from 180 g C m<sup>-2</sup> yr<sup>-1</sup> in tundra (COT) to 1350–1430 g C m<sup>-2</sup> yr<sup>-1</sup> in productive spruce forests of European Russia (FYW and FYD). TER varies between 110 g C m<sup>-2</sup> yr<sup>-1</sup> (COT) and 1280–1310 g C m<sup>-2</sup> yr<sup>-1</sup> (FYW and FYD). The greatest imbalance between GPP (840 g C m<sup>-2</sup> yr<sup>-1</sup>) and TER (605 g C m<sup>-2</sup> yr<sup>-1</sup>) occurred in highly productive larch forests in eastern Siberia (ELL). Differences in measurement periods among sites and the small number of years covered at some sites make it challenging to compare growing season GPP/TER ratios across sites to explain the relative





**Figure 3.** Net ecosystem exchange by eddy covariance method averaged by ecosystem type and area-weighted average (“All”): (a) annual mean fluxes, (b) growing season mean fluxes. FLUXCOM averages for the same locations are given for comparison. By convention, a negative value is a sink of atmospheric CO<sub>2</sub>.

contribution of CO<sub>2</sub> uptake and release in controlling NEE. In general, the growing season GPP/TER ratio for most of the sites varied between 1 and 1.8 (Figure 2d). The only site with a GPP/TER ratio less than 1 (0.7) was the clear-cut forest (FYB) in European Russia. Overall, the differences between GPP and TER between annual and growing season periods are geographically consistent in boreal and temperate zones where they had a value of 40%–50%, aligning with previous studies (Wang et al., 2011). However, in Russia's permafrost regions, the relative difference of GPP and TER [(GPP-TER)/GPP] between growing season and annual mean was considerably lower (<20%), influenced by winter severity and degree of thaw in the frozen layer.

### 3.2. Terrestrial CO<sub>2</sub> Fluxes From the LEA Regional Bottom-Up Accounting Model

Carbon/CO<sub>2</sub> fluxes based on ILIS-LEA are presented by land cover class in Table 1 and for the entire country in Table 2. The fluxes in both tables also include additional data sources. Description of the land cover classes is provided in the notes to Tables 1 and 2, while the methods used to estimate fluxes for individual land classes are described in more detail in Text S1 in Supporting Information S1. From Tables 1 and 2, it follows that during two successive decades, Russia's terrestrial ecosystems decreased their NEE by  $4.1 \pm 11.8 \text{ g C m}^{-2} \text{ yr}^{-1}$ ; thus, in spite of a slight decrease in NEE, we can conclude that the productivity of Russian forests during the period of 2000–2019 remained within the limits of natural variability.

### 3.3. Results From LEA for Terrestrial C Fluxes Individual Land Classes

NPP of Russia's terrestrial ecosystems estimated by LEA increased from  $5,028 \pm 83 \text{ Tg C yr}^{-1}$ , or  $309 \text{ g C m}^{-2} \text{ yr}^{-1}$ , for 2000–2009, to  $5,313 \pm 90 \text{ Tg C yr}^{-1}$ , or  $327 \text{ g C m}^{-2} \text{ yr}^{-1}$ , for 2010–2019 (Table 1). This 5.8% increase in average NPP is defined by interactions between the change in land cover (resulted in the net loss of forest area of 10.2 M ha in 2010–2019), the regrowth of young forests and the increase in productivity of undisturbed ecosystems, basically forests. Young forests restored after fires are usually more productive than old forests, which could explain the overall increase in NPP despite forest area loss from fires. For 2010–2019, NPP estimated by the CMIP5 models is similar to our estimates with  $5,090 \pm 106 \text{ Tg C yr}^{-1}$  ( $314 \text{ g C m}^{-2} \text{ yr}^{-1}$ ), and NPP estimated by the MODIS light-use efficiency model is 10.6% higher (<https://lpdaac.usgs.gov/products/mod17a3hgf061/>). Overall, there is a small positive trend of published NPP estimates for Russia using different methods (Kudeyarov & Kurganova, 1998; Nilsson et al., 2000; Voronin, 2006) with a very high diversity of other publications ranging from 204 to  $614 \text{ g C m}^{-2} \text{ yr}^{-1}$  (Gower et al., 2001; Moiseev & Alyabina, 2007; Shvidenko, Schepaschenko, Nilsson et al., 2008; Shvidenko, Schepaschenko, Vaganov et al., 2008; Zamolodchikov & Utkin, 2000). On average, our estimates of NPP of undisturbed forests with the LEA model are around 7%–10% higher than previous empirical estimates. This could be interpreted as indirect evidence for a fertilization effect of increased atmospheric CO<sub>2</sub> concentrations, or it could just reflect differences in estimation methods (direct estimation NPP through changes in live biomass dynamics).

Soil heterotrophic respiration (SHR) of Russia's terrestrial ecosystems increased by 8%, from 220 to  $238 \text{ g C m}^{-2} \text{ yr}^{-1}$  in 2010–2019 according to the LEA model. The higher increase rate for SHR than for NPP suggests that increasing SHR drives a decreasing net sink. For forests, SHR rates are higher, and increased from

**Table 1**

Bottom-Up C-CO<sub>2</sub> Fluxes of Russia's Terrestrial/Aquatic Ecosystems in 2000–2009 and 2010–2019 From ILIS-LEA Completed by Other Data Sources (Tg C yr<sup>-1</sup>)

Land class <sup>a</sup>	Area, M ha	-1 × NPP	SHR	DEC	EHR	DIS	LM	-1 × NBP	CON	NEE <sup>b</sup>	Confidence interval 0.9
2000–2009 land-atmosphere CO <sub>2</sub> fluxes per land cover type											
Forest FOR <sup>c</sup>	735.2	-2779.8	1716.4	180.2	1896.6	136.2	56.2	-690.8	22.4	-668.4	160.6
Shrub forest SH1	65.9	-87.0	72.5	2.0	74.5	2.4	0.0	-10.1	-	-10.1	3.3
Disturbed forest DSF	40.8	-81.6	124.2	25.0	149.2	5.8	-2.6	+70.8	-	+70.8	24.9
Sparse forests SPF	63.6	-130.1	117.1	3.5	120.6	3.2	0.0	-6.3	0.5	-5.8	2.2
Croplands CRO	87.4	-405.5	268.2	-	268.2	0.2	9.9	-127.2	122.0	-5.2	2.3
Meadows HFP	119.6	-477.1	325.0	2.4	327.4	0.8	0.0	-148.9	64.7	-84.2	24.9
Abandoned agriculture ABL	27.3	-137.9	93.5	-	93.5	1.6	0.0	-42.8	2.6	-40.2	12.8
Peat PEL	141.9	-340.4	295.7	7.6	303.3	6.6	+1.2	-29.3	1.5	-27.8	8.2
Tundra GST	277.1	-415.9	412.9	4.1	417.0	5.8	0.0	+6.9	-	+6.9	10.0
Other Shrubs SH2	65.0	-173.1	152.0	3.8	155.8	4.2	0.0	-13.1	-	-13.1	4.6
Subtotal	1623.8	-5,028.4	3,577.5	228.6	3,806.1	166.8	64.7	-990.8	213.7	-777.1	168.8
2010–2019 land-atmosphere CO <sub>2</sub> fluxes per land cover type											
Forest FOR <sup>c</sup>	725.2	-2905.0	1912.4	204.8	2117.2	166.5	64.0	-557.3	20.7	-536.6	128.4
Shrub forest SH1	66.8	-90.1	76.2	2.5	78.7	2.6		-8.8	1.2	-7.6	2.5
Disturbed forest DSF	45.6	-84.0	131.8	15.7	147.5	5.7	-2.5	+66.7		+66.7	25.0
Sparse forests SPF	68.8	-140.0	125.1	2.0	127.1	3.6		-9.3	0.5	-8.8	3.3
Croplands CRO	86.6	-468.7	307.9	-	307.9	0.3	9.9	-150.6	141.0	-9.6	6.9
Meadows HFP	124.6	-473.5	328.9	2.8	331.5	1.1		-140.7	58.2	-82.5	21.6
Abandoned agriculture ABL	29.9	-149.5	103.2	-	103.2	1.6		-44.7	1.4	-43.3	12.5
Peat PEL	141.9	353.1	299.1	3.8	302.9	13.9	1.4	-34.9	1.0	-33.9	11.2
Tundra GST	272.8	461.7	405.8	4.1	409.9	4.4		-47.4	2.1	-45.3	14.5
Other Shrubs SH2	61.6	187.8	170.4	3.8	174.2	2.1		-11.5	-	-11.5	4.0
Subtotal	1623.8	-5,313.1	3,860.8	239.5	4,100.3	201.8	72.8	-938.5	226.1	-712.4	135.3

<sup>a</sup>Abbreviations of land classes: FOR—Forest (MFFS using the ILIS-LEA classification (see text). SH1—Shrubs growing in harsh growing conditions and considered by the Russian national definition as areas covered by forest. DSF—Disturbed forests (unregenerated forest areas ≤10 years after stand replacing disturbances—burnt areas, stands are killed by insects and pathogens etc.), relative stocking RS < 0.10. SPF—Sparse forests not counted by the Russian definition as forest, but counted in the FAO definition, relative stocking 0.10 ≤ RS ≤ 0.24. CRO—Cropland HFP—Meadow lands, including hayfields, pasture and zonal steppe, recognized by remote sensing. ABL—Abandoned former arable lands. PEL—Peat wetlands with depths of peat level >0.3 m. GST—Treeless land of zonal and mountain tundra, with mosses, lichens, and grasses. SH2—Other shrubs in different zones, except SH1. <sup>b</sup>Main vertical fluxes per land cover type: NPP—Net Primary Production (here -1\*NPP < 0 for C uptake from the atmosphere). SHR—Soil Heterotrophic Respiration (>0 for C release to the atmosphere). DEC—Decomposition of on-the-ground and aboveground CWD (>0 for C release to the atmosphere). DIS—Immediate carbon emission to the atmosphere due to disturbances, including fires and biogenic C emissions, during the year of disturbance events. EHR—Ecosystem heterotrophic respiration defined by Soil heterotrophic respiration (SHR) + DEC. CON—Carbon emission to the atmosphere by the consumption of plant products. LM—Land management (harvest of wood, wood products use, drained forests etc.). NBP—Net Biome Production defined as a total flux for large productive area for period ≥ 1 year, calculated as NBP = NPP-SHR-DEC-DIS-LM (here -1\*NBP is < 0 for C uptake from the atmosphere). NEE\*—part of NEE defined as Ciais et al., 2022 as sum of all non-fossil C fluxes exchanged with atmosphere NEE = NBP-CON for individual land classes; the total value of NEE includes the fluxes, assessed for the whole country is shown in Table 2. <sup>c</sup>In Table 1 FOR means forest of main forest forming tree species. To estimate fluxes corresponding to the Russian national definition of forest, the sum FOR + SH1 should be calculated. To estimate fluxes according to FAO definition, the FOR + DSF + SPF should be calculated.

233 to 264 g C m<sup>-2</sup> yr<sup>-1</sup> in 2010–2019. The increase in SHR reflects the higher loss of forests from stand-replacing disturbances during 2000–2019 mentioned above. Several additional processes also contribute to the trend of SHR: a higher severity of forest fires in 2010–2019, a concurrent higher level of forest natural restoration, and increased partial (not stand-replacing) mortality due to fire and other disturbances (insects, wind damage), as well as the incidence of drought affecting spruce-fir forests in different regions, for example, the loss of about 2 M m<sup>3</sup> of wood annually in the Russian Far East (Man'ko & Gladkova, 2001) or massive drying out the forests in the north of the European part of Russia on the area of over 4 M ha at the beginning of this century (Zhygunov et al., 2015).

**Table 2**

*Bottom-Up Volatile Organic Compound Emissions and C-CO<sub>2</sub> Lateral Fluxes of Russia's Terrestrial/Aquatic Ecosystems and From Geological Processes in 2000–2009 and 2010–2019 From ILIS LEA, and Other Data Sources, Reported for the Entire National Area (Tg C yr<sup>-1</sup>)*

Period	C-CO <sub>2</sub> fluxes from volatile organic compounds/lateral terrestrial transport/aquatic ecosystems/geological								Total NEE
	VOC	NT	WT	IW	DEP	WET	GEO	Subtotals of Table 1	
2000–2009	16.2 ± 5.7	-15.9 ± 5.9	81.0 ± 20.0	115.0 ± 35.0	-56.5 ± 17.0	-7.5 ± 2.5	7.0 ± 2.4	-777.1 ± 168.8	-636.8 ± 171.5
2010–2019	18.5 ± 6.5	-15.6 ± 5.5	81.0 ± 20.0	115.0 ± 35.0	-56.5 ± 17.0	-7.5 ± 2.5	7.0 ± 2.4	-712.4 ± 135.3	-569.5 ± 138.9

*Note.* VOC—Vertical non-CO<sub>2</sub> volatile organic C emissions. NT—Lateral C flux from net trade of crop and wood products (a negative value indicates a net export from Russia). WT—Lateral export of carbon to ocean by rivers and in the lithosphere. IW—Vertical carbon outgassing from inland waters. DEP—Net deposition of organic carbon from wet and dry deposition processes. WET—Atmosphere CO<sub>2</sub> uptake from chemical rock weathering. GEO—Geological (volcanic + diffuse) CO<sub>2</sub> emissions. NEE—Net Ecosystem Exchange obtained by adding NEE from terrestrial ecosystems in Table 1 and the fluxes reported in Table 2. Total land area 1709.7 M ha including 85.9 M ha for inland water and land without soil.

Decomposition of CWD (DEC) was estimated to be a net CO<sub>2</sub> emission to the atmosphere 229 Tg C yr<sup>-1</sup> for 2000–2009 and increased to 239 Tg C yr<sup>-1</sup> for 2010–2019 due to the large and constantly increasing amount of dead wood in forests produced by disturbances during the last two decades, as shown by the LEA model (Table 1).

Two major types of natural disturbances (DIS)—fire and impacts of dangerous insects and pathogens (estimated only for forests) - induce immediate carbon losses during the year of disturbances, with post-disturbance legacy emissions from soils being reported as part of SHR. Increasing the carbon fluxes due to lagged mortality caused by non-stand-replacing fires, which can occur up to 5 years later (with a peak from 1 to 4 years after fire dependent on forest type and fire intensity), were accounted for by matrices of fire severity depending on bioclimatic zone, dominant tree species and time of fire.

An intensification of fire regimes was observed in 2000–2021, accompanied by increasing the extent of burnt area, severity of burning, and frequency of mega-fires (Cho et al., 2025). During this period, 53.6 M ha of forests were killed by fire (Tyukavina et al., 2022); however, the total area covered by forest in Russia decreased by only ~10 M ha since above 20 M ha of previously destroyed forests were restored naturally during the same period. The unprecedented series of severe fires of 2019–2021 in the Russian Far East devastated large areas of primary forests, destroyed the raw material base of the forest industry, and substantially increased the amount of black carbon in the atmosphere and its deposition on snow (Cho et al., 2025; Webb et al., 2024).

The recent estimates of wildfire areas in Russia are very different. Clelland et al. (2024) examined burnt areas in two large Russian regions for 2006–2016. Using 10 remote sensing products (CABAM; SRBA; Fire CCILT11; GFED4s; MCD64A1; FireCC151; ABBA; method based on assessing the perimeter of fire (Talucci et al., 2022); GFED5; and MODIS Active Fires) at 775 M ha in tundra and taiga, they obtained a mean burnt area 3.67 (min 1.70, max 6.77) M ha yr<sup>-1</sup>. For the region of southern taiga (total area 270 M ha, seven RS products, without SRBA, ABBA, and Talucci et al. (2022) from the above list), the burned area was 11.2 (min 5.5, max 22.7) M ha yr<sup>-1</sup>. Note that the estimate of the area by GFED5 exceeded that of MODIS by more than 2.5 times in the northern region and over 4 times in the southern.

The composition of the combustion products depends on the type of fire (i.e., superficial ground; ground steady; crown; and peat fires), the intensity of combustion, the ratio of the flame phase and the smoldering phase. In our study, the mean annual carbon flux emitted by fire in 2000–2009 was 110.8 Tg C yr<sup>-1</sup>, with CO<sub>2</sub> emissions representing 106.3 Tg yr<sup>-1</sup> and the rest being CH<sub>4</sub> and black carbon. Most of these emissions (82%) resulted from forest fires, with stand-replacing forest fires accounting for 1.73 M ha yr<sup>-1</sup>. During 2010–2019, the mean annual carbon flux from fuel combustion was 135.5 Tg C yr<sup>-1</sup>, with 80% originating from forests. Of this, 126.9 Tg C yr<sup>-1</sup> was released as CO<sub>2</sub>. Stand-replacing fires covered a significantly larger area (3.36 M ha yr<sup>-1</sup>) compared to the previous decade. The inter-annual variation in burned areas across all vegetation types ranged from 3 to over 20 M ha yr<sup>-1</sup> with the multi-year average for forest fires reaching 8–10 M ha annually over the past two decades. The inter-annual variability (IAV) was basically defined by mega-fires which occurred in 2003, 2006, 2008 and 2009 during the first decade and in 2010, 2012, 2014 and 2019 during the second decade. The latter unprecedented series of catastrophic fires occurred in 2020–2021. The severity of fires increased during the period 2000–2019 (Zheng et al., 2021). More details on fire are found in Text S1 in Supporting Information S1.

Emissions from biotic disturbances in forest ecosystems were estimated by LEA based on the method from Shvidenko et al. (2010a, 2010b), and were found to be about half of the emissions from fire (56.0 Tg C yr<sup>-1</sup> in 2000–2009 and 66.3 Tg C yr<sup>-1</sup> in 2010–2019). The method is based on the assessment of the sustainability of forest ecosystems as a function of disturbances and unfavorable weather. Some studies estimated the overall insects' damage to be nearly as great as that caused by fire (Isaev, 1997). Official data on areas affected by outbreaks of insects and pathogens were reported by the Russian Federal Service to be about 3.5 M ha annually in 2000–2009, with an increase to 4.9 M ha yr<sup>-1</sup> in 2010–2019. It is likely that all estimates of disturbances based on official statistics are underestimated.

The increasing frequency of drought-induced mortality waves in dark coniferous forests results from the complex interaction between global change and boreal forest processes at the landscape scale and has been observed on many millions of hectares in different regions of the country (Man'ko & Gladkova, 2001; Zhygunov et al., 2015). Our estimates of damage from insects and pathogens likely underestimate the actual biogenic emissions by about 15%, due to insufficient knowledge of important processes such as the spread of stem and root rot and the impact of alien pests.

Summarizing, fires and insect outbreaks caused a total DIS emission of 166.8 Tg C yr<sup>-1</sup> in 2000–2009. Of this, wildfire contributed 112.0 Tg C yr<sup>-1</sup>, with 82% occurring on forest land, while biotic disturbances accounted for 54.8 Tg C yr<sup>-1</sup>. In 2010–2019, the disturbance regimes were more severe, and the resulting immediate DIS carbon emissions were 201.8 Tg C yr<sup>-1</sup> including 135.5 Tg C yr<sup>-1</sup> from wildfires (82% on forest land) and 66.3 Tg C yr<sup>-1</sup> from biotic disturbances (Table 1).

The estimation of GHG emissions due to land management (LM) is challenging for Russia due to the lack of required information. Here we consider the major recognized fluxes related to LM impact on ecosystems. These LM fluxes represent a mean net annual carbon emission of 64.7 and 72.8 Tg C yr<sup>-1</sup> in 2000–2009 and 2010–2019, respectively (Table 1), mostly due to increasing harvest and use of wood and wood products. We also accounted in the LEA model for LM emissions from drained forest land and cultivation of organic arable lands, as well as for the impacts of protective forests and shelter belts in agriculture and of peat mining and use.

In the LEA results for 2000–2009, the removal of wood by harvest was 47.5 Tg C yr<sup>-1</sup> plus the flux of 8.7 Tg C yr<sup>-1</sup> of additional felling emissions from logged areas due to decomposition of residues and damage to soil, giving a total amount of 56.2 Tg C yr<sup>-1</sup>. The removed wood was divided into four carbon pools in the LEA system: (a) long-lived products (10.7 Tg C yr<sup>-1</sup>), (b) net exports from the country (17.8 Tg C yr<sup>-1</sup>), (c) fuel wood (5.4 Tg C yr<sup>-1</sup>), and (d) wood residuals (13.6 Tg C yr<sup>-1</sup>). We assumed that two-thirds of the wood residuals were burned, and one-third was naturally decomposed into waste. Thus, the direct emission to the atmosphere is estimated at 8.6 Tg C yr<sup>-1</sup>, and the remaining 5.0 Tg C yr<sup>-1</sup> increased the waste pool. We estimated a flux of 6.8 Tg C yr<sup>-1</sup> from the accumulation of previous waste from wood processing enterprises in landfills and burial sites, and an emission to the atmosphere of 17.8 Tg C yr<sup>-1</sup> due to decomposition of accumulated long-lived wood products. The total annual flux from the wood products sector was 56.2 Tg C yr<sup>-1</sup> (part of the LM flux in Table 1). Using the same calculation method in the LEA model, the flux due to removal of wood due to harvest was 54.0 Tg C yr<sup>-1</sup> plus “site effects” of 9.8 Tg C yr<sup>-1</sup> in 2010–2019 was 64.0 Tg C yr<sup>-1</sup>, larger due to more harvested wood and produced waste, and changes in the size and structure of the net trade of wood products.

The previous estimate of harvest and use of wood was 48 Tg C yr<sup>-1</sup> for 2003–2008 (Shvidenko, Schepaschenko, & Maksyutov, 2010), while the estimate by Nilsson et al. (2003) for 1990 was 81 Tg C yr<sup>-1</sup>. Larger emissions from harvested wood products in the 1990s are explained by a higher amount of harvested wood and increased amount of waste during the logging and wood processing. Illegal harvest and consumption of wood by local populations were not accounted by official statistics and were considered in the LEA as a specific type of wood product consumption reported in the CON flux, but not as part of LM.

Consumption of plant products (CON) flux estimated by LEA represents the amount of plant products which is consumed or decomposed in the year of production, including human consumption of agricultural products, fodder for livestock; grazing of biomass by domestic and wild animals. We also included in CON illegal harvest and officially unaccounted fuel wood used by local population. The information was derived from available statistics, reports of NGOs, publications and diverse auxiliary data (e.g., from annually published statistical yearbook “Russia's Regions, 2006–2019” (RosStat-RF, 2019).

According to FAO, fuel wood accounts for 34.8% of all wood consumed in the country (FAO, 2005). There are 7.7 million houses with stove heating, of which 3.6 million are in rural areas (Gagarin et al., 2019). Assuming that only rural houses were heated with wood and assuming a minimum rate of 18 m<sup>3</sup> per household per year, the wood volume harvested and consumed by local populations is around 65 M m<sup>3</sup> yr<sup>-1</sup>. According to official statistics, less than 30% of this wood is harvested legally. National (Gagarin et al., 2019; Kuzmichev et al., 2018) and international (Kleinschmit, 2016) analyses estimate illegal logging in Russia between 25% and 35% of the officially reported amount of harvested wood, that is 50–80 M m<sup>3</sup> yr<sup>-1</sup>. Taking into account a wide spectrum of categories of “illegal harvest” (Vaschuk & Shvidenko, 2006) we conservatively estimated that the local illegal harvest and consumption of fuel wood was 22.4 Tg C yr<sup>-1</sup> in 2000–2009 (10.5 Tg C yr<sup>-1</sup> from illegal harvest + 11.9 Tg C yr<sup>-1</sup> from local consumption) and decreased to 20.7 Tg C yr<sup>-1</sup> in 2010–2019 (11.0 Tg C yr<sup>-1</sup> and +9.7 Tg C yr<sup>-1</sup> respectively). These fluxes are part of the CO<sub>2</sub> flux in Table 1, assuming that this wood was burned in the year of harvesting. Overall, this additional harvest adds around one-third to the emissions computed from official harvest statistics.

Fluxes due to the massive abandonment of arable land over 1990–2007 are considered separately in Table 1 (Abandoned Agriculture, ABL). The impact of diverse and fast changing processes on abandoned arable lands on C storage includes the encroachment of trees and shrubs on around 20 M ha by 2007, with a substantial decrease by 2019. The abandonment of arable land to other land-cover categories is considered as a separate category in Table 1 and Text S1 in Supporting Information S1.

### 3.4. LEA for Carbon Fluxes of Tundra and Abandoned Arable Lands

Russia's vast tundra natural zone accounts for 32% to 45% of the world's tundra, depending on definitions. According to Russian estimates, the tundra area is about 2.8 M km<sup>2</sup> (Karelin & Zamolodchikov, 2008; Nilsson et al., 2000). This biome plays a critical yet uncertain role in GHG dynamics due to its extensive territory and significant heterogeneity. Various studies estimated the circumpolar tundra's carbon dioxide (CO<sub>2</sub>) flux in previous decades between −10 and 110 Tg CO<sub>2</sub>-C yr<sup>-1</sup>, the large range reflecting the complexity and rapid environmental changes occurring within these ecosystems, such as permafrost thaw, altered growing seasons, increased productivity, and intensification of disturbances (Karelin & Zamolodchikov, 2008; S. M. Ludwig et al., 2023; Virkkala et al., 2021, 2024). Ramage et al. (2024), based on results from 1000 sites, reported C-CO<sub>2</sub> flux from natural sources in the northern permafrost region for 2000–2020. Using bottom-up methods, they estimated fluxes of −29 (−705, 455), while the top-down approach gave −587 (−862, −312) Tg CO<sub>2</sub>-C yr<sup>-1</sup>. Undisturbed tundra ecosystems were a net sink of −340 (−836, 156) Tg CO<sub>2</sub>-C yr<sup>-1</sup>; however, emissions from inland waters (IW) and fire made the net CO<sub>2</sub> budget of the tundra region neutral, within large uncertainties. Note that all types of permafrost in Russia comprise about 87% of the total permafrost area in the Northern hemisphere.

Long-term measurements from 1993 to 2022 across 69 Russian tundra landscape units provided data for regression models estimating ecosystem respiration (TER) and GPP (Karelin et al., 2020; Zamolodchikov & Karelin, 2001). The results showed that tundra NEE shifted from a carbon sink in the late 20th century to a source in the 2000s, coinciding with increases in both GPP and TER. Winter emissions, often underestimated in models, significantly influence annual CO<sub>2</sub> fluxes (Belshe et al., 2013; Commane et al., 2017).

Recent studies highlight the tundra's response to climate variability, with increasing area and growth intensity of shrubs and “greening” due to rising temperatures and permafrost degradation (Tishkov et al., 2020; Titkova & Vinogradova, 2019). It was also reported that a substantial increase in forest productivity occurred after stand-replacing fire on permafrost (Sedykh, 2009), while tundra affected by fire showed 1.5–2.5 times lower soil CO<sub>2</sub> emissions and primary production compared to the pre-fire state, even 20–26 years after burning (Zamolodchikov et al., 1998). “Browning” has also been detected by satellites in areas affected by bog expansion and anthropogenic disturbances. Despite these changes, in our estimates with the LEA model, the Russian tundra remained close to CO<sub>2</sub> neutrality, with fluctuations driven by annual climate anomalies. This fragile equilibrium suggests that any gains in vegetative productivity might not fully offset increases in winter respiration, especially in the southern and typical tundra subzones (Anisimov et al., 2015). In contrast, a comprehensive meta-analysis across the circumpolar belt suggested a modest net CO<sub>2</sub> sink of around −40 Tg C yr<sup>-1</sup> for Russia's tundra (Bloom et al., 2016; López-Blanco et al., 2019). During the second half of the 2010s, none of the seven EC stations in the Russian tundra indicated a carbon source. This includes the four stations measuring winter respiration, where the difference between the growing season and annual fluxes was not large. The average annual CO<sub>2</sub> sink in the



Russian tundra measured by EC gives a net sink of  $-40$  to  $50 \text{ g C m}^{-2} \text{ yr}^{-1}$ , consistent with Bloom et al. (2016) and López-Blanco et al. (2019) but higher than in the LEA results.

The dynamics of ice wedge degradation/stabilization can cause significant changes in local  $\text{CO}_2$  and  $\text{CH}_4$  fluxes over time. Measurements near Prudhoe Bay, Alaska, combined with repeat imagery analysis to estimate seasonal landscape-level C flux response to geomorphic change showed a net change of  $\text{CO}_2$  and  $\text{CH}_4$  emissions over 69 years of  $-25\%$  and  $+42\%$ , respectively, resulting in a 14% increase in seasonal  $\text{CO}_2$ -eq. emissions (Wickland et al., 2020). For the large and rather homogeneous larch forests growing on continuous permafrost in central Yakutia, four different atmospheric inversions (not considered above) reported net accumulated carbon (sink) in warm months (JJA) of  $-224 \text{ g C m}^{-2} \text{ yr}^{-1}$ , eight biogeochemical models a sink of  $-88 \text{ g C m}^{-2} \text{ yr}^{-1}$  ( $-61\%$ ), two data-driven models a sink of  $-102 \text{ g C m}^{-2} \text{ yr}^{-1}$  ( $-54\%$ ), and EC measurements—a sink of  $-192 \text{ g C m}^{-2} \text{ yr}^{-1}$  ( $-14\%$ ) (Takata et al., 2017).

DGVMs used in combination with atmospheric transport models show the Arctic and boreal regions to be an annual net carbon sink of  $-0.42 \text{ Pg C-CO}_2 \text{ yr}^{-1}$  averaged over the past 40 years (Bruhwiler et al., 2021). Arctic regions ( $60$ – $90^\circ\text{N}$ ) were responsible for almost one-third of this sink ( $-0.13 \text{ Pg C-CO}_2 \text{ yr}^{-1}$ ) and remained relatively consistent over time, whereas the boreal region ( $50$ – $60^\circ\text{N}$ ) has gradually increased its carbon sink strength. Regional atmospheric measurement campaigns with aircraft provide data on local influences (Parazoo et al., 2016). A comprehensive 3-year study found the tundra region of Alaska to be a consistent net carbon source, while the boreal region of Alaska was either carbon neutral or a  $\text{CO}_2$  sink, depending on the year (Commane et al., 2017). Over the course of 3 years, the entire Alaska region was estimated to be a net carbon source of  $0.025 \text{ Pg C-CO}_2 \text{ yr}^{-1}$ . Extrapolating Alaska's study area ( $1.6 \text{ M km}^2$ ) to the entire circumpolar permafrost soil area ( $17.8 \text{ M km}^2$ ) suggests a net carbon source of approximately  $0.3 \text{ Pg C-CO}_2 \text{ yr}^{-1}$ .

The above estimates, along with other publications, come with high uncertainty due to the synthesis of disparate studies and difficulties for upscaling site measurements (Virkkala et al., 2021). Overall, the tundra's role in global carbon cycles continues to be a critical source of uncertainty emphasizing the need for more targeted and extensive monitoring to better understand the response of these dynamic ecosystems to ongoing climatic changes. Based on available information on local fluxes and areas covered by tundra, we concluded that the  $\text{CO}_2$  exchange for undisturbed Russian tundra changed from a small source of  $1.1 \text{ Tg C yr}^{-1}$  for 2000–2009 to a modest sink of  $-47.4 \text{ Tg C yr}^{-1}$  for 2010–2019.

Table 1 contains estimates of  $\text{CO}_2$  fluxes using the flux-based method for agricultural land. For comparison, Text S1 and Table S2 in Supporting Information S1 present aggregated data, basically calculated based on IPCC methodology—the most detailed information to be found on the topic.

Various sources estimated the abandonment area of Russia's croplands in 1990–2007, ranging from 45 to 49 M ha (Kurganova et al., 2015) with  $\sim 39 \text{ M ha}$  abandoned in 1990–2003 (Figure S4 in Supporting Information S1), to 21.6 M ha in 1990–2002 in the official data from (Romanovskaya, 2006). The area of abandoned land remained stable for the decade 2000–2009, but in 2010–2019, partial plowing of abandoned and fallow lands began, reaching 5.6 M ha during the decade. This increased the total area of arable land from 83.1 to 88.7 M ha by the end of 2010s (see Text S2 and Figure S3–S5 in Supporting Information S1 for details).

The process of natural transformation of abandoned arable lands varied by bioclimatic zone. Trees and shrubs encroached in the north and natural grasslands replaced croplands in the south. Around 2010, the forest and shrub cover on abandoned land was assessed at  $\sim 20.0 \text{ M ha}$  (Shvidenko et al., 2010a, 2010b). However, by 2019 this area had decreased to 17.4 M ha, basically due to the lack of management, legislation that prohibited transformation of croplands to other land uses, natural disturbances (mostly fire), and partial plowing. Uncertainties in these estimates are significant. In our study, regenerated forests on abandoned arable land were included in “forest” category, and the rest (recovered as zonal grassland) was designated as “abandoned land.”

During 2000–2019, agricultural land was classified as cropland ( $85$ – $87 \text{ M ha}$ ), meadow land, mostly pasture and hayfields (around  $120$ – $125 \text{ M ha}$ ), fallow lands and zonal steppe areas of the middle latitudes ( $45$ – $50 \text{ M ha}$ ). Starting from the middle of the 2010s, a substantial area of previously abandoned agricultural land is transferred to fodder crop lands that lead to carbon loss. The NPP of croplands reported in Table 1 was calculated based on the estimates of the amount of live biomass produced, reported in published regional assessments. NPP calculated in our study was close to independent estimates for crops by Kudeyarov (2018) and on steppe grasslands by Kurganova et al. (2019).

### 3.5. Biomass and Soil Carbon Stocks and Stocks Changes

Published estimates of biomass dynamics of forests (Bartalev & Stytsenko, 2021; Filipchuk et al., 2023; Shvidenko et al., 2000, 2010a, 2010b; Shvidenko & Schepaschenko, 2014) are difficult to compare because they used different definitions of forest, and most of them do not include estimates of dead woody roots, Coarse Root Debris (CRD) as part of CWD. In our study, both CWD and CRD were defined according to the widely accepted definition (Yan et al., 2006). The mass of CRD of forest ecosystems was assessed based on the input of organic matter (amount of coarse dead roots after fire and biogenic disturbances, harvest, and natural mortality in forests) and the output due to decomposition of the entire mass of below ground wood up to its state when the residual mass of the roots reaches 10%–15% of the original amount. The process of decomposition of CRD lasts 30–80 years with a decay constant 0.020–0.034 dependent on geographical location and landscape specifics (Tuomi et al., 2011; Yatskov et al., 2003) and was considered part of SHR in Table 1.

Pan et al. (2024) reported the dynamics of forest biomass for the last three decades using the FAO definition of forest (840 M ha in Russia by 2020). In this study, we clarified the indicators that are most uncertain in estimating biomass (required by FAO definition of forest) for forest land categories that are not considered forest in the Russian definition. These corrections change the findings of Pan et al. (2024) by several percentage. For 2000, 2010, and 2020, we estimated live forest biomass stocks to be 36.4, 38.6, and 39.1 Pg C, respectively, and CWD stocks (above ground and below ground) to be 12.2 (8.3 + 3.9), 13.0 (8.8 + 4.2) and 14.2 (9.7 + 4.5) Pg C. Thus, the total forest biomass, according to the FAO definition (without soil litter), was 48.6, 51.6, and 53.3 Pg C in 2000, 2010 and 2020, respectively. The high values of CWD stocks result from the widespread area and severity of disturbances over the last two decades. Our estimate of the ratio of the total CWD to live biomass at 36.3% in Russian forests is essentially the same as that reported for managed forests of Canada at 36.3% (both estimates for 2020, (Pan et al., 2024)).

The carbon increment in live forest biomass was  $\sim 220 \text{ Tg C yr}^{-1}$  in 2000–2009 and dropped to  $\sim 40 \text{ Tg C yr}^{-1}$  in 2010–2019, but there was a parallel increase in the change of CWD from 80 to 120  $\text{Tg C yr}^{-1}$  for the same periods (Pan et al., 2024). However, under the increase in forest LB in Europe ( $\sim 70 \text{ Tg C yr}^{-1}$ ), the change in LB in the Asian part was about  $-20 \text{ Tg C yr}^{-1}$ . Such a decline in LB has never before been observed in Russian forest inventories.

The 1<sup>st</sup> cycle of the State Forest Inventory for all forestland (similar, but not exactly to the same as the FAO definition) of the country (the area of 899.5 M ha in 2020), gives a total live biomass stock in forestland of  $46.9 \pm 0.4 \text{ Pg C}$  by the end of the SFI 1st cycle (Filipchuk et al., 2023). This number corresponds to a Growing Stock Volume (GSV) of 113.1 billion  $\text{m}^3$ , higher than our GSV estimate of 101.7 billion  $\text{m}^3$  from the LEA model. Some remote-sensing based results show larger differences. For example, Xu et al. (2021) assumed a Russian forest area of 754.0 M ha and a non-forest woody area of 258.0 M ha, and estimated that the country-level total live biomass stock increased from 2000 to 2020 from 53.33 to 54.56 Pg C, with an annual gross loss of  $362.3 \text{ Tg C yr}^{-1}$ , and a gain of  $407.2 \text{ Tg C yr}^{-1}$ , giving an average net C sink in biomass of  $44.9 \text{ Tg C yr}^{-1}$ . This carbon accumulation rate in biomass is only one-third of the LEA results ( $135 \text{ Tg C yr}^{-1}$ ). Such differences may be explained by the different definitions of forest, the categories of forest land included in the account, and differences in methodology. The higher level of disturbances and unfavorable climate conditions, particularly in Asian Russia in 2010–2019, produced a close to negative rate of forest live biomass accumulation, while the total forest biomass remained a net carbon sink due to the increase in the amount of CWD.

The total live biomass carbon stock of Russia's non-forest vegetation was estimated at 7.1 Pg C for 2000, 7.6 Pg C for 2010 and 7.8 Pg C for 2020 (Nilsson et al., 2000; Shvidenko et al., 2010a, 2010b, 2020), giving a total vegetation live biomass for the above dates of 43.5, 46.2, and 46.7 Tg C, respectively. Adding CWD for forests, the total biomass of vegetation ecosystems in Russia was estimated at 55.7 Pg C in 2000, 59.2 Pg C in 2010, and 59.6 Pg C in 2020.

Soil organic carbon (SOC) dynamics are limited in the LEA carbon accounting model at the country scale due to problems with large uncertainties. The reported estimates of SOC stocks in Russia were based on a soil map at a scale 1:2.5 M and a database of typical soil profiles. A complete regular inventory of SOC in Russia has never been conducted. An estimate of the total stock of SOC in Russia including the litter and the 1-m-thick soil layer below (Figure S6–S8 in Supporting Information S1) is 317.1 Pg C (averaging  $19.2 \text{ kg C m}^{-2}$ ) for the early 2010s (Schepaschenko et al., 2013). Forest ecosystems contain 46% of the total SOC and peatlands 20%. Litter

comprises 14.4 Pg C (averaging 0.90 kg C m<sup>-2</sup>), including 58% in forest and 25% in natural grasslands and shrublands.

Expert estimates of total Russia's SOC uncertainty range from 5% to 7% (10–20 Pg C), making it unsuitable for direct assessments of changes. In the LEA model, we provided an approximate estimate of SOC changes based on input and output of organic matter to the soil, resulting in an average accumulation rate of SOC in Russia's forests of 110 kg C ha<sup>-1</sup> yr<sup>-1</sup> with an uncertainty of around 35% (CI 0.9). This result is within the range of other assessments of SOC change by different models in Scandinavian countries (Ågren et al., 2008; Dalsgaard et al., 2016; de Wit et al., 2006; Liski et al., 2002; Rantakari et al., 2012; Strand et al., 2016). Earth System models support the existence of SOC accumulation in tundra and boreal zones. Eleven Earth System Model simulations used for CMIP5 (Todd-Brown et al., 2014) estimated SOC accumulation rates of 49 ± 59 kg C ha<sup>-1</sup> yr<sup>-1</sup> for Russia's tundra and 108 ± 267 kg C ha<sup>-1</sup> yr<sup>-1</sup> for taiga, without accounting for disturbances.

### 3.6. Other Vertical and Lateral Fluxes of Carbon (Methods Other Than LEA)

The primary source of information for the export and import of basic agricultural commodities used in this study is the Russian Statistical Yearbook (2022). The quantities of products, measured in physical units, were recalculated into dry matter and subsequently into carbon using conversion coefficients (Galkin, 2022; Roy et al., 2001). The import/export ratio changed substantially during the first two decades of this century, from more imports than exports in 2000–2009 (8.8 vs. 6.9 Tg C yr<sup>-1</sup>) to less imports than exports in 2010–2019 (9.6 vs. 15.6 Tg C yr<sup>-1</sup>) (Table 1). The driving forces behind this export growth were primarily from exported cereals, which experienced an increase of 180%, and vegetable oil, which increased by 300%. Since the uncertainty of these estimates is not reported, we used an expert estimate for both fluxes of 30%. Thus, the balance of the net flux of carbon in traded food products is +1.9 ± 0.8 Tg C yr<sup>-1</sup> in 2000–2009 (net import) and -6.0 ± 2.5 Tg C yr<sup>-1</sup> in 2010–2019 (net export).

Outgassing of CO<sub>2</sub> from Russia's IW (including the Caspian sea) was estimated by Lauerwald et al. (2023) at 782 ± 145 Tg CO<sub>2</sub>-eq. yr<sup>-1</sup> (213 ± 30 Tg C-CO<sub>2</sub> yr<sup>-1</sup>). The analysis by Romanovskaya (2023) of inland freshwater data (without the Caspian sea representing 39 M ha) was close to the lower boundary of Lauerwald et al. (2023) although both estimates are poorly constrained by data. As a most likely estimate of the IW flux, we used the first quartile of the Lauerwald et al. (2023) distribution, giving an emission of 115 Tg C yr<sup>-1</sup> assumed to be constant over the last two decades (Table 2).

About 30% of global OC emissions to the atmosphere are emitted as CO, VOCs, and black carbon (Hallquist et al., 2009), part of which is transformed into organic aerosols and removed from the atmosphere through deposition processes (Goldstein & Galbally, 2007). Deposition is the major pathway for the removal of OC from the atmosphere and represents an input to the land. Transfers of OC from the atmosphere to land occur as wet deposition (~60% of the total through precipitation) and as dry deposition (~40% through surface settling of particles (POC) and dissolved organic carbon (DOC), TOC = DOC + POC). In precipitation, most of the carbon is organic (76%–96%) (Fahey et al., 2005; Pan et al., 2010). We used the average aggregated continental estimates (Iavorivska et al., 2016; Noskova et al., 2022) of carbon concentration in precipitation (2.60 ± 2.4 and 2.65 ± 9.9 mg L<sup>-1</sup>) and deposition rates (18 ± 13 and 19 ± 4 kg C ha<sup>-1</sup> yr<sup>-1</sup>) for the European and Asian parts of Russia, respectively. For the entire territory of Russia, this gives a net annual carbon deposition to land (DEP) of -56.5 Tg C yr<sup>-1</sup> (negative values in Table 2 indicate uptake from the atmosphere), composed of -24.5 Tg C yr<sup>-1</sup> from wet deposition and -32.0 Tg C yr<sup>-1</sup> from dry deposition. Uncertainty was estimated at 30% based on expert judgment.

Studies focusing on the impact of climate change and other factors on river runoff across Russian territories from 1976 to around the 2020s reveal a complex pattern of changes. While there is a slight increase in runoff from large northern rivers of about 7%–10%, this change is geographically diverse and not statistically significant for most large river basins. In contrast, river runoff in southern European Russia, particularly in arid regions such as the River Don and lower Volga basins, has decreased significantly by up to 40%–50% (Gelfan et al., 2021; Magritsky, 2022). Despite these regional variations, the average level of river flow across the country has remained relatively stable at about 4,260 km<sup>3</sup> yr<sup>-1</sup>, with no statistically significant trends observed nationally or within individual federal districts in 2000–2019 (Frolova et al., 2020; Rummyancev et al., 2021).

In terrestrial ecosystems, the flux of DOC from organic soil layers to mineral soil in non-permafrost and permafrost boreal terrains varies widely, ranging from 5 to 18 g C m<sup>-2</sup> yr<sup>-1</sup> in forests, 7–12 g C m<sup>-2</sup> yr<sup>-1</sup> in peatlands, and 1.2–2.2 g C m<sup>-2</sup> yr<sup>-1</sup> in various types of tundra (McGuire et al., 2010; Romankevich & Vetrov, 2001). The variability in annual DOC flux is largely driven by annual precipitation patterns. Additionally, wildfires significantly reduce DOC flux by combusting ground vegetation and organic soil layers, resulting in a 40%–50% reduction of DOC in pine forests and 40%–70% in larch forests. In temperate European forests, grasslands, and peatlands, these fluxes are estimated at around  $7 \pm 3$  g C m<sup>-2</sup> yr<sup>-1</sup> (Schulze et al., 2010).

DOC concentrations in inland runoff are notably high in organic rich soils of boreal biomes with discontinuous permafrost. Concentrations in leachates from the soil O horizon and/or peat layers range from 20 to 180 mg C l<sup>-1</sup>, with the highest values observed in needleleaf forests of the northern and middle taiga zones (Gordeev et al., 2024). However, as these waters enter first-order streams, DOC concentrations drop significantly to 20–50 mg C l<sup>-1</sup>, indicating that more than 50% of the produced DOC is retained within subsoils. The most dramatic decrease in DOC concentrations occurs in higher-order rivers, where it eventually drops to 5–10 mg C l<sup>-1</sup> in major rivers. Conversely, dissolved inorganic carbon (DIC) concentrations tend to increase with stream order, reflecting increased contributions from groundwater inputs. The lowest average annual DOC concentrations, around 3.0 mg C l<sup>-1</sup>, are typically found in rivers of the tundra, mountainous regions, and steppes, while DIC concentrations in these regions can peak at up to 50 mg C l<sup>-1</sup>, as observed in rivers like the Don.

Total estimates of riverine carbon export in all forms (DIC, DOC, and particulate OC - POC) from Russian territories to surrounding seas are relatively few. A study by Dolman et al. (2012) estimated a total export of 56.4 Tg C yr<sup>-1</sup> for the period 2000–2009, similar to an earlier estimate of  $61 \pm 31$  Tg C yr<sup>-1</sup> by Shvidenko et al. (2010a, 2010b). For the 2000s, exports to Russia's Arctic seas were estimated between 23.5 and 28.4 Tg C yr<sup>-1</sup> for DOC + POC and 33.8 Tg C yr<sup>-1</sup> for DIC (Romankevich & Vetrov, 2001). These studies highlight the significance of dissolved carbon in understanding the broader impacts of climate change and other environmental drivers on hydrological and carbon cycles in Russian river systems.

In Table 1, we used the estimate for the period of 2000–2019 of the carbon flux to the oceans of  $61 \pm 30$  Tg C yr<sup>-1</sup> and  $20 \pm 10$  Tg C yr<sup>-1</sup> to the lithosphere (Shvidenko et al., 2010a, 2010b). The increase in alkalinity in large Siberian rivers (Drake et al., 2018) noted in recent assessments is not taken into account in the DIC transport assessments due to the lack of data for the entire country. The estimate of flux to the lithosphere should be considered as a conservative expert estimate.

Forest ecosystems of the boreal and mid-latitude zones are the main source of Non-methane Biogenic Volatile Organic Compounds (BVOCs) in the northern hemisphere. The largest emissions were observed in the southern part of the boreal zone, declining toward the north (Tarvainen, 2008). On average, emissions of BVOC are around 1%–2% of NPP (Kesselmeier et al., 2002). Empirical data on BVOC emissions in Russia are limited. For the European part of Russia (the state of land cover at early 1990s), Simpson et al. (1995, 1999) estimated an emission of BVOC at 5.60 Tg yr<sup>-1</sup>, mainly by forests (5.13 Tg BVOC yr<sup>-1</sup>), including 1.72 Tg C from isoprene, 2.06 Tg C from monoterpenes and 1.35 Tg other VOC. Other land classes contributed only 8.4% of total yearly emissions. Isidorov (1994) provided a detailed assessment of BVOC emissions for forests in the European part of Russia based on forest inventory data for 1988, with total emission of the BVOC of  $3.3 \pm 1.2$  Tg BVOC. Taking into account the dynamics of forests in European Russia and changes in the structure of live biomass of trees (Lapenis et al., 2005), a rough estimate for 2019 was around 5.58 Tg yr<sup>-1</sup>, and together with other land classes, 6.03 Tg BVOC yr<sup>-1</sup>. The latest estimate of BVOC emissions for the Russian forest fund land (~1080 M ha) was received as a function of biometric characteristic of forests, temperature and light intensity at 17.3 (13.6, 21.0) Tg BVOC (Isidorov, 2001), of which 61% was isoprene. Scaling up to all vegetated land in Russia and applying a conversion coefficient of 0.882 for isoprene and terpenoids to carbon gives a BVOC emission of  $16.2 \pm 5.7$  Tg C yr<sup>-1</sup> in 2000–2009, and  $18.5 \pm 6.5$  Tg C yr<sup>-1</sup> in 2010–2019. The uncertainty was estimated at 35% based on expert judgment.

Our emission rates seem consistent with those reported in Scandinavian countries. The average annual emission of BVOC at the end 1990s—early 2000s for all 3 Scandinavian countries and Russia normalized by the area of forest lands (Isidorov, 2001) are in the range of 1.8–2.9 g BVOC m<sup>-2</sup> yr<sup>-1</sup>, with Russia being at the lower limit of this range. Nevertheless, the above estimates for Russia should be taken with caution due to insufficient knowledge and the high dependence of emissions and their component structure on numerous factors (geographical location, landscape specifics, type of vegetation, predominant tree species and forest types in

forests, etc.). Regional and national inventories also reflect large diversity in the quantification of the BVOC emissions in the arctic-boreal region (ACIA, 2005; Tarvainen et al., 2007).

The review by Rinne et al. (2009) of seven emission models of BVOC in Finland showed a dominance of terpenoids (mostly monoterpenes, and about twice less isoprene and sesquiterpenes) with an average of about 0.66 Tg BVOC yr<sup>-1</sup>. A series of national emission estimates for Finland by Lindfors and Laurila (2000), Lindfors et al. (2000) and Tarvainen et al. (2007) synthesized empirical knowledge on BVOC emissions from the western Eurasian taiga. Their results indicate that the terpenoid emissions are dominated by monoterpenes, and isoprene represents 10%–15% of monoterpene emissions on a mass basis, while results for Russia differ substantially that could be explained by the dominance of large very cold territories.

CO<sub>2</sub> uptake due to chemical weathering was derived from the map of weathering CO<sub>2</sub> uptake (Xiong et al., 2022). The estimate of the corresponding flux for Russia's territory was estimated as −7.5 Tg C-CO<sub>2</sub> yr<sup>-1</sup> (Table 2, negative value means uptake by land). Aggregated Russian estimates of geological emissions of CO<sub>2</sub> (carbon degassing from the lithosphere including volcanic degassing and diffuse CO<sub>2</sub> emissions) have not been published. Based on fragmented measurements for the Kamchatka arc, the most probable CO<sub>2</sub> volcanic emissions for Russia do not exceed 2 Tg C-CO<sub>2</sub> yr<sup>-1</sup> (Inguaggiato et al., 2017; Taran et al., 2018). Based on data synthesis from (Mörner & Etiope, 2002; Olefeldt et al., 2021; Ramage et al., 2024), we estimated additional CO<sub>2</sub> emissions from the lithosphere in Russia at 5.0 Tg C-CO<sub>2</sub> yr<sup>-1</sup> that gives the total geological flux CO<sub>2</sub> to the atmosphere of 7.0 Tg C-CO<sub>2</sub> yr<sup>-1</sup> (see Table 2).

### 3.7. Bottom-Up Empirical Estimates of CH<sub>4</sub> Emissions From Natural Sources

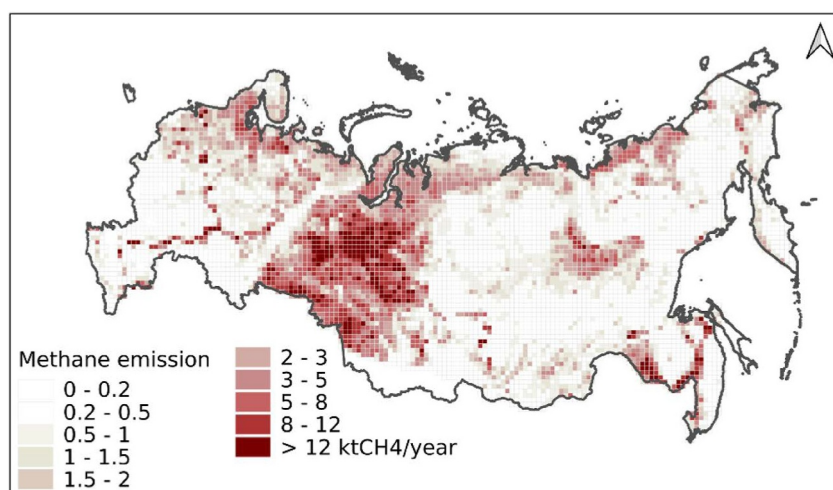
#### 3.7.1. Wetland Emissions

The natural sources of methane in Russia are diverse, such as wetlands, water-saturated soils, lakes, permafrost soils, and fires (Bazhin, 2000). Analyses for the entire permafrost zone (Hugelius et al., 2024; Ramage et al., 2024) include 10 detailed sources of methane emissions. In our study, we used intermedium classification due to the lack of information for Russia. According to forest inventory data, about 142 M ha of treeless bogs with a peat layer thicker than 30 cm are located on the territory of the Russian State Forest Fund—that is, within the area of 1146.3 M ha officially reported as land designated for forest growth (Filipchuk et al., 2022). Vompersky et al. (2005, 2011) estimated that the area of peat bogs thicker than 30 cm in Russia is 139 M ha and an additional area of 369 M ha is covered with shallower peat layers. In this study, we define peatland as areas with a peat depth more than 30 cm, as shallower peat soils are typically covered by other vegetation (forest, shrubland, etc.) and accounted for under other land cover types.

Assessment of wetland CH<sub>4</sub> emissions by bottom-up methods (Table S3 in Supporting Information S1) typically uses empirical regression to relate flux estimates to environmental factors (e.g., temperature, humidity, water table, substrate quality, etc.). Process models (inter alia Cao et al., 1998; Walter et al., 1996, 2001; Zhang et al., 2002) simulate CH<sub>4</sub> production, CH<sub>4</sub> oxidation, and CH<sub>4</sub> transport by plants (in some cases). However, these models give uncertain results at a regional level in Russian territories due to limited information for their parametrization and problems with accurate delineation of wetland areas. Empirical models specifically developed for Russian territories are rare, excluding the empirical “standard model” (Glagolev et al., 2012) which, within bioclimatic zones and for typical ecosystems, use the length of the active period, areas of wetland types, structure of micro landscapes, and specific flux densities for upscaling. Here we used the results from 12 of 15 available studies of methane fluxes from wetlands in Russian territories, excluding three clear outliers (Table S4 in Supporting Information S1). The mean of these bottom-up emissions was 11.3 ± 3.4 Tg CH<sub>4</sub> yr<sup>-1</sup> for 2000–2009 and 10.6 ± 2.7 Tg CH<sub>4</sub> yr<sup>-1</sup> for 2010–2019. The limited number of measurements and an incomplete description of methods likely result in larger uncertainties than calculated.

Another estimate of average CH<sub>4</sub> emissions for all wetland ecosystems of Russia during 2000–2019 was provided for this study by Terentieva et al. (2024). The map produced is based on multi-sensor Landsat composite, PALSAR radar images and extensive field data (20–30 measurements for each wetland types). The studied area included a total area of 174.0 M ha of wetlands and 42.6 M ha of open water. Estimated methane emissions amount to 11.4 Tg CH<sub>4</sub> yr<sup>-1</sup> from wetland and 2.54 Tg CH<sub>4</sub> yr<sup>-1</sup> from open water. In our study, the most likely estimates of emissions used were 11.5 ± 2.9 and 11.2 ± 2.6 Tg CH<sub>4</sub> yr<sup>-1</sup> in 2000–2009 and 2010–2019, respectively. The spatial distribution of emissions is shown in Figure 4.





**Figure 4.** Emissions of CH<sub>4</sub> from Russia's wetlands based on empirical upscaling of site flux measurements by Terentieva et al. (2024).

The recent availability of EC flux towers measuring CH<sub>4</sub> fluxes over wetlands (Delwiche et al., 2021) has enabled the production of machine-learning based estimates of upscaled fluxes by McNicol et al. (2023) and Yuan et al. (2024) (for northern wetlands). Both estimates use maps of flooded areas for wetlands and may thus ignore or underestimate emissions from bogs where the water table lies below the surface most of the year. The total wetland emissions in Russia for the last decade are estimated at 9.18 Tg CH<sub>4</sub> yr<sup>-1</sup> by McNicol et al. (2023) and at 9.85 Tg CH<sub>4</sub> yr<sup>-1</sup> by Yuan et al. (2024), that is, about 2 Tg CH<sub>4</sub> yr<sup>-1</sup> less than the two other estimates given above, possibly because of under-estimated bog emissions. Note that our estimates of wetland CH<sub>4</sub> emissions are only for undisturbed wetlands; therefore, we ignored reduced CH<sub>4</sub> emissions from peat drainage.

### 3.7.2. Tundra Emissions

Ground-based measurements of methane fluxes in the Russian tundra (excluding wetlands) are limited. During the last two decades, there has been a shift from chamber measurements to EC. The study by Hugelius et al. (2020) defined the area for global northern peatlands as  $3.7 \pm 0.5$  M km<sup>2</sup>. When calculated for the area of the Russian tundra from pan-Arctic or global estimates (Kirschke et al., 2013; McGuire et al., 2012; Zona et al., 2015), tundra emissions fall within a range of 1.2–4.2 Tg CH<sub>4</sub> yr<sup>-1</sup>. We used the average of these results;  $2.7 \pm 0.6$  Tg CH<sub>4</sub> yr<sup>-1</sup> for both decades. There is a lack of data for mountain tundra that is considered a sink of CH<sub>4</sub> due to its auto-morphic nature. Emissions from deep permafrost have been assessed globally to be small (Saunois et al., 2025) and were not counted in this study.

### 3.7.3. Methane Sink in Under-Saturated Soils

Information about methane consumption through methanotrophy in under-saturated soils is scarce. At the scale of large regions, the soil sink of CH<sub>4</sub> may play an important role in the global CH<sub>4</sub> budget. Misrepresentation of soil CH<sub>4</sub> sinks may introduce bias into the modeling of net CH<sub>4</sub> emissions. While wet tundra is a source of CH<sub>4</sub>, dry tundra can act as either a small sink or a small source of atmospheric CH<sub>4</sub> (R. K. Harris et al., 1993; Kuhn et al., 2021). Modeling CH<sub>4</sub> oxidation by soils and landfills can rely on direct measurements (Curry, 2007; Grosso et al., 2000; Nozhevnikova et al., 2003; Potter et al., 1996; Sabrekov et al., 2016) or inverse models (Saunois et al., 2020). In Russia, the CH<sub>4</sub> oxidation sink in soils has been assessed using a simple inventory approach based on the average CH<sub>4</sub> consumption rate measured for different biomes (Born et al., 1990), soil textures (Dörr et al., 1993), biome-soil texture combinations (Dutaur & Verchot, 2007), and soil types (Zelenev, 1996) (see Table S5 in Supporting Information S1). We estimated the total soil CH<sub>4</sub> sink in Russian soils using various modeling approaches (see method section in (Glagolev & Filippov, 2011), Table S5 in Supporting Information S1). The best-fitting model yielded an estimate of  $3.6 \pm 2.5$  Tg yr<sup>-1</sup>, while the average value from several available studies after excluding two outliers (min-max) and the model by Dutaur and Verchot (2007), was

$2.9 \pm 2.5 \text{ Tg yr}^{-1}$ . For our assessment, we used the average of these values, resulting in a sink estimate of  $3.2 \pm 2.5 \text{ Tg CH}_4 \text{ yr}^{-1}$  for the period 2000–2019.

### 3.7.4. Fire CH<sub>4</sub> Emissions

We used the emission factor for wildfire CH<sub>4</sub> emissions from Urbanski et al. (2008) and D'Andrea et al. (2010), applying a correction for emissions from organic soils following Hu et al. (2019). The average wildfire CH<sub>4</sub> emissions were estimated at  $1.2 \pm 0.4 \text{ Tg CH}_4 \text{ yr}^{-1}$  for 2000–2009 and  $1.5 \pm 0.5 \text{ Tg CH}_4 \text{ yr}^{-1}$  for 2010–2019.

### 3.7.5. Inland Waters Emissions

Analyzing available sources for CH<sub>4</sub> emissions from IW (outgassing), we estimated emissions of  $6 \text{ Tg CH}_4 \text{ yr}^{-1}$  from lakes (Johnson et al., 2022),  $0.8 \text{ Tg CH}_4 \text{ yr}^{-1}$  from reservoirs (Johnson et al., 2021), and  $1.9 \text{ Tg CH}_4 \text{ yr}^{-1}$  from rivers (Lauerwald et al., 2023). For all IW in Russia, this results in a total emission of  $8.7 \pm 3.6 \text{ Tg CH}_4 \text{ yr}^{-1}$ . Note that we considered reservoir emissions to be natural as in the latest global CH<sub>4</sub> budget study (Saunois et al., 2025).

### 3.7.6. Geological Emissions

Global geological emissions of CH<sub>4</sub> are from different sources (mud volcanoes, micro-interference due to diffuse emissions, underwater seeps, magma volcanoes with a global total of  $40\text{--}64 \text{ Tg CH}_4 \text{ yr}^{-1}$  (Etiope et al., 2008). The emissions from Russia were estimated from Etiope et al. (2019) at  $2.3 \text{ Tg CH}_4 \text{ yr}^{-1}$ .

### 3.7.7. Total Natural and Anthropogenic Emissions of CH<sub>4</sub>

The natural biogenic and wildfire CH<sub>4</sub> emissions from Russia were estimated at  $20.9 \pm 4.7 \text{ Tg CH}_4 \text{ yr}^{-1}$ , or  $564 \pm 323 \text{ Tg CO}_2\text{-eq. yr}^{-1}$ , and were assumed to remain the same for both decades. If we add geological CH<sub>4</sub> emissions from Etiope et al. (2019), we get a total natural CH<sub>4</sub> emission of  $23.2 \pm 5.4 \text{ Tg CH}_4 \text{ yr}^{-1}$  over the period 2000–2019 (Figure S10 in Supporting Information S1). In accordance with the last GHG inventory of Russia, anthropogenic CH<sub>4</sub> emissions without LULUCF (Land Use, Land-Use Change, and Forestry) averaged  $11.3 \pm 0.3 \text{ Tg CH}_4 \text{ yr}^{-1}$  for 2000–2009 and  $10.2 \pm 0.4 \text{ Tg CH}_4 \text{ yr}^{-1}$  for 2010–2019 (NIR, 2024). Anthropogenic emissions have been evaluated by (Saunois et al., 2020), Section 3) at  $19.3 \text{ Tg CH}_4 \text{ yr}^{-1}$  for 2000–2009 and  $19.8 \text{ Tg CH}_4 \text{ yr}^{-1}$  for 2008–2017. Adding natural and anthropogenic CH<sub>4</sub> emissions from Russia gives a total of  $42.5 \pm 9.8 \text{ Tg CH}_4 \text{ yr}^{-1}$  ( $1148 \pm 265 \text{ Tg CO}_2\text{-eq. yr}^{-1}$ ) and  $43.0 \pm 8.7 \text{ Tg CH}_4 \text{ yr}^{-1}$  ( $1161 \pm 235 \text{ Tg CO}_2\text{-eq. yr}^{-1}$ ).

Saunois et al. (2025) anthropogenic CH<sub>4</sub> emissions were estimated at  $23.5 \text{ Tg CH}_4 \text{ yr}^{-1}$  in 2010–2019 while the sectoral estimate in Saunois et al. (2020) was  $29.0 \pm 2.1 \text{ Tg CH}_4 \text{ yr}^{-1}$  ( $783 \pm 54 \text{ Tg CO}_2\text{-eq. yr}^{-1}$ ). The latter estimate includes fossil fuel emissions. For Russia, Bondur et al. (2022) reported bottom-up CH<sub>4</sub> emissions at  $36.8 \pm 8.7 \text{ Tg CH}_4 \text{ yr}^{-1}$ .

### 3.8. Bottom-Up Estimates of N<sub>2</sub>O Natural Emissions

Empirical data on terrestrial natural fluxes of N<sub>2</sub>O are limited in the Arctic zone (Voigt et al., 2020) and scarce for Russia's territory. It has conventionally been assumed that N<sub>2</sub>O emissions in permafrost regions are minimal. However, this assumption has been questioned by recent in situ studies, which have demonstrated that some geologic features in permafrost or other regional specific features may contribute to elevated emissions. Measurements conducted in various forest regions of Siberia on permafrost (Morishita et al., 2003, 2014; Nakano et al., 2004; Takakai et al., 2008) and in the Far East without permafrost (Morishita et al., 2006) revealed that forests may act as a small N<sub>2</sub>O sink. The N<sub>2</sub>O emissions were found to be negatively correlated with soil moisture and not correlated with soil temperature. These studies suggest that high soil moisture and low availability of mineral nitrogen can result in N<sub>2</sub>O uptake by soils through denitrification. Romanovskaya (2023), based on rather limited published field studies (Karelin et al., 2016; B. Ludwig et al., 2006; Repo et al., 2009) and unpublished results of measurement of Russian scientists, used a relatively simple regression model to estimate natural N<sub>2</sub>O emissions at  $0.22 \pm 0.13 \text{ Tg N}_2\text{O yr}^{-1}$  for the period of maximal warming (1980–2017). Another estimate was  $0.17 \pm 0.02 \text{ Tg N}_2\text{O yr}^{-1}$  for 2016 (Korotkov et al., 2023) for the 279 M ha tundra zone.

However, these studies, along with all in situ studies focused on permafrost N<sub>2</sub>O fluxes, used chambers to examine small areas (<50 m<sup>2</sup>). Most of the attempts to estimate the fluxes of this gas are model-based using the top-down approach. According to Schulze et al. (2009), for the Arctic zone of Europe, the value of the N<sub>2</sub>O balance was assumed to be near zero. Although permafrost-affected soils and tundra seem to be a near zero source of nitrous oxide, some hot spots in unvegetated peat and bare soil circles have high emission rates (Voigt et al., 2020). This suggests an underestimation of natural N<sub>2</sub>O emissions in the Arctic related to landforms and freezing and thawing of soils in winter (Voigt et al., 2020), which may also be true for all three GHGs.

Using the 1993–2019 average estimate for N<sub>2</sub>O emissions from permafrost soils from Voigt et al. (2020), we estimated an emission of 12.3 Tg CO<sub>2</sub>-eq. yr<sup>-1</sup> for the Russian tundra zone (279 M ha). Adding 11.6 Tg CO<sub>2</sub>-eq. yr<sup>-1</sup> emissions from IW (Lauerwald et al., 2023) brings the total natural N<sub>2</sub>O emission to 23.9 Tg CO<sub>2</sub>-eq. yr<sup>-1</sup>. Summarizing all available ground data for the Arctic on the N<sub>2</sub>O balance for the period 2004–2022 (Wilkerson et al., 2019) provided an estimate of  $17.9 \pm 5.8$  Tg C-CO<sub>2</sub>-eq. yr<sup>-1</sup> for the Russian tundra zone, which is comparable although a bit smaller than our estimate. Finally, we included fire as a small source of N<sub>2</sub>O emissions with an emission factor of 0.20–0.25 g N<sub>2</sub>O emissions per kg of consumed fuel, giving a total emission from fires of  $0.051 \pm 0.025$  Tg N<sub>2</sub>O yr<sup>-1</sup> in 2000–2009 and  $0.065 \pm 0.028$  Tg N<sub>2</sub>O yr<sup>-1</sup> in 2010–2019.

Based on this synthesis, the total natural N<sub>2</sub>O emission from Russia is estimated at  $0.33 \pm 0.17$  and  $0.34 \pm 0.16$  Tg N<sub>2</sub>O yr<sup>-1</sup> for 2000–2009 and 2010–2019, respectively. Empirical N<sub>2</sub>O bottom-up anthropogenic emissions measured for all of Russia are not available, and published values include data from a GHG inventory of Russia where anthropogenic N<sub>2</sub>O emissions without LULUCF are  $0.0189 \pm 0.006$  in 2000–2009 and  $0.207 \pm 0.012$  Tg N<sub>2</sub>O yr<sup>-1</sup> in 2010–2019 (NIR, 2024). Therefore, we used the EDGAR database (2023) for anthropogenic N<sub>2</sub>O emissions,  $0.216 \pm 0.008$  and  $0.245 \pm 0.012$  Tg N<sub>2</sub>O yr<sup>-1</sup> that gives a total N<sub>2</sub>O emissions  $0.55 \pm 0.17$  and  $0.58 \pm 0.17$  Tg N<sub>2</sub>O for 2000–2009 and 2010–2019, respectively.

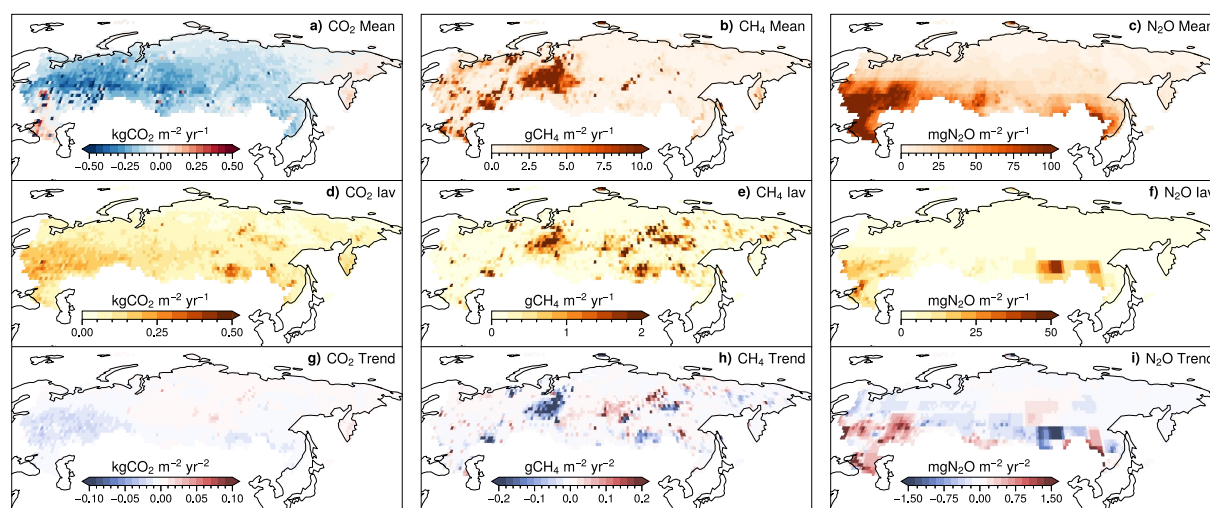
Overall, based on a bottom-up approach, natural Russia's ecosystems were a net sink of the three major GHG gases (CO<sub>2</sub>, CH<sub>4</sub>, and N<sub>2</sub>O) at  $-1618 \pm 645$  Tg CO<sub>2</sub>-eq. yr<sup>-1</sup> in 2000–2009 and  $-1357 \pm 532$  Tg CO<sub>2</sub>-eq. yr<sup>-1</sup> in 2010–2019. This flux includes: (a) C-CO<sub>2</sub> fluxes estimated as a net sink of  $-637 \pm 172$  and  $-570 \pm 139$  Tg C yr<sup>-1</sup> in 2000–2009 and 2010–2019, respectively; (b) CH<sub>4</sub> emissions from natural sources of  $23.2 \pm 5.4$  Tg CH<sub>4</sub> yr<sup>-1</sup> for 2000–2019; (c) N<sub>2</sub>O natural emissions of  $0.33 \pm 0.17$  and  $0.34 \pm 0.16$  Tg N<sub>2</sub>O yr<sup>-1</sup>, for two considered decades, respectively. For all GHGs, including natural and anthropogenic sources, terrestrial vegetation served as a net sink of  $-1032 \pm 682$  Tg CO<sub>2</sub>-eq. and  $-768 \pm 559$  Tg CO<sub>2</sub>-eq. for two decades.

### 3.9. Estimates From Global Vegetation (BU) and Inverse (TD) Models

#### 3.9.1. Spatial Distributions of 3 Gases Fluxes and Variability by TD Models

Figure 5 shows the spatial distribution of CO<sub>2</sub>, CH<sub>4</sub> and N<sub>2</sub>O fluxes across Russia by inverse models, presenting mean values, IAV and long-term trends. Spatial variability in these fluxes is influenced by land cover types such as taiga forests, tundra, wetlands, permafrost regions and agricultural land, as well as anthropogenic activities such as fossil fuel extraction and agriculture. The maps highlight the interplay between natural ecosystems and industrial development, particularly in regions such as Western and Eastern Siberia where oil and gas extraction is prominent.

The left-hand column in Figure 5 presents the mean CO<sub>2</sub> flux over the period 2000–2019, the IAV of annual CO<sub>2</sub> fluxes defined by the standard deviation of annual fluxes averaged from the six inversions, and the linear trend of CO<sub>2</sub> fluxes over the period 2000–2019. The inversions locate a CO<sub>2</sub> sink of stronger magnitude in European Russia and central Siberia, while the Russian Far East is a small source of CO<sub>2</sub> as tundra and permafrost regions in the north have lower CO<sub>2</sub> fluxes due to limited plant activity, shorter growing seasons and intensive wildfire. IAV is low over most of the Russian territory except in some regions of southern Siberia and European Russia, partly related to wildfire variations. Taiga regions show relatively higher IAV of fluxes compared with tundra regions. The trend of CO<sub>2</sub> fluxes shows a dipole with negative values, indicating an increasing CO<sub>2</sub> sink in the South of European Russia and central Siberia and in the Far East. In contrast, over most of Siberia and northern European Russia, the trend of CO<sub>2</sub> fluxes is slightly negative, indicating a weaker CO<sub>2</sub> sink or an increasing CO<sub>2</sub> source to the atmosphere, with a hotspot in the region between Ob' and Yenisei rivers, representing the heavy industrial zone.



**Figure 5.** Maps of  $\text{CO}_2$ ,  $\text{CH}_4$ , and  $\text{N}_2\text{O}$  fluxes (left column; a, d, g), flux inter-annual variability (middle column; b, e, h) and spread between inversion model estimations (right column; c, f, i) for Russia in top, middle and bottom rows, respectively. The maps were produced using the recent versions of the inverse models participating in Global Carbon Project budget activity of  $\text{CO}_2$  (van der Woude et al., GBC, this issue),  $\text{CH}_4$  (Saunois et al., 2025) and  $\text{N}_2\text{O}$  (Tian et al., 2024). The following inversions were used, which cover the analysis period of 2000–2019:  $\text{CO}_2$ —MIROC4-ACTM; Carbo-Scope; CTE; NISMOM; CAMS; CT-NOAA; UoE; IACAS;  $\text{CH}_4$ —MIROC4-ACTM; CTE-LMDZ; CTE; NISMOM; NIES-Inv1;  $\text{N}_2\text{O}$  - MIROC4-ACTM; GEOS-CHEM; INVICAT; PYVAR.

For  $\text{CH}_4$  (Figure 5, central column), the highest emissions are concentrated over wetlands and oil/gas extraction areas in western Siberia and over densely populated parts of Russia. Wetlands are known hotspots for methane emissions due to anaerobic decomposition of organic matter, while fossil fuel extraction activities also contribute significantly to  $\text{CH}_4$  emissions. The IAV of  $\text{CH}_4$  is most pronounced in wetlands and fossil fuel extraction areas, fluctuations in wetland water levels or variations in oil/gas production being the main drivers. Eastern Siberia, with its newly established oil and gas complexes, exhibits high variability in methane emissions, driven by the rapidly growing industrial activity in the region.  $\text{CH}_4$  trends indicate increasing emissions from Western and Eastern Siberia, particularly in regions with expanding fossil fuel industries, highlighting the impact of human activities on methane dynamics. Regions with high IAV and a negative trend in sparsely populated areas may indicate the occurrence of intense wildfires.

For  $\text{N}_2\text{O}$  (Figure 5, right-hand column), the highest mean fluxes are observed over agricultural areas in southern European Russia, where nitrogen-based fertilizers were historically intensively applied. The IAV of  $\text{N}_2\text{O}$  shows remarkable year-to-year variability not only in agricultural zones but also in Yakutia, suggesting that permafrost dynamics play a role in  $\text{N}_2\text{O}$  emission patterns. Interestingly, the IAV of  $\text{N}_2\text{O}$  emissions along the Lena River basin overlaps significantly with that of  $\text{CH}_4$ , indicating that both gases are affected by similar environmental processes, such as permafrost thaw and water saturation in wetlands. Trend analysis for  $\text{N}_2\text{O}$  shows a general increase in emissions over most of northern Russia. In contrast, agricultural areas in southern Russia show stable or slightly decreasing  $\text{N}_2\text{O}$  trends, possibly due to reduced fertilizer use over the last three decades. Significant decreases in  $\text{N}_2\text{O}$  emissions occur in eastern Russia, which is characterized by undisturbed soils with minimal human activity. In localized regions, such as the Lake Baikal, where  $\text{N}_2\text{O}$  and  $\text{CH}_4$  trends overlap significantly, increasing  $\text{N}_2\text{O}$  emissions may be associated with thawing permafrost or intense forest fires.

### 3.9.2. Evaluation of Fluxes by DGVMs and Atmospheric Inversions for $\text{CO}_2$ , $\text{CH}_4$ and $\text{N}_2\text{O}$

*C-CO<sub>2</sub>*. Contributions by  $\text{CO}_2$  fertilization, climate change and land-use to net sink simulated by DGVMs from TRENDY v11 are presented in Table 3 (Sitch et al., 2024). Despite faster than average global warming in Russia, the carbon sink change appears to be driven mostly by the increase in  $\text{CO}_2$ .

For comparison with BU fluxes, we prepared a summary of eight inversion model fluxes from the GCB 2023 (selected to cover a whole period), and 13 DGVM models/model versions from Trendy v11, shown in Table 4. Inversion fluxes adjusted for lateral fluxes by Deng et al. (2022) are also added.



**Table 3**

Decadal NBP ( $\pm 1$  Standard Deviation) in  $\text{Pg C yr}^{-1}$  and Drivers' Attribution for 2000–2009 and 2012–2021 for the RECCAP2 Region Russia (Sitch et al., 2024)

Period	Fluxes according to drivers' attribution, $\text{Pg C yr}^{-1}$			
	$\text{CO}_2$	Climate	LULCC	Net flux
2000–2009	$0.31 \pm 0.13$	$0.15 \pm 0.19$	$-0.04 \pm 0.03$	$0.41 \pm 0.03$
2012–2021	$0.35 \pm 0.16$	$0.12 \pm 0.19$	$-0.07 \pm 0.06$	$0.41 \pm 0.27$

The difference between inversions and DGVMs is within their respective uncertainty range despite rather high uncertainties of both individual inversions and DGVMs. Unlike LEA, the inversions suggest a slightly increasing carbon sink during 2000–2019 (concurring with projections by Tagesson et al. (2020)). This contradiction to LEA and some other results can be explained by the coarseness of global models and their inability to fully account for regional details and the impact of disturbances, particularly during short time periods (Gustafson et al., 2024). The annual fluxes by inversions (GCB2023 inversions) and TRENDY v11  $\text{CO}_2$  Table 4), DGVMs, EC and LEA bottom-up values averaged by decades are presented in Figure 6.

A subregional analysis of flux time series points to a larger divergence between DGVMs and inversion trends that is centered on West and Central Siberia (Figure S11 in Supporting Information S1).

The spread between individual inverse models continues to be large, even as many inverse models are now using the  $\text{CO}_2$  observations over Russia (e.g., Sasakawa et al., 2010). The impact of including the observations over Siberia could result in either lowering (Saeki et al., 2013) or increasing (Maksyutov et al., 2003) the Siberian sink estimate depending on the inverse model setup. Further reduction of the inverse model spread may be achieved by addressing existing model vertical transport differences in mid-to high latitudes (Remaud et al., 2018). Chandra et al. (2022) reported lower NEE values of  $-0.31 \pm 0.04$  and  $-0.39 \pm 0.06 \text{ Pg C yr}^{-1}$  for 2000–2009 and 2010–2019, respectively. On the other hand, based on outputs from the v10 OCO-2 Orbiting Carbon Observatory modeling inter-comparison project, Byrne et al. (2023) estimated a median NBP (change of amount of carbon in terrestrial ecosystems after correcting inversions for  $\text{CO}_2$  fluxes produced by lateral transfer processes) for 2015–2019  $-0.67 \pm 0.07 \text{ Pg C yr}^{-1}$ . LEA's estimate of our study was closer to GCB 2023 inversions (Figure 7).

Using the Bayesian method to harmonize the C- $\text{CO}_2$  budget obtained by methods and data indicated in Figure 6, we have for two decades  $-537 \pm 215$  and  $-538 \pm 220 \text{ Tg C-CO}_2 \text{ yr}^{-1}$ . The Bayesian averaging approach provides useful insights, though numerical results should be interpreted with caution, considering the different nature of uncertainties between the BU and TD methods and additional uncertainties from the regional incompleteness of adjusted lateral fluxes.

The CMIP6 Earth System (Jones et al., 2024) for 2010–2019 presents basic indicators of terrestrial ecosystem productivity close to LEA. The means ( $\text{Pg C yr}^{-1}$ ) are: GPP  $9.65 \pm 1.08$  and  $9.41 \pm 1.12$  and NPP  $5.09 \pm 1.06$  and  $5.31 \pm 1.10$ , respectively by CMIP6 and LEA. The NEE is estimated at  $-0.37 \pm 0.16 \text{ Pg C yr}^{-1}$  by the Earth models and at  $-0.57 \pm 0.13 \text{ Pg C yr}^{-1}$  by the LEA.

The estimates of the book-keeping models are given in Table 5 (data from the GCB (Friedlingstein et al., 2023)).

According to definitions used by the GCB, the flux of  $\text{CO}_2$  from land-use, land-use change, and forestry includes  $\text{CO}_2$  fluxes from deforestation, afforestation, logging, and forest degradation, shifting cultivation and regrowth of forests. Results of Table 5 allow us to conclude that they are extremely diverse, with a high probability that they do not belong to samplings from the same population, and therefore we did not use this type of model in the aggregated analysis.

A number of studies based on inventories and models reported a net carbon sink in live woody biomass for the entire boreal zone from 2000–2015 (or to 2019) on average at  $-0.22 \pm 0.14 \text{ Pg C yr}^{-1}$  (N. L. Harris et al., 2021; Liu et al., 2015; Tagesson et al., 2020; Xu et al., 2021). Our study gives an average sink of woody biomass in Russia for 2000–2019  $-0.21 \pm 0.09 \text{ Pg C yr}^{-1}$ .

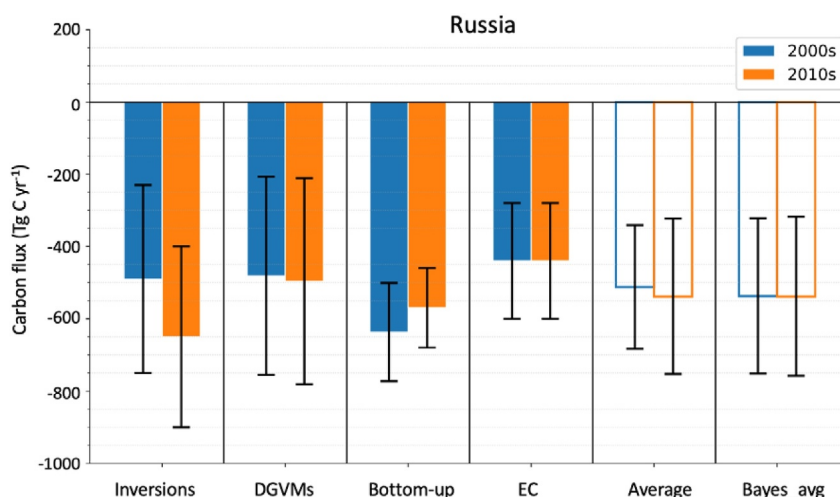
**Table 4**

Summary of the Evaluation of Net Ecosystem Exchange for Russia's Terrestrial Ecosystems by Inverse Models (INV), DGVMs, and LEA in 2000–2019

Period	DGVMs	INV	INV with lateral adjustment	LEA
2000–2009	$-0.48 \pm 0.27$	$-0.56 \pm 0.26$	$-0.49 \pm 0.26$	$-0.64 \pm 0.17$
2010–2019	$-0.48 \pm 0.28$	$-0.73 \pm 0.27$	$-0.65 \pm 0.27$	$-0.57 \pm 0.14$

Note. Data units  $\text{Pg C yr}^{-1}$ .





**Figure 6.** Fluxes of C-CO<sub>2</sub> in Russia's terrestrial ecosystems according to inversions using surface CO<sub>2</sub> data, dynamic global vegetation models simulations, bottom-up land-ecosystem approach and eddy covariance for the whole of Russia. By convention, a negative value denotes carbon removal from the atmosphere. The subregional time series of annual mean fluxes and flux seasonal cycles are shown in Figure S11 in Supporting Information S1.

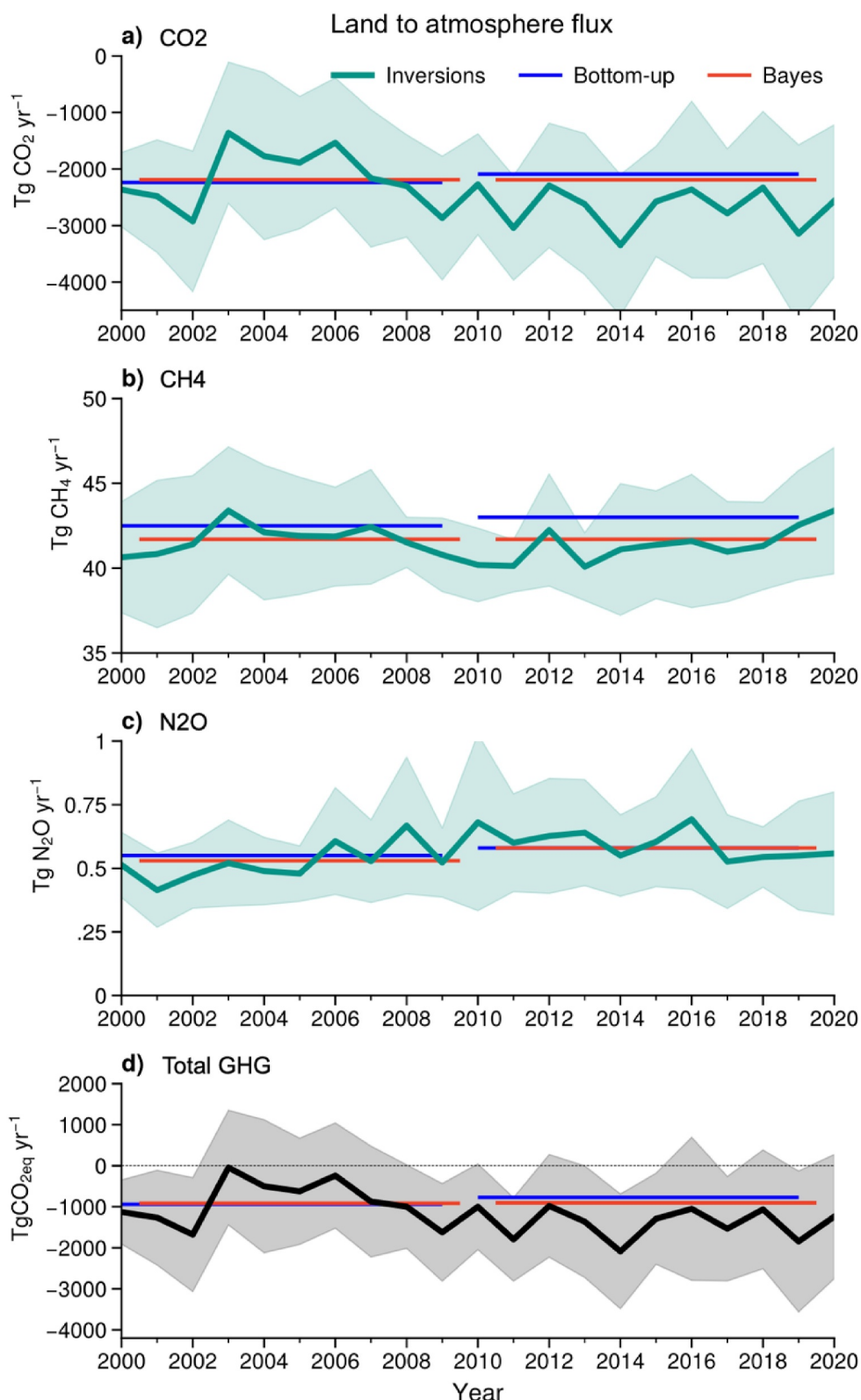
Average CH<sub>4</sub> emissions by inverse modeling from Russia's territory over periods 2000–2009 and 2008–2017 (Tg CH<sub>4</sub> yr<sup>-1</sup>) as presented in Saunio et al. (2020) were estimated for two considered decades at  $30.9 \pm 8.3$  and  $30.7 \pm 3.7$  Tg CH<sub>4</sub> yr<sup>-1</sup> and included anthropogenic sources of  $19.3 \pm 8.1$  and  $19.8 \pm 6.8$  Tg CH<sub>4</sub> yr<sup>-1</sup>, respectively (Table S7 in Supporting Information S1). Anthropogenic emissions of CH<sub>4</sub> by sectors were estimated for 2000–2017 based on different sources (CEDSgridded, EDGARv432, GAINSgridded, USEPA, FAO, CEDScount). The estimated anthropogenic methane emissions amount to  $29.7 \pm 4.3$  Tg CH<sub>4</sub> yr<sup>-1</sup> and include emissions from fossil fuel extraction of  $17.2 \pm 1.9$  Tg CH<sub>4</sub> yr<sup>-1</sup> (Table S8 in Supporting Information S1).

Table 6 summarizes net N<sub>2</sub>O emission estimates from inverse models for Russia during 2000–2019. For comparison, flux estimates from a set of DGVMs are also included, specifically DLEM (Tian et al., 2015), LPJ-GUESS (Olin et al., 2015), ORCHIDEE-CNP (Goll et al., 2017) and VISIT (Ito et al., 2018). The comparison indicates that the spread between inverse models is below 20%, and the difference between inverse model estimates and DGVM averages is smaller than the spread within the DGVM and inverse model ensembles. Given the large uncertainty in N<sub>2</sub>O emissions and emission factors, the close agreement between the atmospheric top-down approach and process-based modeling appears encouraging for assessing N<sub>2</sub>O emissions (Figure 7c). However, this similarity may be illusive, considering the scarcity of direct N<sub>2</sub>O emissions measurements across Russia. NIR (2024) reports average annual emissions of 0.33 Tg N<sub>2</sub>O yr<sup>-1</sup> for 2016–2020, with 0.05 Tg N<sub>2</sub>O yr<sup>-1</sup> attributed to energy, industrial, and waste sectors, while the remaining emissions originate from land use and agriculture.

Based on 13 DGVMs (CLASS-CTEM, LLEM, ELM, JSBACH, JULES, LPJ-GUESS, LPJ-MPI, LPJ-WSL, LPX, ORCHIDEE, TEM-MDM, TRIPLEX-GHG and VISIT), the CH<sub>4</sub> flux for wetlands in 2000–2017 was estimated at  $10.99 \pm 5.46$  Tg CH<sub>4</sub> yr<sup>-1</sup> (Saunio et al., 2020). The spread of the model results was large.

Wittig et al. (2023), based on inverse modeling using Siberian observations, estimated CH<sub>4</sub> emission for Northern Eurasia over 2008–2019: total emissions of 42.8 Tg CH<sub>4</sub> yr<sup>-1</sup> (of which 79% in East Eurasia), including emissions from wetlands of 16.2 Tg CH<sub>4</sub> yr<sup>-1</sup>, other natural emissions of 6.4 Tg CH<sub>4</sub> yr<sup>-1</sup>, and anthropogenic emissions of 20.2 Tg CH<sub>4</sub> yr<sup>-1</sup>. That is close to the global inversion results for this region (Figure 7b).

Anthropogenic sources in database EDGARv8 are estimated at 2164 and 2361 Tg CO<sub>2</sub>-eq. yr<sup>-1</sup> in 2000–2009 and 2010–2019, respectively, indicating slight changes in the composition of emitted GHGs: CO<sub>2</sub> 78.7%, CH<sub>4</sub> 18.5% and 2.8% in the first decade, and 76.6% CO<sub>2</sub>, 20.5% CH<sub>4</sub> and 2.9% N<sub>2</sub>O in the second decade (Table S9 in Supporting Information S1).



**Figure 7.** Annual average flux timeseries of  $\text{CO}_2$  (a),  $\text{CH}_4$  (b),  $\text{N}_2\text{O}$  (c) and Greenhouse gas total (d) for Russia as estimated by TD models and bottom-up empirical approaches. The following inversions were used:  $\text{CO}_2$ —MIROC4-ACTM; Carbo-Scope; CTE; NISMON; CAMS; CT-NOAA; UoE; IACAS;  $\text{CH}_4$ —MIROC4-ACTM; CTE-LMDZ; CTE; NISMON; NIES-Inv1;  $\text{N}_2\text{O}$ —MIROC4-ACTM; GEOSHEM; INVICAT; PYVAR.

**Table 5**  
*Emissions From Land-Use Change (ELUC) According to the Book-Keeping Models*

Models	2000–2009	2010–2019
BLUE	$3.1 \pm 21.6$	$84.7 \pm 36.3$
H&C	$-95.2 \pm 12.3$	$-28.2 \pm 20.3$
OSCAR	$-10.0 \pm 9.4$	$25.6 \pm 20.8$

Note. Units: Tg C yr<sup>-1</sup>.

Historical emissions of all GHG from all sources including land use can be found in Our World in Data based on Jones et al. (2024). The emissions for 2000–2009 and 2010–2019 are estimated at 1990 Tg CO<sub>2</sub>-eq. yr<sup>-1</sup> (including 77.0% of CO<sub>2</sub>, 19.5% of CH<sub>4</sub>, and 3.5% of N<sub>2</sub>O) and 2418 Tg CO<sub>2</sub>-eq. yr<sup>-1</sup> (77.8% CO<sub>2</sub>, 19.1% CH<sub>4</sub> and 3.1% N<sub>2</sub>O) Tg CO<sub>2</sub>-eq. yr<sup>-1</sup> (Table S6 in Supporting Information S1).

### 3.10. Total Greenhouse Gases Budget

Figure 7 presents GHG emissions estimates for 2000–2009 and 2010–2019, obtained using two methods with similar final goals: inversions and LEA.

While the difference in C-CO<sub>2</sub> emissions is not substantial, the observed temporal trends are opposite. Inversions show a clear increase in the carbon sink over two decades of about 30% (from 2,047 to 2,676 Tg CO<sub>2</sub>-eq. yr<sup>-1</sup>), whereas LEA estimates indicate an 11% decline in the CO<sub>2</sub> carbon sink (from 2,300 to 2,087 Tg CO<sub>2</sub>-eq. yr<sup>-1</sup>).

Evidently, LEA is based on more detailed information, but the uncertainties associated with such data may be less reliable. The second decade of this century was marked by critical seasonal weather instability and drought across vast boreal regions in Russia, leading to severe fires and the death of 33.6 M ha of forests, compared to 19.3 M ha in the previous decade. Increased biogenic disturbances and harvest further expand the area of damaged forests. Nevertheless, the decrease in total forest area (according to MFFS) across the country was only 10.2 M ha in 2010–2019, with substantial natural reforestation of previously disturbed areas contributing to a higher carbon sink over a major part of the boreal zone, along with increased vegetation cover on abandoned arable lands. The LEA method of estimation of productivity of forests has a certain inertia because it depends on periodic forest inventory updates. Conversely, inversions have their own limitations, particularly with rapidly and heterogeneously changing environments and land cover.

However, according to the calculated uncertainties, the estimate of accuracy of LEA is substantially higher than that of the inversions. In the Bayesian context, there is a reversal of the cumulative sign of trends of CO<sub>2</sub> emissions in Russian ecosystems from negative to positive. Considering the similarity in fluxes of CH<sub>4</sub> and N<sub>2</sub>O estimated by the various methods for the periods being compared, we concluded that the effect on the global GHG budget of Russian lands is that those ecosystems remain a sink in the 21st century, slightly decreasing from  $-993 \pm 924$  to  $-912 \pm 812$  Tg CO<sub>2</sub>-eq. yr<sup>-1</sup> between 2000–2009 and 2010–2019.

We can conclude that, according to Bayesian averaging, Russia's land served a net sink in 2000–2009 and 2010–2019, respectively, at  $-2,263$  and  $-2,188$  Tg CO<sub>2</sub>-eq. yr<sup>-1</sup>; at  $-1,547$  and  $-1,469$ , if anthropogenic GHG emissions from natural sources are also included (Table 7). If all of Russia's fossil fuel emissions are included, the sink decreases to  $-865$  and  $-455$  Tg CO<sub>2</sub>-eq. yr<sup>-1</sup>. Inclusion of all anthropogenic GHG emissions over the country transforms Russia into a source of about 1,100–1,500 Tg CO<sub>2</sub>-eq. yr<sup>-1</sup>. However, we note that all results received by the Bayesian averaging should be taken with caution because of uncertainties resulting from this procedure.

**Table 6**  
*N<sub>2</sub>O Emissions From Natural Sources Estimated by Inverse Modeling (INV) and DGVMs From the NMIP Intercomparison Project (Tg N<sub>2</sub>O yr<sup>-1</sup>)*

Period	Inverse models							DGVMs (NMIP)	
	PYVAR	PYVAR2	GEOS-CHEM	MIROC4-ACTM	INVICAT	INV mean	INV std	Mean	std
2000–2009	0.28	0.28	0.38	0.31	0.26	0.30	0.05	0.32	0.16
2010–2019	0.28	0.33	0.41	0.30	0.29	0.33	0.05	0.33	0.14

**Table 7**

*Bayesian Averaging of Empirical Bottom-Up and Top-Down (Inversion) GHG Balance for The Terrestrial Ecosystem of Russia*

Period	Greenhouse gases (Tg CO <sub>2</sub> -eq. yr <sup>-1</sup> )				Balance
	CO <sub>2</sub>	CH <sub>4</sub>	N <sub>2</sub> O	Total	
2000–2009					
Natural fluxes	−2263 ± 901	626 ± 146	90 ± 46	−1547 ± 914	
Anthropogenic fluxes	1386 ± 69	1126 ± 202	148 ± 46	2660 ± 218	1113 ± 940
2010–2019					
Natural fluxes	−2188 ± 803	626 ± 146	94 ± 44	−1469 ± 813	
Anthropogenic fluxes	1666 ± 117	1126 ± 202	148 ± 46	2940 ± 238	1471 ± 847

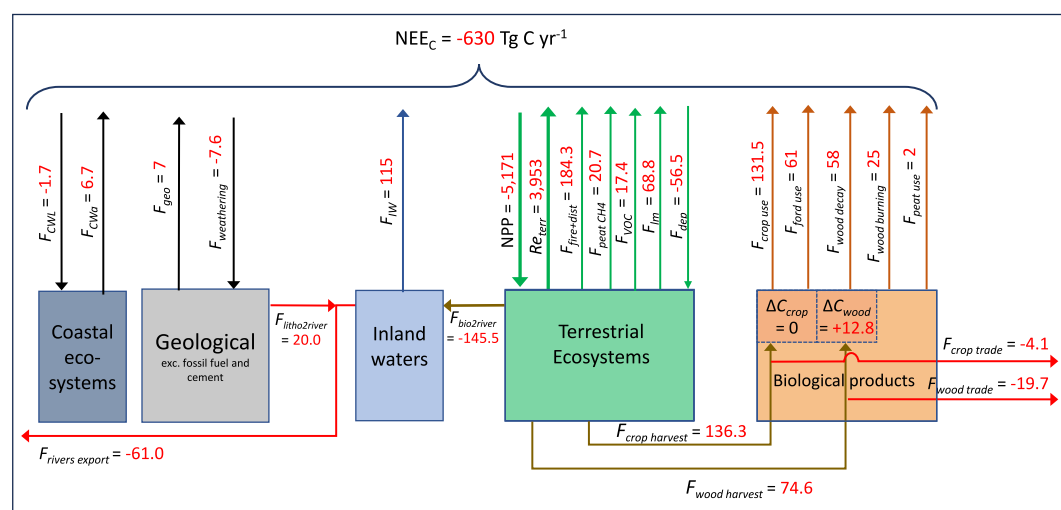
#### 4. Discussion

The calculated estimates of the major components of the bottom-up carbon budget in this study are presumed to be free from substantial unrecognized biases. The developed multi-dimensional regional models are based on solid methodology, supported by sufficient empirical data, and have high spatial resolution.

Two major indicators of dynamics of ecosystem productivity—Net Primary Production and SHR—demonstrate an increase during 2000–2019. Overall, the immediate post-disturbance increase in SHR is significant in boreal forests (Harmon et al., 2011). However, when the entire post-disturbance succession period is considered (on average 50–60 years for coniferous forest), the accumulated change in SHR is small (Schepaschenko et al., 2025). SHR also increases after the conversion of forests to agricultural lands and some other land uses (Fan & Han, 2020; Paustian et al., 2000). Before the 1990s, about 7 M ha of wetlands were drained and converted to agriculture. Most of these drainage systems did not function in recent decades, and the current officially reported area of drained wetlands used for agriculture is 4.2 M ha, with an uncertain impact on SHR. Recently published average values of SHR (264–318 g C m<sup>-2</sup> yr<sup>-1</sup>) by bioclimatic zones and land classes in Russia (Kudeyarov, 2018) are similar to the LEA estimates of this study. Historically, published SHR estimates have slightly increased since the early 2000s: from around 170 g C m<sup>-2</sup> yr<sup>-1</sup> (Golubyatnikov et al., 2005; Golubyatnikov & Svirezhev, 2008; Kudeyarov & Kurganova, 2005; Kurganova, 2003; Kurganova et al., 2010) to 190 g C m<sup>-2</sup> yr<sup>-1</sup> (Mukhortova et al., 2021). As for NPP estimates, this increase in SHR between earlier and recent studies may reflect higher respiration rates NPP inputs and/or increased decomposition, but methodological differences could also play a role. In our study, total heterotrophic respiration of forest ecosystems, defined as the sum of SHR (Mukhortova et al., 2021) and decomposition flux from CWD (DEC), shows an increase during the last two decades. The ratios of SHR and ecosystem heterotrophic respiration to net primary production (i.e., SHR:NPP and EHR:NPP) were 0.62 and 0.68, respectively, in 2000–2009, and increased to 0.68 and 0.77 in 2010–2019, mainly because of increased natural disturbances and harvest.

A specific conclusion from these assessments of NPP, SHR and Heterotrophic Ecosystem Respiration (HER) is that while NPP and HER in non-forest land classes increased by 1.05% and 1.03% in 2010–2019 compared to 2000–2009, respectively, forest NPP rose by 4.5%, whereas HER increased by 12.1%. The primary driver of these changes was the unprecedented rise in natural disturbances (mostly fire) during the second decade (in 2010–2021) when the extent of fire in arctic and boreal regions in Eurasia and Northern America nearly tripled (Jones et al., 2024). Additionally, biogenic disturbances, including outbreaks of harmful insects expanding into new northern forest regions, significantly contributed to tree mortality.

Overall, the bottom-up approach estimated that Russia's land ecosystems acted as a net carbon sink, with C-CO<sub>2</sub> fluxes of  $-636.8 \pm 171.5$  Tg C yr<sup>-1</sup> for 2000–2009 and  $-569.5 \pm 138.9$  Tg C yr<sup>-1</sup> for 2010–2019, with the errors at a 90% confidence level. The reliability of these estimates depends on the comprehensiveness of accounting systems and estimated uncertainty. The completeness of fuzzy systems can be estimated only by professional expert judgments. Analyses of the accounting systems used in our study lead to a conclusion that very likely not less than 96%–98% of the recognized carbon fluxes have been accounted.



**Figure 8.** Net Ecosystem Exchange of carbon for land of Russia following Ciais et al. (2022) with some modification to the sectoral details.

In Figure 8, we present a comparison of the carbon stock change in land ecosystems of Russia (average for 2000–2019) derived from LEA and supplemented by published data not included in LEA. The net change was estimated at 630 Tg C yr<sup>-1</sup> that is close to the conclusion of this study. Net trade was not included in the account.

However, some problems with strict assessment of uncertainty within bottom-up approaches applied to Russian ecosystems remain. Despite control procedures of input data quality and a large number of observations in most cases, the assessment of uncertainty of fuzzy systems (or problems of full complexity) cannot be comprehensive. First, much of the information used in the bottom-up approach does not come from planned experiments, and the actual accuracy of various Russia's inventories is not known. Strictly speaking, the estimated uncertainty is, to some extent, a result of statistical exercises, leaving the problem of “uncertainty of uncertainties” unaddressed from a systems point of view.

Data for other GHGs—methane and nitrous oxide—have a weaker empirical basis for Russian terrestrial ecosystems than CO<sub>2</sub>, and estimates of their fluxes substantially use results from international studies and global models. Our estimates indicate that CH<sub>4</sub> emissions from natural and anthropogenic sources remained stable across both decades at  $42.5 \pm 9.7$  and  $43.0 \pm 8.7$  Tg CH<sub>4</sub> yr<sup>-1</sup>. Inverse modeling (Figure 7) reports similar values of  $41.7 \pm 3.06$  and  $41.2 \pm 2.69$  Tg CH<sub>4</sub> yr<sup>-1</sup>, but with lower uncertainties. Some recent studies showed a positive trend in CH<sub>4</sub> emissions during recent decades. Yuan et al. (2024) reported a positive (+8.9%) robust increasing trend from Boreal-Arctic wetlands with strong IAV. This trend is mainly explained by two hot spot regions, one of which is the West Siberian Wetlands (52–74°N, 60–94.5°E), where the increase in emissions CH<sub>4</sub> was estimated at 11%, from 6.1 to 6.9 Tg CH<sub>4</sub> yr<sup>-1</sup> over 2000–2020. McNicol et al. (2023), using Upscaling Wetland Methane Emission from the FLUXNET-CH<sub>4</sub> EC Network (UpCH<sub>4</sub> v 1.0), provided a new and independent bottom-up global estimate of CH<sub>4</sub> emission from EC measurements for the period 2001–2018 at  $146 \pm 42.7$  Tg CH<sub>4</sub> yr<sup>-1</sup>, which is very close to bottom-up (BU) emissions from the GCP (mean 149 Tg CH<sub>4</sub> yr<sup>-1</sup>, (Saunois et al., 2020)). This model, trained on 119 site-years of EC CH<sub>4</sub> flux data from 43 freshwater wetland sites in the FLUXNET-CH<sub>4</sub> Community Product, accurately reproduced site-level annual means and average seasonal cycles of CH<sub>4</sub> fluxes in major bioclimatic tundra, boreal, and temperate regions. The average estimate by McNicol et al. (2023) for the West Siberian Lowlands was 6.5 Tg CH<sub>4</sub> yr<sup>-1</sup>, almost identical to the average by Yuan et al. (2024).

These two studies could be compared with the results of an intensive research experiment in the West Siberian Lowland, WETCHIMP-WSL, where three approaches were used: 21 large-scale process-based models, five inversions, and in situ observations. While the range of individual estimates was high, the 12-year average emissions (for 1993–2004) were rather consistent with bottom-up models ( $5.34 \pm 0.54$  Tg CH<sub>4</sub> yr<sup>-1</sup>) and inversions ( $6.06 \pm 1.26$ ), but in situ observation gave a lower estimate at  $3.91 \pm 1.24$  Tg CH<sub>4</sub> yr<sup>-1</sup> (Bohn et al., 2015).



Some studies also report an increase in  $\text{N}_2\text{O}$  emissions. Voigt et al. (2017, 2020) reported increasing probability of  $\text{N}_2\text{O}$  emissions as the permafrost thaws on about one quarter of subarctic peatlands, with the highest post-thaw emissions from bare peat surfaces. The presence of vegetation decreased emissions (by  $\sim 90\%$ ) but did not prevent thaw-induced  $\text{N}_2\text{O}$  release. Waterlogged conditions also suppressed emissions. Yuan et al. (2023) found increased  $\text{N}_2\text{O}$  emissions in 1969–2019 caused by warming, using the improved Terrestrial Ecosystem Model.  $\text{N}_2\text{O}$  uptake from the atmosphere was  $0.1 \text{ Tg N yr}^{-1}$  with a small IAV. Perhaps our estimation underestimated  $\text{CH}_4$  and  $\text{N}_2\text{O}$  emissions during the last two decades, but this underestimation is within the limits of the calculated uncertainty, and there were insufficient empirical data to further improve these estimates.

Our study demonstrates that consistent results can be produced by different methods, that is, the bottom-up empirical Land Ecosystem Account (LEA) and other estimates upscaled from in situ observations, inverse modeling (IM), and, with some reservations, EC and DGVMs. The spread of differences in the estimates is within the limits of assessed uncertainties. Some differences might be explained by either specifics of the methods or unusual dynamics within ecosystems during 2000–2019. However, some results from DGVMs require more detailed discussion as follows.

DGVM estimates of forest  $\text{CO}_2$  emissions for Russia should be taken with caution. Several estimates of the carbon budget for 2000–2014 (Dolman et al., 2012; Quegan et al., 2011; Shvidenko et al., 2007; Shvidenko & Schepaschenko, 2014) reported similar estimates of forest NPP by both DGVMs and LEA for the previous decades. However, the partitioning of NBP in component fluxes in these two approaches is different: the DGVMs find NPP to be nearly balanced by heterotrophic respiration, fluxes from disturbances are clearly underestimated, and land classes are oversimplified. In the LEA, heterotrophic respiration is substantially lower than NPP, and disturbances play a much larger role in the overall carbon balance. The DGVM ensembles we used do not account for a substantial part of disturbances and some other fluxes. Additionally, the official ground data used for adjustment (usually NIR) substantially underestimate the actual NEE for Russian forests.

Therefore, when comparing results from different methods, it is critical to use the same flux component structure. O'Sullivan et al. (2024) concluded that DGVMs simulate a sink about 50% lower than inverse modeling for Russia and other northern countries over 2001–2021, mainly caused by overestimation of fire emissions in DGVMs and by the lack of robust forest demography resulting in lower forest regrowth rates. Our study generally supports this conclusion, but the underestimation of the sink is lower, about 25%. LEA directly or indirectly accounts for almost all common recognized disturbances in forests. Our explanation is that DGVMs tend to overestimate HER in cold regions, especially areas with permafrost. Note that the results of O'Sullivan et al. (2024) do not show an increase in net carbon sink by inversions for the entire northern belt, of which Russian forests cover two-thirds of the total area.

The empirical bottom-up approach demonstrates (within limits of uncertainties) a relatively small negative trend on NEE over 2000–2019 in contrast to the calculated results of the inversions used. The reason may lie in the contradictory effects of climate change and disturbances on the regional functioning of terrestrial ecosystems. On one hand, overall warming increases ecosystem productivity in cold regions during the seasons with a satisfactory amount of water. On the other hand, warming leads to a marked increase in wildfires and pathological processes in regions experiencing dryer fire seasons. Due to the increased frequency and severity of catastrophic fire seasons in Russia in 2010–2019, resulting in a net loss of 10 M ha of Russian forests, it is not easy to find a logical explanation for the increasing net carbon sink in this decade. Nevertheless, across the entire country, the average productivity of terrestrial ecosystems grew during the entire period of 2000–2019, except for years with catastrophic fires and accompanied disturbances. This was especially true for forests.

The challenge of rigorously assessing uncertainty persists, but there is increasing evidence that the Bayesian method offers improvements. As demonstrated in this study, the magnitude of uncertainty can significantly influence the statistical conclusions when using different methods. Thus, the problem of “uncertainty of uncertainties” is still waiting for a solution.

Two studies were recently published by Russian researchers: a detailed report on the assessment of GHG fluxes in Russian (Korotkov et al., 2023) and a condensed journal paper (Romanovskaya & Korotkov, 2024) that describes a bottom-up assessment of the budgets for major GHGs from natural and anthropogenic sources for the single year 2016. These publications are important for two reasons: they are largely based on official statistics without excluding unmanaged forests and broadly follow the IPCC methodology. Overall, the classification of land

classes in these publications is similar to that used in our study; the anthropogenic components cover the energy, industry, livestock, and waste sectors, which were mostly taken from the NIR reports (NIR, 2024). The GHG balance of Russia's terrestrial ecosystems (natural fluxes) is reported by Romanovskaya and Korotkov (2024) as  $-1129 \text{ Tg CO}_2\text{-eq. yr}^{-1}$ , resulting from  $-2686 \text{ Tg CO}_2 \text{ yr}^{-1}$  (or  $-733 \text{ Tg C yr}^{-1}$ ) and  $+1557 \text{ Tg CO}_2\text{-eq. yr}^{-1}$  from the two other GHGs ( $\text{CH}_4$  and  $\text{N}_2\text{O}$ ). The reported uncertainty is very high, often exceeding hundred percent, and is presented only for a few basic indicators. When anthropogenic emissions are included, Russia is considered a significant source at  $879 \text{ Tg CO}_2\text{-eq. yr}^{-1}$ . Notably, while the total C- $\text{CO}_2$  estimates in the cited papers are close to those obtained in our work, many component fluxes differ by 100% or more due to different data sources—official statistics (Romanovskaya & Korotkov, 2024) versus constraints from empirical data, models, and remote sensing in this study.

A key takeaway from a comparison of these studies is that critical evaluation and verification of both the data and methodology is crucial. A rigorous systems analysis approach is essential, incorporating both ground-based and remote sensing data to improve the accuracy of national and international GHG assessments (Chevallier, 2021). Comprehensive integration of such diverse information sources is the only viable strategy for advancing our understanding of the Earth system. Ideally, the uncertainty in both scientific studies and policy-relevant reports should remain within limits that are acceptable to decision-makers. However, there is no consensus on what constitutes an acceptable uncertainty range. For regional and national GHG budget assessments, based on the conception of “total utility,” we propose a target uncertainty in limits of 25%–30% with a confidence level 0.9 within the framework of a comprehensive and verifiable account of major GHGs. Requiring that assessments meet this standard would enhance their utility for both scientific research and policymaking.

## 5. Conclusions

This study shows that Russia's terrestrial vegetation served as a sustainable carbon sink in 2000–2019, despite unfavorable climate change and the accompanying increase in natural disturbances, especially fires. Nevertheless, fires and outbreaks of harmful insects may have decreased the annual carbon sink in forests by 30%–40% compared to years with low fire danger. Transition to sustainable forest and LM is one of the urgent actions needed to significantly reduce carbon losses in ecosystems.

The study confirms that the use of system analyses does not have alternatives in the scientific explanation of biogeochemical processes in the Earth system. This is particularly important for bottom-up empirical methods. However, our study identified a number of shortcomings that hinder the full application of this approach in the Russian context, particularly regarding the availability and reliability of the necessary information. A significant drawback is the lack of system integration across the different methods used to estimate the GHG budget, particularly due to incompatibility in some basic definitions and classification schemes between top-down and bottom-up approaches.

Unresolved issues persist in quantifying and understanding Russia's GHG cycling. While remote sensing and modeling capacities have advanced, they often outpace the corresponding ground-based knowledge, especially in the development of multidimensional models for morphologically complex ecosystems such as forests, which include components “hidden” from remote sensing. These gaps include insufficient data on age structure in forests (e.g., even-aged vs. uneven-aged stands), the role of lower forest layers and soil, both live and dead roots (particularly fine roots), and varied definitions and classifications of shrubs. There is also insufficient knowledge and lack of a solid methodology for assessing the impacts of biotic agents and climate change on natural forests. This situation underscores the urgent need to improve national systems of forest inventory and monitoring, especially in countries like Russia, where historical data collection has not prioritized the biosphere and ecological functions of forests.

The results of this study provide additional information for addressing one of the critical issues in organizing international efforts to mitigate undesirable climate change. The special emphasis on managed ecosystems (especially forests) in IPCC documents seems logical, but this does not change the fact that knowledge of a part of a fuzzy system does not necessarily provide reliable knowledge of the entire system. In addition, modern definitions of “managed” ecosystems and their justification are, strictly speaking, not fully scientifically robust. Therefore, compiling a comprehensive and verifiable GHG budget is probably not possible when studying only part of the systems in isolation.

## Conflict of Interest

The authors declare no conflicts of interest relevant to this study.

## Data Availability Statement

Most of the data sets used in this study are published by third parties, with references provided in the text. Data sets generated by the co-authors are listed below. Soil Respiration Field Measurements Database: Used for assessing heterotrophic soil respiration efflux in this study. Available at the IIASA PURE repository via (<https://doi.org/10.22022/ESM/10-2020.107>) under a CC BY-NC 4.0 license (Mukhortova et al., 2020). (Not Available in CrossRef) (Not Available in External Pubmed). Dead Wood Field Measurements Database: Used for assessing the dead wood carbon pool in this study. Available at the Zenodo repository via (<https://doi.org/10.5281/zenodo.7455326>) under a CC 4.0 license (Shvidenko et al., 2022). (Not Available in CrossRef) (Not Available in External Pubmed). Live Biomass Destructive Sampling Database: Available at the PANGAEA repository via (<https://doi.org/10.1594/PANGAEA.871492>) under a CC BY-NC 4.0 license (Schepaschenko et al., 2017). Random-ForestCode Version 2020.02.19: Used for soil respiration modeling and preserved in Supporting Information S1 via (<https://doi.org/10.1016/j.scitotenv.2021.147314>) under a CC 4.0 license (Mukhortova et al., 2021). (Not Available in CrossRef) (Not Available in External Pubmed). Map of Russian forest for the year 2009 is available at the Zenodo repository via (<https://doi.org/10.5281/zenodo.6056054>) with a CC 4.0 license (Schepaschenko et al., 2018). Map of growing stock volume for the year 2014 is available at the Zenodo repository via (<https://doi.org/10.5281/zenodo.3981198>) with CC 4.0 license (Schepaschenko et al., 2020). Russian Wetlands and Methane Fluxes Data Set: Mapping and methane flux estimation. Available at the Zenodo repository via (<https://doi.org/10.5281/zenodo.13997236>) under a CC 4.0 license (Terentieva et al., 2024).

## Acknowledgments

I.K. was supported by the Ministry of Science and High Education of the Russian Federation (State assignment #122040500037-6). M.G. and I.K. were supported by the Ministry of Science and High Education of the Russian Federation (theme No. 121040800146-3 "Physical bases of ecological functions of soils: technologies of monitoring, forecasting and management"). V.M. was supported by the state assignment of Ministry of Science and High Education of Russian Federation FFER-2022-0002 (Theme No. 1022031600002-1-1.6.19). J.K., I.K. was supported as a part of the most important innovative project of national importance "Development of a system for ground-based and remote monitoring of carbon pools and greenhouse gas fluxes in the territory of the Russian Federation, ensuring the creation of recording data systems on the fluxes of climate-active substances and the carbon budget in forests and other terrestrial ecological systems" (Registration number: 123030300031-6). R.L. and P.C. acknowledge funding from French state aid, managed by ANR under the "Investissements d'avenir" programme (ANR-16-CONV-0003, "CLand"). P.C. acknowledges support from the European Space Agency Climate Change Initiative RECCAP2 Project (ESRIN/4000123002/18/I-NB). P.K.P. and N.C. are supported by the Arctic Challenge for Sustainability phase II (ARCS-II; JPMXD1420318865), and P.K.P., D.B. and N.C. are supported by the Environment Research and Technology Development Fund (JPMEERF24S12205). A.P. and L.M. were supported by the state assignment of Ministry of Science and High Education of the Russian Federation FWES-2024-0023 (Theme No. 124012900558-7).

## References

- ACIA. (2005). *Arctic climate impact assessment*. Cambridge University Press.
- Ågren, G. I., Hyvönen, R., & Nilsson, T. (2008). Are Swedish forest soils sinks or sources for CO<sub>2</sub>—Model analyses based on forest inventory data. *Biogeochemistry*, 89(1), 139–149. <https://doi.org/10.1007/s10533-007-9151-x>
- Anisimov, O. A., Zhiltcova, Y. L., & Rashvin, V. Y. (2015). Modelling biological productivity in the Russian arctic using satellite observations. *Izvestiya - Atmospheric and Oceanic Physics*, 3, 60–70. <https://doi.org/10.1134/S0001433815090042>
- Bartalev, S. A., & Stytsenko, F. V. (2021). An assessment of the forest stands destruction by fire based on the remote sensing data on a seasonal distribution of burnt areas. *Forest Science*, 2, 115–122. <https://doi.org/10.31857/S0024114821020029>
- Bazhin, N. M. (2000). Methane in the atmosphere. *Soros Educational Journal*, 6(3), 52–57. <https://mpira.ub.uni-muenchen.de/50844/>
- Belshe, E. F., Schuur, E. A. G., & Bolker, B. M. (2013). Tundra ecosystems observed to be CO<sub>2</sub> sources due to differential amplification of the carbon cycle. *Ecology Letters*, 16(10), 1307–1315. <https://doi.org/10.1111/ele.12164>
- Bloom, A. A., Exbrayat, J.-F., van der Velde, I. R., Feng, L., & Williams, M. (2016). The decadal state of the terrestrial carbon cycle: Global retrievals of terrestrial carbon allocation, pools, and residence times. *Proceedings of the National Academy of Sciences*, 113(5), 1285–1290. <https://doi.org/10.1073/pnas.1515160113>
- Bohn, T. J., Melton, J. R., Ito, A., Kleinen, T., Spahni, R., Stocker, B. D., et al. (2015). WETCHIMP-WSL: Intercomparison of wetland methane emissions models over west siberia. *Biogeosciences*, 12(11), 3321–3349. <https://doi.org/10.5194/bg-12-3321-2015>
- Bondur, V. G., Mokhov, I. I., & Makosko, A. A. (Eds.) (2022). In *Methane and climate change: Scientific problems and technological aspect*. Russian Academy of Sciences.
- Born, M., Dörr, H., & Levin, I. (1990). Methane consumption in aerated soils of the temperate zone. *Tellus B: Chemical and Physical Meteorology*, 42(1), 2–8. <https://doi.org/10.1034/j.1600-0889.1990.00002.x>
- Bruhwyler, L., Parmentier, F.-J. W., Crill, P., Leonard, M., & Palmer, P. I. (2021). The arctic carbon cycle and its response to changing climate. *Current Climate Change Reports*, 7(1), 14–34. <https://doi.org/10.1007/s40641-020-00169-5>
- Byrne, B., Baker, D. F., Basu, S., Bertolacci, M., Bowman, K. W., Carroll, D., et al. (2023). National CO<sub>2</sub> budgets (2015–2020) inferred from atmospheric CO<sub>2</sub> observations in support of the global stocktake. *Earth System Science Data*, 15(2), 963–1004. <https://doi.org/10.5194/essd-15-963-2023>
- Cao, M., Gregson, K., & Marshall, S. (1998). Global methane emission from wetlands and its sensitivity to climate change. *Atmospheric Environment*, 32(19), 3293–3299. [https://doi.org/10.1016/s1352-2310\(98\)00105-8](https://doi.org/10.1016/s1352-2310(98)00105-8)
- Chandra, N., Patra, P. K., Bisht, J. S. H., Ito, A., Umezawa, T., Saigusa, N., et al. (2021). Emissions from the oil and gas sectors, coal mining and ruminant farming drive methane growth over the past three decades. *Journal of the Meteorological Society of Japan Service*, 119(2), 309–337. <https://doi.org/10.2151/jmsj.2021-015>
- Chandra, N., Patra, P. K., Niwa, Y., Ito, A., Iida, Y., Goto, D., et al. (2022). Estimated regional CO<sub>2</sub> flux and uncertainty based on an ensemble of atmospheric CO<sub>2</sub> inversions. *Atmospheric Chemistry and Physics*, 22(14), 9215–9243. <https://doi.org/10.5194/acp-22-9215-2022>
- Chevallier, F. (2021). Fluxes of carbon dioxide from managed ecosystems estimated by national inventories compared to atmospheric inverse modeling. *Geophysical Research Letters*, 48(15), e2021GL093565. <https://doi.org/10.1029/2021GL093565>
- Cho, Y., Kim, H., Park, R. J., & Kim, S.-W. (2025). Unprecedented east Siberian wildfires intensify Arctic snow darkening through enhanced poleward transport of black carbon. *Science of The Total Environment*, 961, 178423. <https://doi.org/10.1016/j.scitotenv.2025.178423>
- Ciais, P., Bastos, A., Chevallier, F., Lauerwald, R., Poulter, B., Canadell, J. G., et al. (2022). Definitions and methods to estimate regional land carbon fluxes for the second phase of the REgional Carbon Cycle Assessment and Processes Project (RECCAP-2). *Geoscientific Model Development*, 15(3), 1289–1316. <https://doi.org/10.5194/gmd-15-1289-2022>

- Clelland, A. A., Marshall, G. J., Baxter, R., Potter, S., Talucci, A. C., Rady, J. M., et al. (2024). Annual and seasonal patterns of burned area products in arctic-boreal North America and Russia for 2001–2020. *Remote Sensing*, 16(17), 3306. <https://doi.org/10.3390/rs16173306>
- Commene, R., Lindaas, J., Benmergui, J., Luus, K. A., Chang, R. Y.-W., Daube, B. C., et al. (2017). Carbon dioxide sources from Alaska driven by increasing early winter respiration from arctic tundra. *Proceedings of the National Academy of Sciences*, 114(21), 5361–5366. <https://doi.org/10.1073/pnas.1618567114>
- Curry, C. L. (2007). Modeling the soil consumption of atmospheric methane at the global scale. *Global Biogeochemical Cycles*, 21(4), GB4012. <https://doi.org/10.1029/2006GB002818>
- Dalsgaard, L., Astrup, R., Antón-Fernández, C., Borgen, S. K., Breidenbach, J., Lange, H., et al. (2016). Modeling soil carbon dynamics in northern forests: Effects of spatial and temporal aggregation of climatic input data. *PLoS One*, 11(2), e0149902. <https://doi.org/10.1371/journal.pone.0149902>
- D'Andrea, M., Fiorucci, P., & Holmes, T. P. (2010). A stochastic forest fire model for future land cover scenarios assessment. *Natural Hazards and Earth System Sciences*, 10, 2161–2167. <https://doi.org/10.5194/nhess-10-2161-2010>
- Delwiche, K. B., Knox, S. H., Malhotra, A., Fluet-Chouinard, E., McNicol, G., Feron, S., et al. (2021). FLUXNET-CH<sub>4</sub>: A global, multi-ecosystem dataset and analysis of methane seasonality from freshwater wetlands. *Earth System Science Data*, 13(7), 3607–3689. <https://doi.org/10.5194/essd-13-3607-2021>
- Deng, Z., Ciais, P., Tzompa-Sosa, Z. A., Saunio, M., Qiu, C., Tan, C., et al. (2022). Comparing national greenhouse gas budgets reported in UNFCCC inventories against atmospheric inversions. *Earth System Science Data*, 14(4), 1639–1675. <https://doi.org/10.5194/essd-14-1639-2022>
- de Wit, H. A., Palosuo, T., Hylen, G., & Liski, J. (2006). A carbon budget of forest biomass and soils in southeast Norway calculated using a widely applicable method. *Forest Ecology and Management*, 225(1), 15–26. <https://doi.org/10.1016/j.foreco.2005.12.023>
- Dolman, A. J., Shvidenko, A., Schepaschenko, D., Ciais, P., Tchepakova, N., Chen, T., et al. (2012). An estimate of the terrestrial carbon budget of Russia using inventory-based, eddy covariance and inversion methods. *Biogeosciences*, 9(12), 5323–5340. <https://doi.org/10.5194/bg-9-5323-2012>
- Dörr, H., Katruff, L., & Levin, I. (1993). Soil texture parameterization of the methane uptake in aerated soils. *Chemosphere*, 26(1), 697–713. [https://doi.org/10.1016/0045-6535\(93\)90454-D](https://doi.org/10.1016/0045-6535(93)90454-D)
- Drake, T. W., Tank, S. E., Zhulidov, A. V., Holmes, R. M., Gurtovaya, T., & Spencer, R. G. M. (2018). Increasing alkalinity export from large Russian arctic Rivers. *Environmental Science & Technology*, 52(15), 8302–8308. <https://doi.org/10.1021/acs.est.8b01051>
- Dutaur, L., & Verchot, L. V. (2007). A global inventory of the soil CH<sub>4</sub> sink. *Global Biogeochemical Cycles*, 21(4), GB4013. <https://doi.org/10.1029/2006GB002734>
- Etiopie, G., Ciotoli, G., Schwietzke, S., & Schoell, M. (2019). Gridded maps of geological methane emissions and their isotopic signature. *Earth System Science Data*, 11(1), 1–22. <https://doi.org/10.5194/essd-11-1-2019>
- Etiopie, G., Lassey, K. R., Klusman, R. W., & Boschi, E. (2008). Reappraisal of the fossil methane budget and related emission from geologic sources. *Geophysical Research Letters*, 35(9), L09307. <https://doi.org/10.1029/2008GL033623>
- Fahey, T. J., Siccama, T. G., Driscoll, C. T., Likens, G. E., Campbell, J., Johnson, C. E., et al. (2005). The biogeochemistry of carbon at Hubbard Brook. *Biogeochemistry*, 75(1), 109–176. <https://doi.org/10.1007/s10533-004-6321-y>
- Fan, L., & Han, W. (2020). Soil respiration after forest conversion to tea gardens: A chronosequence study. *Catena*, 190, 104532. <https://doi.org/10.1016/j.catena.2020.104532>
- FAO. (2005). *State of the World's forests 2005*. FAO. Retrieved from <https://openknowledge.fao.org/handle/20.500.14283/y5574e>
- Filipchuk, A. N., Malysheva, N. V., Zolina, T. A., Fedorov, S. V., Berdov, A. M., Kositsyn, V. N., et al. (2022). Analytical review of the quantitative and qualitative characteristics of forests in the Russian Federation: Results of the first cycle of the state forest inventory. *Forestry Information*, 1, 5–34. <https://doi.org/10.24419/LHL.2304-3083.2022.1.01>
- Filipchuk, A. N., Malysheva, N. V., Zolina, T. A., & Seleznev, A. A. (2023). Carbon stock in living biomass of Russian forests: New quantification based on data from the first cycle of the state forest inventory. *Central European Forestry Journal*, 69(4), 248–261. <https://doi.org/10.2478/forj-2023-0021>
- Friedlingstein, P., O'Sullivan, M., Jones, M. W., Andrew, R. M., Bakker, D. C. E., Hauck, J., et al. (2023). Global carbon budget 2023. *Earth System Science Data*, 15(12), 5301–5369. <https://doi.org/10.5194/essd-15-5301-2023>
- Friedlingstein, P., O'Sullivan, M., Jones, M. W., Andrew, R. M., Hauck, J., Landschützer, P., et al. (2025). Global carbon budget 2024. *Earth System Science Data*, 17(3), 965–1039. <https://doi.org/10.5194/essd-17-965-2025>
- Frolova, N. L., Kireeva, M. B., Kharlamov, M. A., Samsonov, T. E., Entin, A. L., & Lurie, I. K. (2020). Mapping the current state and transformation of the water regime of Rivers in the European territory of Russia. *Geodesy and Cartography*, 96(1), 14–26. <https://doi.org/10.22389/0016-7126-2020-961-7-14-26>
- Gagarin, Y. N., Dobrovolsky, A. A., & Smirnov, A. P. (2019). Situation with protection of forests against illegal loggings in Russian Federation. *Forest Science Issues*, 2(4), 1–22. <https://doi.org/10.31509/2658-607x-2019-2-4-1-22>
- Galkin, S. S. (Ed.) (2022). *Russian Statistical yearbook 2022*. Moscow: Federal state Statistical service (ROSSTAT). Retrieved from <https://rosstat.gov.ru/folder/210/document/12994>
- Gasser, T., Crepin, L., Quilcaille, Y., Houghton, R. A., Ciais, P., & Obersteiner, M. (2020). Historical CO<sub>2</sub> emissions from land use and land cover change and their uncertainty. *Biogeosciences*, 17(15), 4075–4101. <https://doi.org/10.5194/bg-17-4075-2020>
- Gelfan, A., Frolova, N., Magritsky, D., Kireeva, M., Grigoriev, V., Motovilov, Y., & Gusev, Y. (2021). Climate change impact on annual and maximum runoff of Russian rivers: Diagnosis and projections. *Fundamental and Applied Climatology*, 7(1), 36–79. <https://doi.org/10.21513/2410-8758-2021-1-36-79>
- Glagolev, M. V., & Filippov, I. V. (2011). Inventory of soil methane consumption. *Environmental Dynamics and Global Climate Change*, 2(2), 3–22. <https://doi.org/10.17816/edgcc221>
- Glagolev, M. V., Sabrekov, A. F., Kleptsova, I. E., Filippov, I. V., Lapshina, E. D., Machida, T., & Maksyutov, S. S. (2012). Methane emission from bogs in the subtaiga of Western Siberia: The development of standard model. *Eurasian Soil Science*, 45(10), 947–957. <https://doi.org/10.1134/S106422931210002X>
- Goldstein, A. H., & Galbally, I. E. (2007). Known and unexplored organic constituents in the Earth's atmosphere. *Environmental Science & Technology*, 41(5), 1514–1521. <https://doi.org/10.1021/es072476p>
- Goll, D. S., Vuichard, N., Maignan, F., Jornet-Puig, A., Sardans, J., Violette, A., et al. (2017). A representation of the phosphorus cycle for ORCHIDEE (revision 4520). *Geoscientific Model Development*, 10(10), 3745–3770. <https://doi.org/10.5194/gmd-10-3745-2017>
- Golubiyatnikov, L. L., Mokhov, I. I., Denisov, E. A., & Tikhonov, V. A. (2005). Model estimates of climate change impact on the vegetation cover and atmospheric carbon sink. *Izvestiya RAS. Atmospheric and Oceanic Physics*, 41(1), 25–35.



- Golubiatnikov, L. L., & Svirezhev, Y. M. (2008). Life-cycle model of terrestrial carbon exchange. *Ecological Modelling*, 213(2), 202–208. <https://doi.org/10.1016/j.ecolmodel.2007.12.001>
- Gordeev, V. V., Pokrovsky, O. S., Zhulidov, A. V., Filippov, A. S., Gurtovaya, T. Y., Holmes, R. M., et al. (2024). Dissolved Major and trace elements in the largest Eurasian Arctic Rivers: Ob, Yenisey, Lena, and Kolyma. *Water*, 16(2), 316. <https://doi.org/10.3390/w16020316>
- Gower, S. T., Krankina, O., Olson, R. J., Apps, M., Linder, S., & Wang, C. (2001). Net primary production and carbon allocation patterns of boreal Forest ecosystems. *Ecological Applications*, 11(5), 1395–1411. <https://doi.org/10.2307/3060928>
- Grosso, S. J. D., Parton, W. J., Mosier, A. R., Ojima, D. S., Potter, C. S., Borken, W., et al. (2000). General CH<sub>4</sub> oxidation model and comparisons of CH<sub>4</sub> Oxidation in natural and managed systems. *Global Biogeochemical Cycles*, 14(4), 999–1019. <https://doi.org/10.1029/1999GB001226>
- Gustafson, E. J., Lucash, M. S., Shvidenko, A. Z., Sturtevant, B. R., Miranda, B. R., Schepaschenko, D., & Matsumoto, H. (2024). Climate change and disturbance interact to alter landscape reflectivity (albedo) in boreal forests across a large latitudinal gradient in Siberia. *Science of The Total Environment*, 956, 177043. <https://doi.org/10.1016/j.scitotenv.2024.177043>
- Hallquist, M., Wenger, J. C., Baltensperger, U., Rudich, Y., Simpson, D., Claeys, M., et al. (2009). The formation, properties and impact of secondary organic aerosol: Current and emerging issues. *Atmospheric Chemistry and Physics*, 9(14), 5155–5236. <https://doi.org/10.5194/acp-9-5155-2009>
- Hansen, M. C., Potapov, P. V., Moore, R., Hancher, M., Turubanova, S. A., Tyukavina, A., et al. (2013). High-Resolution global maps of 21st-Century forest cover change. *Science*, 342(6160), 850–853. <https://doi.org/10.1126/science.1244693>
- Hansis, E., Davis, S. J., & Pongratz, J. (2015). Relevance of methodological choices for accounting of land use change carbon fluxes. *Global Biogeochemical Cycles*, 29(8), 1230–1246. <https://doi.org/10.1002/2014GB004997>
- Harmon, M. E., Bond-Lamberty, B., Tang, J., & Vargas, R. (2011). Heterotrophic respiration in disturbed forests: A review with examples from North America. *Journal of Geophysical Research*, 116(G4), G00K04. <https://doi.org/10.1029/2010JG001495>
- Harris, N. L., Gibbs, D. A., Baccini, A., Birdsey, R. A., de Bruin, S., Farina, M., et al. (2021). Global maps of twenty-first century forest carbon fluxes. *Nature Climate Change*, 11(3), 1–7. <https://doi.org/10.1038/s41558-020-00976-6>
- Harris, R. K., Bartlett, S., Froking, S., & Crill, P. (1993). Methane emissions from northern high latitude wetlands. In *Biogeochemistry of global change: Radiatively active trace gases* (pp. 449–486). Chapman and Hall.
- Houghton, R. A., & Castanho, A. (2023). Annual emissions of carbon from land use, land-use change, and forestry from 1850 to 2020. *Earth System Science Data*, 15(5), 2025–2054. <https://doi.org/10.5194/essd-15-2025-2023>
- Hu, Y., Christensen, E., Restuccia, F., & Rein, G. (2019). Transient gas and particle emissions from smouldering combustion of peat. *Proceedings of the Combustion Institute*, 37(3), 4035–4042. <https://doi.org/10.1016/j.proci.2018.06.008>
- Hugelius, G., Loisel, J., Chadburn, S., Jackson, R. B., Jones, M., MacDonald, G., et al. (2020). Large stocks of peatland carbon and nitrogen are vulnerable to permafrost thaw. *Proceedings of the National Academy of Sciences*, 117(34), 20438–20446. <https://doi.org/10.1073/pnas.1916387117>
- Hugelius, G., Ramage, J., Burke, E., Chatterjee, A., Smallman, T. L., Aalto, T., et al. (2024). Permafrost region greenhouse gas budgets suggest a weak CO<sub>2</sub> sink and CH<sub>4</sub> and N<sub>2</sub>O sources, but magnitudes differ between top-down and Bottom-Up methods. *Global Biogeochemical Cycles*, 38(10), e2023GB007969. <https://doi.org/10.1029/2023GB007969>
- Iavorivska, L., Boyer, E. W., & DeWalle, D. R. (2016). Atmospheric deposition of organic carbon via precipitation. *Atmospheric Environment*, 146, 153–163. <https://doi.org/10.1016/j.atmosenv.2016.06.006>
- Inguaggiato, S., Cardellini, C., Taran, Y., & Kalacheva, E. (2017). The CO<sub>2</sub> flux from hydrothermal systems of the karymsky volcanic centre, Kamchatka. *Journal of Volcanology and Geothermal Research*, 346, 1–9. <https://doi.org/10.1016/j.jvolgeores.2017.07.012>
- Isaev, A. S. (Ed.) (1997). In *Program of extraordinary activities on biological struggle with pests in forests of Krasnoyarsk kray*. Federal Forest Service of Russia.
- Isidorov, V. A. (1994). Volatile emissions of plant: Composition, emission rate, and ecological significance. *Sankt-Petersburg: Alga-Fund*.
- Isidorov, V. A. (2001). *Organic chemistry of the atmosphere*. Chemical Literature Publishing House.
- Ito, A., Nishina, K., Ishijima, K., Hashimoto, S., & Inatomi, M. (2018). Emissions of nitrous oxide (N<sub>2</sub>O) from soil surfaces and their historical changes in east Asia: A model-based assessment | progress in Earth and planetary science | full text. *Progress in Earth and Planetary Science*, 5(55), 55. <https://doi.org/10.1186/s40645-018-0215-4>
- Johnson, M. S., Matthews, E., Bastviken, D., Deemer, B., Du, J., & Genovese, V. (2021). Spatiotemporal methane emission from global reservoirs. *Journal of Geophysical Research: Biogeosciences*, 126(8), e2021JG006305. <https://doi.org/10.1029/2021JG006305>
- Johnson, M. S., Matthews, E., Du, J., Genovese, V., & Bastviken, D. (2022). Methane emission from global Lakes: New spatiotemporal data and observation-driven modeling of methane dynamics indicates lower emissions. *Journal of Geophysical Research: Biogeosciences*, 127(7), e2022JG006793. <https://doi.org/10.1029/2022JG006793>
- Jones, M. W., Andrew, R. M., Peters, G. P., Janssens-Maenhout, G., De-Gol, A. J., Ciais, P., et al. (2021). Gridded fossil CO<sub>2</sub> emissions and related O<sub>2</sub> combustion consistent with national inventories 1959–2018. *Scientific Data*, 8(1), 2. <https://doi.org/10.1038/s41597-020-00779-6>
- Jones, M. W., Veraverbeke, S., Andela, N., Doerr, S. H., Kolden, C., Mataveli, G., et al. (2024). Global rise in forest fire emissions linked to climate change in the extratropics. *Science*, 386(6719), ead15889. <https://doi.org/10.1126/science.ad15889>
- Jung, M., Schwalm, C., Migliavacca, M., Walther, S., Camps-Valls, G., Koirala, S., et al. (2020). Scaling carbon fluxes from eddy covariance sites to globe: Synthesis and evaluation of the FLUXCOM approach. *Biogeosciences*, 17(5), 1343–1365. <https://doi.org/10.5194/bg-17-1343-2020>
- Karelin, D. V., Goriachkin, S. V., Zamolodchikov, D. G., Dolgikh, A. V., Zazovskaya, E. P., Shishkov, V. A., et al. (2016). The influence of local anthropogenic factors on soil emission of biogenic greenhouse gases in cryogenic ecosystems. *Biology Bulletin Reviews*, 77(3), 167–181.
- Karelin, D. V., Goryachkin, S., Zazovskaya, E., Shishkov, V., Pochikalov, A., Dolgikh, A., et al. (2020). Greenhouse gas emission from the cold soils of Eurasia in natural settings and under human impact: Controls on spatial variability. *Geoderma Regional*, 22, e00290. <https://doi.org/10.1016/j.geodrs.2020.e00290>
- Karelin, D. V., & Zamolodchikov, D. G. (2008). *Carbon exchange in cryogenic ecosystems*. Nauka.
- Karger, D. N., Conrad, O., Böhrer, J., Kawohl, T., Kreft, H., Soria-Auza, R. W., et al. (2017). Climatologies at high resolution for the earth's land surface areas. *Scientific Data*, 4(1), 170122. <https://doi.org/10.1038/sdata.2017.122>
- Kendall, M. G., & Stuart, A. (1966). *Distribution theory*. Nauka.
- Kesselmeier, J., Ciccioli, P., Kuhn, U., Stefani, P., Biesenthal, T., Rottenberger, S., et al. (2002). Volatile organic compound emissions in relation to plant carbon fixation and the terrestrial carbon budget. *Global Biogeochemical Cycles*, 16(4), 73–173–9. <https://doi.org/10.1029/2001GB001813>
- Kharuk, V. I., Im, S. T., Petrov, I. A., Dvinskaya, M. L., Shushpanov, A. S., & Golyukov, A. S. (2021). Climate-driven conifer mortality in siberia. *Global Ecology and Biogeography*, 30(2), 543–556. <https://doi.org/10.1111/geb.13243>
- Kirschke, S., Bousquet, P., Ciais, P., Saunoy, M., Canadell, J. G., Dlugokencky, E. J., et al. (2013). Three decades of global methane sources and sinks. *Nature Geoscience*, 6(10), 813–823. <https://doi.org/10.1038/ngeo1955>



- Kleinschmit, D. (2016). *Illegal logging and related timber trade – Dimensions, drivers, impacts and responses. A global scientific rapid response assessment report*. IUFRO, 146. Retrieved from <https://www.iufro.org/publications/series/world-series/article/2016/12/03/world-series-vol-35-illegal-logging-and-related-timber-trade-dimensions-drivers-impacts-and-t/>
- Korotkov, V. N., Romanovskaya, A. A., Karelin, D. V., Kurganova, I. N., Sirin, A. A., Korzukhin, M. D., et al. (2023). Assessment of greenhouse gas flows in ecosystems of regions of the Russian Federation. In A. A. Romanovskaya (Ed.), *Assessment of greenhouse gas flows in ecosystems of regions of the Russian Federation* (pp. 45–345). Yu. A. Izrael Institute of Global Climate and Ecology
- Kudeyarov, V. N. (2018). Soil respiration and biogenic carbon dioxide sink in the territory of Russia: An analytical review. *Eurasian Soil Science*, 51(6), 599–612. <https://doi.org/10.1134/S1064229318060091>
- Kudeyarov, V. N., & Kurganova, I. N. (1998). Carbon dioxide emissions and net primary production of Russian terrestrial ecosystems. *Biology and Fertility of Soils*, 27(3), 246–250. <https://doi.org/10.1007/s003740050428>
- Kudeyarov, V. N., & Kurganova, I. N. (2005). Respiration of Russian soils: Database analysis, long-term monitoring, and general estimates. *Eurasian Soil Science*, 38(9), 983–992.
- Kuhn, M. A., Varner, R. K., Bastviken, D., Crill, P., MacIntyre, S., Turetsky, M., et al. (2021). BAWLD-CH<sub>4</sub>: A comprehensive dataset of methane fluxes from boreal and arctic ecosystems. *Earth System Science Data*, 13(11), 5151–5189. <https://doi.org/10.5194/essd-13-5151-2021>
- Kurganova, I. N. (2003). *Carbon dioxide emissions from soils of Russian terrestrial ecosystems (interim report no. IR-02-070)*. IIASA, 69. Retrieved from <https://pure.iiasa.ac.at/id/eprint/6717/>
- Kurganova, I. N., Lopes de Gerenyu, V. O., Zengaliyev, A. T., & Kudeyarov, V. N. (2019). Carbon budget in the steppe ecosystems of Russia. *RAS Reports*, 485(No 6), 732–735.
- Kurganova, I. N., Lopes de Gerenyu, V., & Kuzyakov, Y. (2015). Large-scale carbon sequestration in post-agrogenic ecosystems in Russia and Kazakhstan. *Catena*, 133, 461–466. <https://doi.org/10.1016/j.catena.2015.06.002>
- Kurganova, I. N., Lopes de Gerenyu, V. O., Shvidenko, A. Z., & Sapozhnikov, P. M. (2010). Changes in the organic carbon pool of abandoned soils in Russia (1990–2004). *Eurasian Soil Science*, 43(3), 333–340. <https://doi.org/10.1134/s1064229310030129>
- Kuzmichev, E. P., Trushina, I. G., & Lopatin, E. V. (2018). Volumes of illegal forest logging in Russian Federation. *Forestry Information*, 1, 63–77. <https://doi.org/10.24419/LHI.2304-3083.2018.1.06>
- Lapenis, A., Shvidenko, A., Shepaschenko, D., Nilsson, S., & Aiyer, A. (2005). Acclimation of Russian forests to recent changes in climate. *Global Change Biology*, 11(12), 2090–2102. <https://doi.org/10.1111/j.1365-2486.2005.001069.x>
- Lauerwald, R., Allen, G. H., Deemer, B. R., Liu, S., Maavara, T., Raymond, P., et al. (2023). Inland water greenhouse gas budgets for RECCAP2: 2. Regionalization and homogenization of estimates. *Global Biogeochemical Cycles*, 37(5), e2022GB007658. <https://doi.org/10.1029/2022GB007658>
- Li, W., Ciais, P., Wang, Y., Peng, S., Broquet, G., Ballantyne, A. P., et al. (2016). Reducing uncertainties in decadal variability of the global carbon budget with multiple datasets. *Proceedings of the National Academy of Sciences*, 113(46), 13104–13108. <https://doi.org/10.1073/pnas.1603956113>
- Lindfors, V., & Laurila, T. (2000). Biogenic volatile organic compound (VOC) emissions from forests in Finland. *Boreal Environment Research*, 5(2), 95–113.
- Lindfors, V., Laurila, T., Hakola, H., Steinbrecher, R., & Rinne, J. (2000). Modeling speciated terpenoid emissions from the European boreal forest. *Atmospheric Environment*, 34(29), 4983–4996. [https://doi.org/10.1016/S1352-2310\(00\)00223-5](https://doi.org/10.1016/S1352-2310(00)00223-5)
- Liski, J., Perruchoud, D., & Karjalainen, T. (2002). Increasing carbon stocks in the forest soils of Western Europe. *Forest Ecology and Management*, 169(1–2), 159–175. [https://doi.org/10.1016/S0378-1127\(02\)00306-7](https://doi.org/10.1016/S0378-1127(02)00306-7)
- Liu, Y. Y., van Dijk, A. I. J. M., de Jeu, R. A. M., Canadell, J. G., McCabe, M. F., Evans, J. P., & Wang, G. (2015). Recent reversal in loss of global terrestrial biomass. *Nature Climate Change*, 5(5), 470–474. <https://doi.org/10.1038/nclimate2581>
- López-Blanco, E., Exbrayat, J.-F., Lund, M., Christensen, T. R., Tamstorf, M. P., Slevin, D., et al. (2019). Evaluation of terrestrial pan-arctic carbon cycling using a data-assimilation system. *Earth System Dynamics*, 10(2), 233–255. <https://doi.org/10.5194/esd-10-233-2019>
- Ludwig, B., Teepe, R., Lopes de Gerenyu, V., & Flessa, H. (2006). CO<sub>2</sub> and N<sub>2</sub>O emissions from gleyic soils in the Russian tundra and a German forest during freeze–thaw Periods—A microcosm study. *Soil Biology and Biochemistry*, 38(12), 3516–3519. <https://doi.org/10.1016/j.soilbio.2006.06.006>
- Ludwig, S. M., Schiferl, L., Hung, J., Natali, S. M., & Commane, R. (2023). Resolving heterogeneous fluxes from tundra halves the growing season carbon budget. *Biogeosciences Discussions*, 1–30. preprint(bg-2023-119). <https://doi.org/10.5194/bg-2023-119>
- Magritsky, D. V. (2022). New data on the distribution of the water runoff in the northeast of Russia and the water flow into arctic seas. *Water Management in Russia: Problems, Technologies, Management*, 6, 70–85. [https://doi.org/10.35567/19994508\\_2022\\_6\\_5](https://doi.org/10.35567/19994508_2022_6_5)
- Maksyutov, S., Machida, T., Mukai, H., Patra, P. K., Nakazawa, T., Inoue, G., et al. (2003). Effect of recent observations on Asian CO<sub>2</sub> flux estimates by transport model inversions. *Tellus Series B Chemical and Physical Meteorology*, 55(2), 522–529. <https://doi.org/10.1034/j.1600-0889.2003.00052.x>
- Man'ko, Y. I., & Gladkova, G. A. (2001). Spruce decline in the light of global deterioration of dark-coniferous forests. *Vladivostok*. Retrieved from [https://www.phantastike.com/nature/spruce\\_shrinking\\_light/pdf/](https://www.phantastike.com/nature/spruce_shrinking_light/pdf/)
- McGlynn, E., Li, S., F. Berger, M., Amend, M., & L. Harper, K. (2022). Addressing uncertainty and bias in land use, land use change, and forestry greenhouse gas inventories. *Climatic Change*, 170(1), 5. <https://doi.org/10.1007/s10584-021-03254-2>
- McGuire, A. D., Christensen, T. R., Hayes, D., Heroult, A., Euskirchen, E., Kimball, J. S., et al. (2012). An assessment of the carbon balance of arctic tundra: Comparisons among observations, process models, and atmospheric inversions. *Biogeosciences*, 9(8), 3185–3204. <https://doi.org/10.5194/bg-9-3185-2012>
- McGuire, A. D., Hayes, D. J., Kicklighter, D. W., Zhuang, Q., Chen, M., Gurney, R. K., et al. (2010). Analysis of the carbon balance of boreal Asia from 1997 to 2006. In *Proc. Int. Conf. On environmental observations, modeling and information system ENVIROMIS* (pp. 53–58).
- McNicol, G., Fluet-Chouinard, E., Ouyang, Z., Knox, S., Zhang, Z., Aalto, T., et al. (2023). Upscaling wetland methane emissions from the FLUXNET-CH<sub>4</sub> eddy covariance network (UpCH<sub>4</sub> v1.0): Model development, network assessment, and budget comparison. *AGU Advances*, 4(5), e2023AV000956. <https://doi.org/10.1029/2023AV000956>
- Meroni, M., Mollicone, D., Belelli, L., Manca, G., Rosellini, S., Stivanello, S., et al. (2002). Carbon and water exchanges of regenerating forests in central siberia. *Forest Ecology and Management*, 169(1), 115–122. [https://doi.org/10.1016/S0378-1127\(02\)00302-X](https://doi.org/10.1016/S0378-1127(02)00302-X)
- Moiseev, B. N., & Alyabina, I. O. (2007). Evaluation and mapping of the components of carbon and nitrogen balances in the main biomes of Russia. *Izvestia of the Russian Academy of Sciences. Geographical series*, 5, 116–127.
- Morishita, T., Hatano, R., & Desyatkin, R. V. (2003). CH<sub>4</sub> flux in an alas ecosystem formed by forest disturbance near yakutsk, eastern siberia, Russia. *Soil Science & Plant Nutrition*, 49(3), 369–377. <https://doi.org/10.1080/00380768.2003.10410022>

- Morishita, T., Matsuura, Y., Kajimoto, T., Osawa, A., Zyryanova, O. A., & Prokushkin, A. S. (2014). CH<sub>4</sub> and N<sub>2</sub>O dynamics of a Larix gmelinii forest in a continuous permafrost region of central siberia during the growing season. *Polar Science*, 8(2), 156–165. <https://doi.org/10.1016/j.polar.2014.01.004>
- Morishita, T., Matsuura, Y., Zyryanova, O. A., & Prokushkin, A. S. (2006). CO<sub>2</sub>, CH<sub>4</sub> and N<sub>2</sub>O fluxes from a larch forest soil in central siberia. In R. Hatano & G. Guggenberger (Eds.), *Symptom of environmental change in Siberian permafrost region* (pp. 1–9).
- Mörner, N.-A., & Etiope, G. (2002). Carbon degassing from the lithosphere. *Global and Planetary Change*, 33(1), 185–203. [https://doi.org/10.1016/S0921-8181\(02\)00070-X](https://doi.org/10.1016/S0921-8181(02)00070-X)
- Mukhortova, L. V., Schepaschenko, D., Moltchanova, E., Shvidenko, A., Khabarov, N., & See, L. (2021). Respiration of Russian soils: Climatic drivers and response to climate change. *Science of The Total Environment*, 785, 147314. <https://doi.org/10.1016/j.scitotenv.2021.147314>
- Mukhortova, L. V., Schepaschenko, D., & Shvidenko, A. (2020). Soil respiration database [Dataset]. *IIASA PURE*. <https://doi.org/10.22022/ESM/10-2020.107>
- Nakano, T., Inoue, G. E. N., & Fukuda, M. (2004). Methane consumption and soil respiration by a birch forest soil in west siberia. *Tellus B: Chemical and Physical Meteorology*, 56(3), 223–229. <https://doi.org/10.3402/tellusb.v56i3.16421>
- Nilsson, S., Shvidenko, A., Jonas, M., McCallum, I., Thomson, A., & Baltzer, H. (2007). Uncertainties of a regional terrestrial biota full carbon account: A systems analysis. *Water, Air, and Soil Pollution: Focus*, 7, 425–441. [https://doi.org/10.1007/978-1-4020-5930-8\\_2](https://doi.org/10.1007/978-1-4020-5930-8_2)
- Nilsson, S., Shvidenko, A., Stolbovoi, V., Gluck, M., Jonas, M., & Obersteiner, M. (2000). Full carbon account for Russia (interim report no. IR-00-021), 180. Retrieved from <https://pure.iiasa.ac.at/id/eprint/6224/>
- Nilsson, S., Vaganov, E. A., Shvidenko, A. Z., Stolbovoi, V., Rozhkov, V. A., MacCallum, I., & Ionas, M. (2003). Carbon budget of vegetation ecosystems of Russia. *Doklady Earth Sciences*, 393, 1281–1283.
- NIR. (2024). *National inventory report of anthropogenic emissions by sources and removals by sinks of GHGs of the Russian Federation. National inventory document*. Roshydromet, 406. Retrieved from <https://unfccc.int/documents/645136>
- Noskova, T. V., Lovtskaya, O. V., Panina, M. S., Podchufarova, D. P., & Papina, T. S. (2022). Organic carbon in atmospheric precipitation in the urbanized territory of the south of Western siberia, Russia. *Pure and Applied Chemistry*, 94(3), 309–315. <https://doi.org/10.1515/pac-2021-0321>
- Nozhevnikova, A., Glagolev, M., Nekrasova, V., Einola, J., Sormunen, K., & Rintala, J. (2003). The analysis of methods for measurement of methane oxidation in landfills. *Water Science and Technology*, 48, 45–52. <https://doi.org/10.2166/wst.2003.0218>
- Olefeldt, D., Hovemyr, M., Kuhn, M. A., Bastviken, D., Bohn, T. J., Connolly, J., et al. (2021). The boreal–arctic wetland and lake dataset (BAWLD). *Earth System Science Data*, 13(11), 5127–5149. <https://doi.org/10.5194/essd-13-5127-2021>
- Olin, S., Lindeskog, M., Pugh, T. A. M., Schurgers, G., Wärilind, D., Mishurov, M., et al. (2015). Soil carbon management in large-scale Earth system modelling: Implications for crop yields and nitrogen leaching. *Earth System Dynamics*, 6(2), 745–768. <https://doi.org/10.5194/esd-6-745-2015>
- O'Sullivan, M., Sitch, S., Friedlingstein, P., Luijckx, I. T., Peters, W., Rosan, T. M., et al. (2024). The key role of forest disturbance in reconciling estimates of the northern carbon sink. *Communications Earth and Environment*, 5(1), 1–10. <https://doi.org/10.1038/s43247-024-01827-4>
- Pan, Y., Birdsey, R. A., Phillips, O. L., Houghton, R. A., Fang, J., Kauppi, P. E., et al. (2024). The enduring world forest carbon sink. *Nature*, 631(8021), 563–569. <https://doi.org/10.1038/s41586-024-07602-x>
- Pan, Y., Wang, Y., Xin, J., Tang, G., Song, T., Wang, Y., et al. (2010). Study on dissolved organic carbon in precipitation in northern China. *Atmospheric Environment*, 44(19), 2350–2357. <https://doi.org/10.1016/j.atmosenv.2010.03.033>
- Parazoo, N. C., Commane, R., Wofsy, S. C., Koven, C. D., Sweeney, C., Lawrence, D. M., et al. (2016). Detecting regional patterns of changing CO<sub>2</sub> flux in Alaska. *Proceedings of the National Academy of Sciences of the United States of America*, 113(28), 7733–7738. <https://doi.org/10.1073/pnas.1601085113>
- Patra, P. K., Dlugokencky, E. J., Elkins, J. W., Dutton, G. S., Tohjima, Y., Sasakawa, M., et al. (2022). Forward and inverse modelling of atmospheric nitrous oxide using MROCA-Atmospheric chemistry-transport model. *Journal of the Meteorological Society of Japan. Ser. II*, 100(2), 361–386. <https://doi.org/10.2151/jmsj.2022-018>
- Patra, P. K., Houweling, S., Krol, M., Bousquet, P., Belikov, D., Bergmann, D., et al. (2011). TransCom model simulations of CH<sub>4</sub> and related species: Linking transport, surface flux and chemical loss with CH<sub>4</sub> variability in the troposphere and lower stratosphere. *Atmospheric Chemistry and Physics*, 11(24), 12813–12837. <https://doi.org/10.5194/acp-11-12813-2011>
- Paustian, K., Six, J., Elliott, E. T., & Hunt, H. W. (2000). Management options for reducing CO<sub>2</sub> emissions from agricultural soils. *Biogeochemistry*, 48(1), 147–163. <https://doi.org/10.1023/A:1006271331703>
- Piao, S., Wang, X., Park, T., Chen, C., Lian, X., He, Y., et al. (2020). Characteristics, drivers and feedbacks of global greening. *Nature Reviews Earth and Environment*, 1(1), 14–27. <https://doi.org/10.1038/s43017-019-0001-x>
- Potter, C. S., Davidson, E. A., & Verchot, L. V. (1996). Estimation of global biogeochemical controls and seasonality in soil methane consumption. *Chemosphere*, 32(11), 2219–2246. [https://doi.org/10.1016/0045-6535\(96\)00119-1](https://doi.org/10.1016/0045-6535(96)00119-1)
- Pulliaainen, J., Luoju, K., Derksen, C., Mudryk, L., Lemmetyinen, J., Salminen, M., et al. (2020). Patterns and trends of northern hemisphere snow mass from 1980 to 2018. *Nature*, 581(7808), 294–298. <https://doi.org/10.1038/s41586-020-2258-0>
- Quegan, S., Beer, C., Shvidenko, A., McCallum, I., Handoh, I. C., Peylin, P., et al. (2011). Estimating the carbon balance of central siberia using a landscape-ecosystem approach, atmospheric inversion and dynamic global vegetation models. *Global Change Biology*, 17(1), 351–365. <https://doi.org/10.1111/j.1365-2486.2010.02275.x>
- Ramage, J., Kuhn, M., Virkkala, A.-M., Voigt, C., Maruschak, M. E., Bastos, A., et al. (2024). The net GHG balance and budget of the permafrost region (2000–2020) from ecosystem flux upscaling. *Global Biogeochemical Cycles*, 38(4), e2023GB007953. <https://doi.org/10.1029/2023GB007953>
- Rantakari, M., Lehtonen, A., Linkosalo, T., Tuomi, M., Tamminen, P., Heikkinen, J., et al. (2012). The Yasso07 soil carbon model – Testing against repeated soil carbon inventory. *Forest Ecology and Management*, 286, 137–147. <https://doi.org/10.1016/j.foreco.2012.08.041>
- Remaud, M., Chevallier, F., Cozic, A., Lin, X., & Bousquet, P. (2018). On the impact of recent developments of the LMDz atmospheric general circulation model on the simulation of CO<sub>2</sub> transport. *Geoscientific Model Development*, 11(11), 4489–4513. <https://doi.org/10.5194/gmd-11-4489-2018>
- Repo, M. E., Susiluoto, S., Lind, S. E., Jokinen, S., Elsakov, V., Biasi, C., et al. (2009). Large N<sub>2</sub>O emissions from cryoturbated peat soil in tundra. *Nature Geoscience*, 2(3), 189–192. <https://doi.org/10.1038/ngeo434>
- Rinne, J., Bäck, J., & Hakola, H. (2009). Biogenic volatile organic compound emissions from the Eurasian taiga: Current knowledge and future directions. *Boreal Environment Research*, 14, 807–826.
- Romankevich, E. A., & Vetrov, A. A. (2001). *The carbon cycle in arctic seas of Russia*. Nauka.
- Romanovskaya, A. A. (2006). Organic carbon in long-fallow lands of Russia. *Eurasian Soil Science*, 39(1), 44–52. <https://doi.org/10.1134/S1064229306010066>

- Romanovskaya, A. A. (Ed.) (2023). In *Assessment of greenhouse gas fluxes in ecosystems of regions of the Russian Federation*. IGKE. Retrieved from [http://www.igke.ru/wp-content/uploads/2023/11/Monograph\\_corr\\_15112023\\_2.pdf](http://www.igke.ru/wp-content/uploads/2023/11/Monograph_corr_15112023_2.pdf)
- Romanovskaya, A. A., & Korotkov, V. N. (2024). Balance of anthropogenic and natural greenhouse gas fluxes of all inland ecosystems of the Russian Federation and the contribution of sequestration in forests. *Forests*, 15(4), 707. <https://doi.org/10.3390/f15040707>
- Roshydromet. (2022). Report on climate features on territory of Russian Federation in 2021. *Moscow Times: Federal Agency on Hydrometeorology of the Russian Federation*. Retrieved from <https://www.meteorf.gov.ru/images/news/20220324/4/Doklad.pdf>
- RosStat, R. F. (2019). Regions of Russia. Social and economic indicators. *Federal Agency of State Statistics of the Russian Federation*. Retrieved from <https://rosstat.gov.ru/folder/210/document/13204>
- Roy, J., Saugier, B., & Mooney, H. A. (2001). *Terrestrial global productivity*. Elsevier. Retrieved from <https://doi.org/10.1016/B978-0-12-505290-0.X5000-5>
- Rumyantsev, V. A., Koronkevich, N. I., Izmailova, A. V., Georgiadi, A. G., Zaitseva, I. S., Barabanova, E. A., et al. (2021). Water resources of Rivers, Lakes and reservoirs of Russia and anthropogenic impacts on them. *Izvestiya Rossiiskoi Akademii Nauk. Seriya Geograficheskaya*, 85(1), 120–135. <https://doi.org/10.31857/S258755662101012X>
- Sabrekov, A. F., Glagolev, M. V., Alekseychik, P. K., Smolentsev, B. A., Terentiev, I. E., Krivenok, L. A., & Maksyutov, S. S. (2016). A process-based model of methane consumption by upland soils. *Environmental Research Letters*, 11(7), 075001. <https://doi.org/10.1088/1748-9326/11/7/075001>
- Sacki, T., Maksyutov, S., Sasakawa, M., Machida, T., Arshinov, M., Tans, P., et al. (2013). Carbon flux estimation for siberia by inverse modeling constrained by aircraft and tower CO<sub>2</sub> measurements. *Journal of Geophysical Research: Atmospheres*, 118(2), 1100–1122. <https://doi.org/10.1002/jgrd.50127>
- Sasakawa, M., Shimoyama, K., Machida, T., Tsuda, N., Suto, H., Arshinov, M., et al. (2010). Continuous measurements of methane from a tower network over Siberia. *Tellus Series B Chemical and Physical Meteorology*, 62(5), 403–416. <https://doi.org/10.1111/j.1600-0889.2010.00494.x>
- Saunio, M., Martinez, A., Poulter, B., Zhang, Z., Raymond, P., Regnier, P., et al. (2025). Global Methane Budget 2000–2020. *Earth System Science Data*, 17(5), 1873–1958. <https://doi.org/10.5194/essd-17-1873-2025>
- Saunio, M., Stavert, A. R., Poulter, B., Bousquet, P., Canadell, J. G., Jackson, R. B., et al. (2020). The Global Methane Budget 2000–2017. *Earth System Science Data*, 12(3), 1561–1623. <https://doi.org/10.5194/essd-12-1561-2020>
- Schellnhuber, H. J. (2003). Integration assessments of adaptation and mitigation. In *World climate change conference* (pp. 94–95).
- Schepaschenko, D., McCallum, I., Shvidenko, A., Fritz, S., Kraxner, F., & Obersteiner, M. (2011). A new hybrid land cover dataset for Russia: A methodology for integrating statistics, remote sensing and in situ information. *Journal of Land Use Science*, 6(4), 245–259. <https://doi.org/10.1080/1747423X.2010.511681>
- Schepaschenko, D., Moltchanova, E., Fedorov, S., Karminov, V., Ontikov, P., & Santoro, M. (2020). Map of growing stock volume of Russian forests for the year 2014 (version 1) [Dataset]. *Zenodo*. <https://doi.org/10.5281/zenodo.3981198>
- Schepaschenko, D., Moltchanova, E., Fedorov, S., Karminov, V., Ontikov, P., Santoro, M., et al. (2021). Russian forest sequesters substantially more carbon than previously reported. *Scientific Reports*, 11(1), 12825. <https://doi.org/10.1038/s41598-021-92152-9>
- Schepaschenko, D., Mukhortova, L., & Shvidenko, A. (2025). Estimation of impact of disturbances on soil respiration in forest ecosystems of Russia. *Forests*, 16(6), 925. <https://doi.org/10.3390/f16060925>
- Schepaschenko, D., Mukhortova, L. V., Shvidenko, A. Z., & Vedrova, E. F. (2013). The pool of organic carbon stock in the soils of Russia. *Eurasian Soil Science*, 46(2), 107–116. <https://doi.org/10.1134/s1064229313020129>
- Schepaschenko, D., Shvidenko, A., & Moltchanova, E. (2018). Map of Russian forest for the year 2009 [Dataset]. *Zenodo*. <https://doi.org/10.5281/zenodo.6056054>
- Schepaschenko, D., Shvidenko, A., Usoltsev, V. A., Lakyda, P., Luo, Y., Vasylyshyn, R., et al. (2017). A database of forest biomass structure for Eurasia [Dataset]. *Scientific Data*, 4(1), 170070. <https://doi.org/10.1038/sdata.2017.70>
- Schulze, E. D., Ciais, P., Luyssaert, S., Schrumpp, M., Janssens, I. A., Thiruchittampalam, B., et al. (2010). The European carbon balance. Part IV: Integration of carbon and other trace-gas fluxes. *Global Change Biology*, 16(5), 1451–1469. <https://doi.org/10.1111/j.1365-2486.2010.02215.x>
- Schulze, E. D., Luyssaert, S., Ciais, P., Freibauer, A., Janssens, I. A., Soussana, J. F., et al. (2009). Importance of methane and nitrous oxide for Europe's terrestrial greenhouse-gas balance. *Nature Geoscience*, 2(12), 842–850. <https://doi.org/10.1038/ngeo686>
- Sedykh, V. N. (2009). *Forest forming process*. Nauka Publishing.
- See, L., Schepaschenko, D., Lesiv, M., McCallum, I., Fritz, S., Comber, A., et al. (2015). Building a hybrid land cover map with crowdsourcing and geographically weighted regression. *ISPRS Journal of Photogrammetry and Remote Sensing*, 103, 48–56. <https://doi.org/10.1016/j.isprsjprs.2014.06.016>
- Shvidenko, A., Mukhortova, L., Kapitsa, E., Kraxner, F., See, L., Pyzhev, A., et al. (2023). A modelling System for dead wood assessment in the forests of Northern Eurasia. *Forests*, 14(1), 45. <https://doi.org/10.3390/f14010045>
- Shvidenko, A., Mukhortova, L., Kapitsa, E., Pyzhev, A., Gordeev, R., Fedorov, S., & Schepaschenko, D. (2022). Dead wood in the forests of Northern Eurasia: Field measurements database [Dataset]. *Zenodo*. <https://doi.org/10.5281/zenodo.7455327>
- Shvidenko, A., & Nilsson, S. (2003). A synthesis of the impact of Russian forests on the global carbon budget for 1961–1998. *Tellus Series B Chemical and Physical Meteorology*, 55(2), 391–415. <https://doi.org/10.1034/j.1600-0889.2003.00046.x>
- Shvidenko, A., Nilsson, S., Rozhkov, V., & Strakhov, V. (1996). Carbon budget of the Russian boreal forests: A system analysis approach to uncertainty. In *Forest ecosystems, forest management, and the global carbon cycle* (Vol. 40, pp. 145–162). Springer Verlag.
- Shvidenko, A., Nilsson, S., Stolbovoi, V. S., Gluck, M., Shchepaschenko, D. G., & Rozhkov, V. A. (2000). Aggregated estimation of the basic parameters of biological production and the carbon budget of Russian terrestrial ecosystems: 1. Stocks of plant organic mass. *Russian Journal of Ecology*, 31(6), 371–378. <https://doi.org/10.1023/a:1026631523999>
- Shvidenko, A., & Schepaschenko, D. (2014). Carbon budget of Russian forests. *Siberian Journal of Forest Science*, 1, 69–92.
- Shvidenko, A., & Schepaschenko, D. (2021). Development of a system model for assessment of carbon emissions by Russia's forests for improvements of international reporting of Russian Federation (IMGAR-II). Science report.228
- Shvidenko, A., Schepaschenko, D., Kraxner, F., & Fritz, S. (2015). Full verified carbon account of forest ecosystems as a fuzzy system: An attempt to assess uncertainty. In *Proceedings of the 4th international workshop on uncertainties in atmospheric emissions* (pp. 1–8). Systems Research Institute, Polish Academy of Sciences. Retrieved from <https://pure.iiasa.ac.at/id/eprint/11890/>
- Shvidenko, A., Schepaschenko, D., & Maksyutov, S. (2010). Impact of terrestrial ecosystems of Russia on the global carbon cycle from 2003–2008: An attempt of synthesis. In *Int. Conf. On environmental observation, modeling and information systems* (pp. 48–52). Enviromis'2010.
- Shvidenko, A., Schepaschenko, D., & McCallum, I. (2010b). *GEF-2. Bottom-up inventory of the carbon fluxes in northern eurasia for comparison with GOSAT level 4 products. Report to the global environmental forum*. Japan. Laxenburg. IIASA.210
- Shvidenko, A., Schepaschenko, D., McCallum, I., & Nilsson, S. (2010a). Can the uncertainty of full carbon accounting of forest ecosystems be made acceptable to policymakers? *Climatic Change*, 103(1–2), 137–157. <https://doi.org/10.1007/s10584-010-9918-2>



- Shvidenko, A., Schepaschenko, D., Nilsson, S., & Bouloui, Y. (2007). Semi-empirical models for assessing biological productivity of northern Eurasian forests. *Ecological Modelling*, 204(1–2), 163–179. <https://doi.org/10.1016/j.ecolmodel.2006.12.040>
- Shvidenko, A., Schepaschenko, D. G., Nilsson, S., & Buluy, Y. I. (2008). Tables and models of growth and productivity of forests of major forest forming species of northern Eurasia. In *Federal agency of forest management* (2nd ed.) Standard and reference materials
- Shvidenko, A., Schepaschenko, D. G., Vaganov, E. A., & Nilsson, S. (2008). Net primary production of forest ecosystems of Russia: A new estimate. *Doklady Earth Sciences*, 421(2), 1009–1012. <https://doi.org/10.1134/s1028334x08060330>
- Shvidenko, A., Zamolodchikov, D., Valentini, R., & Linder, M. (2020). Ecosystem functions and services of Russia's forests. In *Russian forests and climate change* (pp. 28–34). European Forest Institute. <https://doi.org/10.36333/wscu11>
- Simpson, D., Guenther, A., Hewitt, C. N., & Steinbrecher, R. (1995). Biogenic emissions in Europe: 1. Estimates and uncertainties. *Journal of Geophysical Research*, 100(D11), 22875–22890. <https://doi.org/10.1029/95JD02368>
- Simpson, D., Winiwarter, W., Börjesson, G., Cinderby, S., Ferreiro, A., Guenther, A., et al. (1999). Inventorying emissions from nature in Europe. *Journal of Geophysical Research*, 104(D7), 8113–8152. <https://doi.org/10.1029/98JD02747>
- Sitch, S., O'Sullivan, M., Robertson, E., Friedlingstein, P., Albergel, C., Anthoni, P., et al. (2024). Trends and drivers of terrestrial sources and sinks of carbon dioxide: An overview of the TRENDY project. *Global Biogeochemical Cycles*, 38(7), e2024GB008102. <https://doi.org/10.1029/2024GB008102>
- Strand, L. T., Callesen, I., Dalsgaard, L., & de Wit, H. A. (2016). Carbon and nitrogen stocks in Norwegian forest soils—The importance of soil formation, climate, and vegetation type for organic matter accumulation. *Canadian Journal of Forest Research*, 46(12), 1459–1473. <https://doi.org/10.1139/cjfr-2015-0467>
- Tagesson, T., Schurgers, G., Horion, S., Ciais, P., Tian, F., Brandt, M., et al. (2020). Recent divergence in the contributions of tropical and boreal forests to the terrestrial carbon sink. *Nature Ecology & Evolution*, 4(2), 202–209. <https://doi.org/10.1038/s41559-019-1090-0>
- Takakai, F., Desyatkin, A. R., Lopez, C. M. L., Fedorov, A. N., Desyatkin, R. V., & Hatano, R. (2008). Influence of forest disturbance on CO<sub>2</sub>, CH<sub>4</sub> and N<sub>2</sub>O fluxes from larch forest soil in the permafrost taiga region of eastern Siberia. *Soil Science and Plant Nutrition*, 54(6), 938–949. <https://doi.org/10.1111/j.1747-0765.2008.00309.x>
- Takata, K., Patra, P. K., Kotani, A., Mori, J., Belikov, D., Ichii, K., et al. (2017). Reconciliation of top-down and bottom-up CO<sub>2</sub> fluxes in Siberian larch forest. *Environmental Research Letters*, 12(12), 125012. <https://doi.org/10.1088/1748-9326/aa926d>
- Talucci, A. C., Lorant, M. M., & Alexander, H. D. (2022). Siberian taiga and tundra fire regimes from 2001–2020. *Environmental Research Letters*, 17(2), 025001. <https://doi.org/10.1088/1748-9326/ac3f07>
- Taran, Y., Zelenski, M., Chaplygin, I., Malik, N., Campion, R., Inguaggiato, S., et al. (2018). Gas emissions from volcanoes of the kuril island arc (NW Pacific): Geochemistry and fluxes. *Geochemistry, Geophysics, Geosystems*, 19(6), 1859–1880. <https://doi.org/10.1029/2018GC007477>
- Tarvainen, V. (2008). *Development of biogenic VOC emission inventories for the boreal forest* (Finish Meteorological Institute Contribution No. 72). Finish Meteorological Institute, 64. Retrieved from <https://helda.helsinki.fi/bitstreams/274f9b7d-19b1-4ffb-963c-1f902fca335b/download>
- Tarvainen, V., Hakola, H., Rinne, J., Hellén, H., & Haapanala, S. (2007). Towards a comprehensive emission inventory of terpenoids from boreal ecosystems. *Tellus B: Chemical and Physical Meteorology*, 59(3), 526–534. <https://doi.org/10.1111/j.1600-0889.2007.00263.x>
- Terentieva, I., Glagolev, M., Maksyutov, S., & Sabrekov, A. (2024). Mapping Russian wetlands and estimating methane fluxes [Dataset]. Zenodo. <https://doi.org/10.5281/zenodo.13997236>
- Thompson, R. L., Chevallier, F., Crotwell, A. M., Dutton, G., Langenfelds, R. L., Prinn, R. G., et al. (2014). Nitrous oxide emissions 1999 to 2009 from a global atmospheric inversion. *Atmospheric Chemistry and Physics*, 14(4), 1801–1817. <https://doi.org/10.5194/acp-14-1801-2014>
- Tian, H., Chen, G., Lu, C., Xu, X., Ren, W., Zhang, B., et al. (2015). Global methane and nitrous oxide emissions from terrestrial ecosystems due to multiple environmental changes. *Ecosystem Health and Sustainability*, 1(1), 1–20. <https://doi.org/10.1890/EHS14-0015.1>
- Tian, H., Pan, N., Thompson, R. L., Canadell, J. G., Suntharalingam, P., Regnier, P., et al. (2024). Global nitrous oxide budget (1980–2020). *Earth System Science Data*, 16(6), 2543–2604. <https://doi.org/10.5194/essd-16-2543-2024>
- Tian, H., Xu, R., Canadell, J. G., Thompson, R. L., Winiwarter, W., Suntharalingam, P., et al. (2020). A comprehensive quantification of global nitrous oxide sources and sinks. *Nature*, 586(7828), 248–256. <https://doi.org/10.1038/s41586-020-2780-0>
- Tishkov, A. A., Belonovskaya, E. A., Vaisfeld, M. A., Glazov, P. M., Lappo, E. G., Morozova, O. V., et al. (2020). Regional biogeographic effects of “fast” climate changes in the Russian arctic in the 21st century. *Arctic: Ecological Economy*, 2(38), 31–44. <https://doi.org/10.25283/2223-4594-2020-2-31-44>
- Titkova, T. B., & Vinogradova, V. V. (2019). Climate change in transitional natural zones of the north of Russia and their manifestation in the spectral characteristics of landscapes. *Modern Problems of Remote Sensing of the Earth from Space*, 16(5), 310–323. <https://doi.org/10.21046/2070-7401-2019-16-5-310>
- Todd-Brown, K. E. O., Randerson, J. T., Hopkins, F., Arora, V., Hajima, T., Jones, C., et al. (2014). Changes in soil organic carbon storage predicted by Earth system models during the 21st century. *Biogeosciences*, 11(8), 2341–2356. <https://doi.org/10.5194/bg-11-2341-2014>
- Tuomi, M., Laiho, R., Repo, A., & Liski, J. (2011). Wood decomposition model for boreal forests. *Ecological Modelling*, 222(3), 709–718. <https://doi.org/10.1016/j.ecolmodel.2010.10.025>
- Tyukavina, A., Potapov, P., Hansen, M. C., Pickens, A. H., Stehman, S. V., Turubanova, S., et al. (2022). Global trends of forest loss due to fire from 2001 to 2019. *Frontiers in Remote Sensing*, 3, 825190. <https://doi.org/10.3389/frsen.2022.825190>
- Urbanski, S. P., Hao, W. M., & Baker, S. (2008). Chapter 4 chemical composition of wildland fire emissions. In A. Bytnerowicz, M. J. Arbaugh, A. R. Riebau, & C. Andersen (Eds.), *Developments in environmental science* (Vol. 8, pp. 79–107). Elsevier. [https://doi.org/10.1016/S1474-8177\(08\)00004-1](https://doi.org/10.1016/S1474-8177(08)00004-1)
- Vaschuk, L. N., & Shvidenko, A. Z. (2006). Dynamics of forests of Irkutsk region.
- Vashchuk, N. L. (2016). On reliability of the state Forest register data of the forests studied and ways to eliminate defects. *Siberian Journal of Forest Science*(4), 26–38. <https://doi.org/10.15372/SJFS20160403>
- Virkkala, A.-M., Aalto, J., Rogers, B. M., Tagesson, T., Treat, C. C., Natali, S. M., et al. (2021). Statistical upscaling of ecosystem CO<sub>2</sub> fluxes across the terrestrial tundra and boreal domain: Regional patterns and uncertainties. *Global Change Biology*, 27(17), 4040–4059. <https://doi.org/10.1111/gcb.15659>
- Virkkala, A.-M., Rogers, B. M., Watts, J. D., Arndt, K. A., Potter, S., Wargowsky, I., et al. (2024). An increasing arctic-boreal CO<sub>2</sub> sink despite strong regional sources. *bioRxiv*. <https://doi.org/10.1101/2024.02.09.579581>
- Voigt, C., Marushchak, M. E., Abbott, B. W., Biasi, C., Elberling, B., Siciliano, S. D., et al. (2020). Nitrous oxide emissions from permafrost-affected soils. *Nature Reviews Earth and Environment*, 1(8), 420–434. <https://doi.org/10.1038/s43017-020-0063-9>
- Voigt, C., Marushchak, M. E., Lamprecht, R. E., Jackowicz-Korczyński, M., Lindgren, A., Mastepanov, M., et al. (2017). Increased nitrous oxide emissions from arctic peatlands after permafrost thaw. *Proceedings of the National Academy of Sciences*, 114(24), 6238–6243. <https://doi.org/10.1073/pnas.1702902114>

- Vompersky, S. E., Sirin, A. A., Sal'nikov, A. A., Tsyganova, O. P., & Valyaeva, N. A. (2011). Estimation of forest cover extent over peatland and paludified shallow peatlands in Russia. *Contemporary Problems of Ecology*, 4(7), 734–741.
- Vompersky, S. E., Sirin, A. A., Tsyganova, O. P., Valyaeva, N. A., & Maikov, D. A. (2005). Peatlands and paludified lands of Russia: An attempt of analysis of spatial distribution and diversity. *Izvestia of the Russian Academy of Sciences. Geographical Series*, 5, 39–50.
- Voronin, P. Y. (2006). Chlorophyll index and photosynthetic carbon sequestration in northern Eurasia. *Russian Journal of Plant Physiology*, 53(5), 689–697. <https://doi.org/10.1134/S1021443706050141>
- Walter, B. P., Heimann, M., & Matthews, E. (2001). Modeling modern methane emissions from natural wetlands: 1. Model description and results. *Journal of Geophysical Research*, 106(D24), 34189–34206. <https://doi.org/10.1029/2001JD900165>
- Walter, B. P., Heimann, M., Shannon, R. D., & White, J. R. (1996). A process-based model to derive methane emissions from natural wetlands. *Geophysical Research Letters*, 23(25), 3731–3734. <https://doi.org/10.1029/96GL03577>
- Wang, T., Ciais, P., Piao, S. L., Ottlé, C., Brender, P., Maignan, F., et al. (2011). Controls on winter ecosystem respiration in temperate and boreal ecosystems. *Biogeosciences*, 8(7), 2009–2025. <https://doi.org/10.5194/bg-8-2009-2011>
- Webb, E. E., Alexander, H. D., Paulson, A. K., Loranty, M. M., DeMarco, J., Talucci, A. C., et al. (2024). Fire-Induced carbon loss and tree mortality in Siberian larch forests. *Geophysical Research Letters*, 51(1), e2023GL105216. <https://doi.org/10.1029/2023GL105216>
- Wells, K. C., Millet, D. B., Bousserez, N., Henze, D. K., Chaliyakunnel, S., Griffis, T. J., et al. (2015). Simulation of atmospheric N<sub>2</sub>O with GEOS-chem and its adjoint: Evaluation of observational constraints. *Geoscientific Model Development*, 8(10), 3179–3198. <https://doi.org/10.5194/gmd-8-3179-2015>
- Wickland, K. P., Jorgenson, M. T., Koch, J. C., Kanevskiy, M., & Striegl, R. G. (2020). Carbon dioxide and methane flux in a dynamic arctic tundra landscape: Decadal-scale impacts of ice wedge degradation and stabilization. *Geophysical Research Letters*, 47(22), e2020GL089894. <https://doi.org/10.1029/2020GL089894>
- Wilkerson, J., Dobosy, R., Sayres, D. S., Healy, C., Dumas, E., Baker, B., & Anderson, J. G. (2019). Permafrost nitrous oxide emissions observed on a landscape scale using the airborne eddy-covariance method. *Atmospheric Chemistry and Physics*, 19(7), 4257–4268. <https://doi.org/10.5194/acp-19-4257-2019>
- Wilson, C., Chipperfield, M. P., Gloor, M., & Chevallier, F. (2014). Development of a variational flux inversion system (INVICAT v1.0) using the TOMCAT chemical transport model. *Geoscientific Model Development*, 7(5), 2485–2500. <https://doi.org/10.5194/gmd-7-2485-2014>
- Wittig, S., Berchet, A., Pison, I., Saunio, M., Thanwerdas, J., Martinez, A., et al. (2023). Estimating methane emissions in the arctic nations using surface observations from 2008 to 2019. *Atmospheric Chemistry and Physics*, 23(11), 6457–6485. <https://doi.org/10.5194/acp-23-6457-2023>
- Xiong, L., Bai, X., Zhao, C., Li, Y., Tan, Q., Luo, G., et al. (2022). High-resolution data sets for global carbonate and silicate rock weathering carbon sinks and their change trends. *Earth's Future*, 10(8), e2022EF002746. <https://doi.org/10.1029/2022EF002746>
- Xu, L., Saatchi, S. S., Yang, Y., Yu, Y., Pongratz, J., Bloom, A. A., et al. (2021). Changes in global terrestrial live biomass over the 21st century. *Science Advances*, 7(27), eabe9829. <https://doi.org/10.1126/sciadv.abe9829>
- Yan, E., Wang, X., & Huang, J. (2006). Concept and classification of coarse woody debris in forest ecosystems. *Frontiers of Biology in China*, 1(1), 76–84. <https://doi.org/10.1007/s11515-005-0019-y>
- Yatskov, M., Harmon, M. E., & Krankina, O. N. (2003). A chronosequence of wood decomposition in the boreal forests of Russia. *Canadian Journal of Forest Research*, 33(7), 1211–1226. <https://doi.org/10.1139/x03-033>
- Yuan, K., Li, F., McNicol, G., Chen, M., Hoyt, A., Knox, S., et al. (2024). Boreal–arctic wetland methane emissions modulated by warming and vegetation activity. *Nature Climate Change*, 14(3), 282–288. <https://doi.org/10.1038/s41558-024-01933-3>
- Yuan, Y., Zhuang, Q., Zhao, B., & Shurpali, N. (2023). Nitrous oxide emissions from pan-arctic terrestrial ecosystems: A process-based biogeochemistry model analysis from 1969 to 2019 (pp. 1–37). EGUSphere. <https://doi.org/10.5194/egusphere-2023-1047>
- Zamolodchikov, D. G., & Karelin, D. V. (2001). An empirical model of carbon fluxes in Russian tundra. *Global Change Biology*, 7(2), 147–161. <https://doi.org/10.1046/j.1365-2486.2001.00380.x>
- Zamolodchikov, D. G., Karelin, D. V., & Ivashchenko, A. I. (1998). Postfire changes of the carbon cycle in southern tundra. *Russian Journal of Ecology*, 29(4), 236–240.
- Zamolodchikov, D. G., & Utkin, A. I. (2000). A system of conversion relations for calculating net primary production of forest ecosystems by growing stocks. *Lesovedenie*, 6, 54–63.
- Zelenev, M. M. (1996). *Assessment of the average annual methane flux from the soils of Russia (no. WP-96-051)*. IIASA, 45. Retrieved from <https://pure.iiasa.ac.at/id/eprint/4975/>
- Zhang, Y., Li, C., Trettin, C. C., Li, H., & Sun, G. (2002). An integrated model of soil, hydrology, and vegetation for carbon dynamics in wetland ecosystems. *Global Biogeochemical Cycles*, 16(4), 9–1–9–17. <https://doi.org/10.1029/2001GB001838>
- Zheng, P., Wang, D., Yu, X., Jia, G., Liu, Z., Wang, Y., & Zhang, Y. (2021). Effects of drought and rainfall events on soil autotrophic respiration and heterotrophic respiration. *Agriculture, Ecosystems & Environment*, 308, 107267. <https://doi.org/10.1016/j.agee.2020.107267>
- Zhou, X., Zhou, T., & Luo, Y. (2012). Uncertainties in carbon residence time and NPP-Driven carbon uptake in terrestrial ecosystems of the conterminous USA: A Bayesian approach. *Tellus B: Chemical and Physical Meteorology*, 64(1), 17223. <https://doi.org/10.3402/tellusb.v64i0.17223>
- Zhygunov, A. V., Semakova, T. A., & Shabunin, D. A. (2015). Massive drying out of forests in north-west Russia. *Proceedings of the St. Petersburg Forestry Academy*, 211, 32–52.
- Zona, D., Gioli, B., Lindaas, J., Wofsy, S., Miller, C. E., Dinardo, S. J., et al. (2015). Cold season emissions dominate the arctic tundra methane budget | PNAS. *PNAS*, 113(1), 40–45. <https://doi.org/10.1073/pnas.1516017111>